UNDERSTANDING THE SUPPLY AND DEMAND OF CRITICAL MATERIALS FOR CLEAN ENERGY TECHNOLOGIES: AN AGENT-BASED MODELING APPROACH

by

Jinjian Cao

A Dissertation

Submitted to the Faculty of Purdue University

In Partial Fulfillment of the Requirements for the degree of

Doctor of Philosophy

Division of Environmental and Ecological Engineering

West Lafayette, Indiana

December 2021

THE PURDUE UNIVERSITY GRADUATE SCHOOL
STATEMENT OF COMMITTEE APPROVAL

Dr. Fu Zhao, Chair

School of Mechanical Engineering and Environmental & Ecological Engineering

Dr. John W. Sutherland

School of Environmental & Ecological Engineering

Dr. Seokcheon Lee

School of Industrial Engineering

Dr. Hongyue Jin

Department of Systems and Industrial Engineering, University of Arizona

Approved by:

Dr. John A. Howarter

I dedicate this work to my dear parents, who always supported me during my life oversea.

ACKNOWLEDGMENTS

I would like to acknowledge my advisor Dr. Fu Zhao, who takes care of me in the past 7 years. He has always been helpful and teaches me a lot in how to do research and writing. Meanwhile, he is always forgiving about my mistakes and guide me thorough numerous difficulties. I would also acknowledge my committee members, Dr. John W. Sutherland, Dr. Seokcheon Lee and Dr. Hongyue Jin. Dr. Sutherland has provided precious opinions on my works and writings. Dr. Lee is a great mentor and provides excellent guidance in classes. Dr. Jin has always been kind and it is a great pleasure to work with her. I would also address Dr. Chul Hun Choi for his invaluable collaboration on several works. He is full of ideas and inspired me a lot. Finally, I would like to acknowledge my dear family and friends, who support me all along across the sea. My parents Yang Cao and Xiaohe Chen encourages my studies abroad for 9 years, I cannot thank them enough for their greatest love.

This work was supported by the National Science Foundation under Grant No. 1336534. Any opinions, findings, and conclusions or recommendations expressed in this material are those of the authors and do not necessarily reflect the views of the National Science Foundation.

This research is funded by the Critical Materials Institute, an Energy Innovation Hub funded by the U.S. Department of Energy, Office of Energy Efficiency and Renewable Energy, Advanced Manufacturing Office. The APC was funded by the Critical Materials Institute. All data presented in this study are available in corresponding publicly accessible sources. All data sources are referenced individually.

Additional funding was provided by School of Mechanical Engineering in TA and RA positions I was granted.

TABLE OF CONTENTS

LIST OF TABLES

LIST OF FIGURES

ABBREVIATIONS

ABM	Agent-based modeling
CFL	Compact fluorescent lamp
CH	Cost heuristic
CIGS	Copper indium gallium selenide
DOE	Department of Energy
EOL	End of life
EV	Electric Vehicle
GDP	Gross domestic product
GHG	Greenhouse gas
GWP	Global warming potential
ITO	Indium-tin-oxide
LCA	Life-cycle assessment
LCD	Liquid crystal display
LED	Light-emitting diode
LFP	Lithium iron phosphate
NAH	Network attitude heuristic
NMC	Lithium nickel manganese cobalt oxide
NREL	National Renewable Energy Laboratory
PPM	Parts per million
SAH	Self attitude heuristic
USGS	United States Geological Survey

ABSTRACT

With the rapid development of clean energy technologies, various bottlenecks on supplies of related critical materials emerged. Since supply chains of critical materials often involved with multiple layers of markets with different characteristics, to better identify bottlenecks and increase critical material availability, it is vital to have better understanding and projection on these markets.

Agent-based modeling is a bottom-up approach that can imitate heterogenous objects in a changing environment. Therefore, it is an excellent tool to simulate markets with fierce competition and fast revolution. This work demonstrates the application of agent-based modeling by discussing three different topics related to critical material demand and supply induced by clean energy products.

The first application focused on LED residential lighting market. LED lighting market grew rapidly and introduced potential demand on several critical materials including indium. The work modeled consumers as heterogenous and irrational agents in network purchasing new bulbs based on their own preferences towards different technologies. Projections of LED market were made based on different assumptions reflecting possible policies and events.

The second model explained the indium refining market. Indium is an important by-product metal in LCD display and CIGS photovoltaics manufacturing. Refineries competition on indium supply market was modeled based on agent-based modeling and game theory. Since indium is a by-product metal, facilities capacities and expansions were also taken into consideration. Multiple uncertainties in the market were modeled as scenarios.

The last work dedicated to end-of-life electric vehicles recycling market. Spent EV batteries contain valuable critical materials and are usually sold to recyclers by end-use consumers. However, a large portion of EOL EV batteries were sold to illegal recyclers with cost advantages. This work established an agent-based model utilizing biding mechanics to identify cost gaps between legal and illegal recyclers. Several scenarios representing uncertainties and possible policies were explored.

1. INTRODUCTION

Clean energy technologies are those technologies linked with sustainable and environmental-friendly energy sources, including solar, wind, water, geothermal, bioenergy and nuclear. It also includes energy-saving and fossil-fuel replacement technologies, such as light-emitting diodes (LED) lighting and electric vehicles (EV). In 2013, Department of Energy (DOE) listed four clean energy technologies as most promising, including wind power, solar power, LED, and EV [1]. These technologies grew rapidly in the last decade. For example, LED lighting occupied 15% of total lighting market in 2016, and 30% in 2018 [2]. With the development of these technologies, demand for several type of rare material, known as critical materials, increased significantly. In 2011, DOE listed 16 materials as critical to clean energy technologies. These materials are important to one or several clean energy technologies and are usually facing potential supply risk [3]. Meanwhile, EU and China also listed several materials as "critical" or "strategic" [4] [5]. To better advance clean energy technologies, it is vital to secure a steady supply of such materials to matching the demand.

1.1 Understanding the Supply and Demand of Critical Materials

Several methods have been utilized to analysis critical material supplies from an overview perspective. Material flow analysis is an excellent tool to track the supply-demand balance of a certain moment. Studies have been conducted on Lithium-ion batteries [6], indium [7], and rare earth elements [8]. U.S. Geological Survey also provided annual demand and supply data for materials, including critical materials listed [9]. Several studies modeled critical material supplies as economic models using regression tools [10] [11] [12]. To illustrate the temporal changes on supply-demand balance, system dynamics are employed in addition to material flow analysis to create a projection critical material supply and demand markets [13] [14].

Taking a closer look at the supply chain, the clean energy technologies market often involves with a multi-layer market structure [6], as shown in Figure 1.1. Studies can be focused on one or more chains of the market to provide a more detailed insight. Economic reports and reserve analysis on critical material mines have been conducted [15] [16]. Renewable energy markets penetration studies can be used to assess critical material demand [17]. Analysis on EOL renewable energy products to retrieve critical materials have also been conducted [18] [19] [20]. It has been concluded that critical materials can only be recycled when material price is high enough, and the EOL product contains viable amount of economic feasible material. Several studies are also interested in the adoption of clean energy technologies, including economical model [21] and consumer behavior model [22].

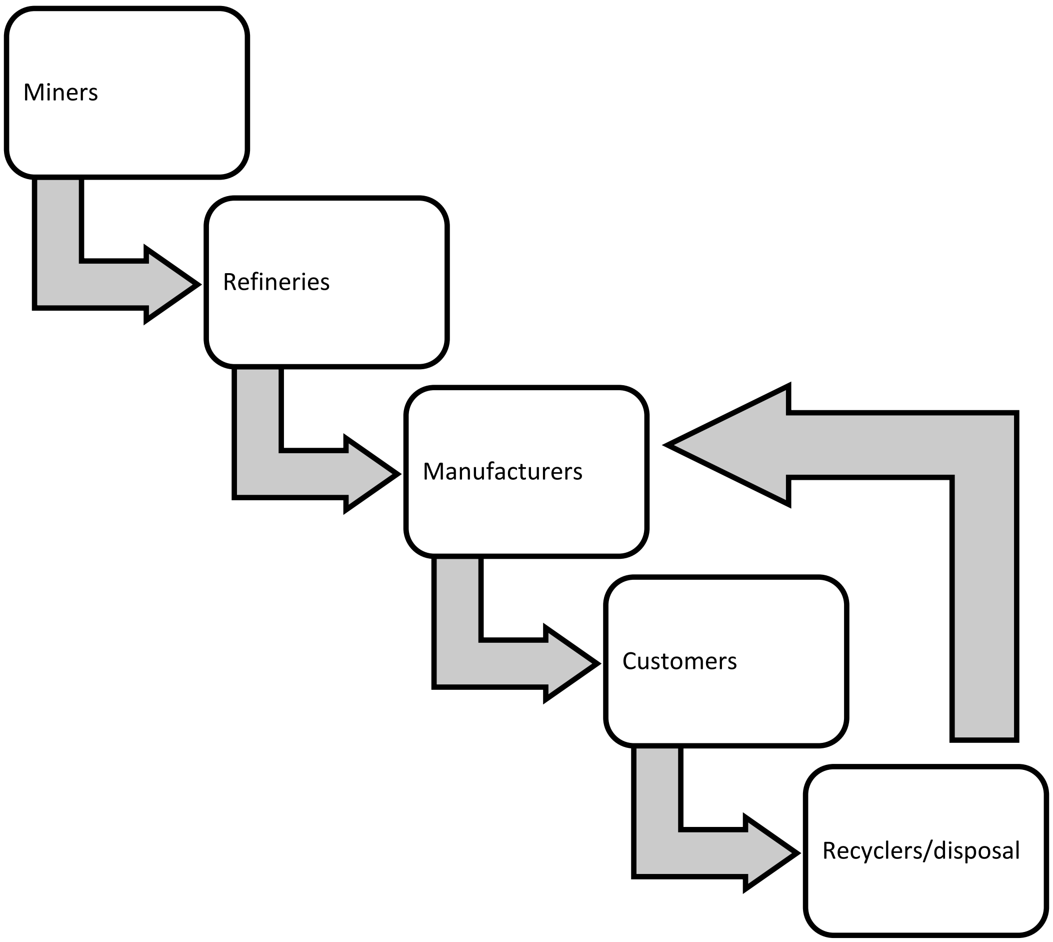

Figure 1.1. Market layers

Inevitably, competition exists in every layer of the market. Research have been conducted trying to establish an economic model for critical metal supply competition [11] [23], clean energy market competition [24] and recycler competition for EOL products [25] [26].

Riddle et. al. developed an agent-based model on global rare earth market [27] [28] [29]. Their model focused on country level behaviors of the market and included multiple layers of elements form miners to manufacturers. Their model provided an excellent example of providing a bottom-up based view of the markets and connection between multiple market layers.

1.2 Introduction to Studies

The studies mentioned above provide abundant views of various clean energy markets and critical material supply-demand balance behind them. However, most of these studies are conducted with a top-down view of the problem. Also, most study did not provide enough insights over the nature of a competing market. Creating a bottom-up, dynamic and competing market model will provide new insights on the non-corporative market behaviors, which already be proven in various other fields, such as network channel assignment [30] and power markets [31]. These existing models are usually based on game theory, multi-agent optimization problem or agent-based modeling [32].

Critical material related markets are usually with high price volatility and uncertainties due to limited market sizes and frequent innovations. Therefore, these markets are extremely sensitive to policies, situations, and irregular market behaviors [33] [34]. Agent-based modeling (ABM) is a flexible tool to address uncertainties and had been applied to model various markets with high uncertainties, such as wind-power electricity market [35] and uncertainty of consumer behaviors [36]. ABM adopts a bottom-up computational approach with “agents” imitating decision makers in real world events. Agents make interactions with each other and with the “environment”, which is the representation of corresponding scenarios in the real world [37]. In a competing market model, actors are usually heterogeneous suppliers or customers making decisions.

This study originally focused on indium supply and demand markets. Indium consumption was mainly driven by LCD manufacturing industry. However, several new applications of indium, including LED and CIGS thin film photovoltaics, may induce further indium demand [38]. Meanwhile, as indium is a by-product of host metal mining and refining, especially zinc, indium supply may not increase accordingly to maintain supply-demand balance due to economic and raw material availability issue [39]. To investigate both the demand and supply potential of indium, two separate models were established. In Chapter 2, an agent-based model focusing on LED lighting market is presented as LED may become a new demand source of indium. This model demonstrates clean energy technology adaption with heterogeneous customers under stochastic behaviors. In Chapter 3, ABM is applied to global indium refineries competing in indium supply market facing demand from emerging photovoltaic cell technology. The market is highly volatile, and several market uncertainties are modeled as separate scenarios to assess their influence. The research also considered about EOL recycling for indium as a secondary supply. However, indium EOL recycling is not economically feasible at the moment and little indium EOL recycling data are available [40]. To illustrate that this method could be applied to EOL recycling market containing critical materials, another emerging market was chosen by the study. In Chapter 4, a model of EOL EV batteries recycling in China is discussed. Both regular and irregular recyclers bid for waste batteries and the importance for policy maker to get involved in the market is shown.

In all, this study provides insights on the various ways of implementing ABM on critical material and clean energy technology market, while also makes up examples to provide predictions and understandings on several interesting markets with different natures.

1.3 References

[1] Tillemann, L., Beck, F., Brodrick, J., Brown, A., Feldman, D., Nguyen, T., & Ward, J. (2013). Revolution Now: The Future Arrives for Four Clean Energy Technologies. US Department of Energy, 20.

[2] Elliott, C., & Lee, K. (2020). Adoption of Light-Emitting Diodes in Common Lighting Applications (No. DOE/EE-2120). Guidehouse.

[3] Chu, S. (Ed.). (2011). Critical materials strategy. DIANE publishing.

[4] European Commission (2020). Critical Raw Materials Resilience: Charting a Path towards greater Security and Sustainability. Retrieved from https://ec.europa.eu/growth/sectors/raw-materials/areas-specific-interest/critical-raw-materials_en

[5] The Ministry of Land and Resources of the People's Republic of China (2016) . National Mineral Resources Plan (2016-2020) Retrieved from http://www.mnr.gov.cn/gk/ghjh/201811/t20181101_2324927.html (In Chinese)

[6] Song, J., Yan, W., Cao, H., Song, Q., Ding, H., Lv, Z., ... & Sun, Z. (2019). Material flow analysis on critical raw materials of lithium-ion batteries in China. Journal of Cleaner Production, 215, 570-581.

[7] Yoshimura, A., Daigo, I., & Matsuno, Y. (2013). Global substance flow analysis of indium. Materials transactions, 54(1), 102-109.

[8] Guyonnet, D., Planchon, M., Rollat, A., Escalon, V., Tuduri, J., Charles, N., ... & Fargier, H. (2015). Material flow analysis applied to rare earth elements in Europe. Journal of Cleaner Production, 107, 215-228.

[9] USGS (2021). Mineral Commodity Summaries. Retrieved From https://www.usgs.gov/centers/nmic/mineral-commodity-summaries

[10] Fizaine, F. 2013. Byproduct production of minor metals: Threat or opportunity for the development of clean technologies? The PV sector as an illustration. Resources Policy, 38(3), 373-383.

[11] Afflerbach, P., Fridgen, G., Keller, R., Rathgeber, A. W., & Strobel, F. 2014. The by-product effect on metal markets–new insights to the price behavior of minor metals. Resources Policy, 42, 35-44.

[12] Gu, G. H., Noh, J., Kim, I., & Jung, Y. (2019). Machine learning for renewable energy materials. Journal of Materials Chemistry A, 7(29), 17096-17117.

[13] Choi, C. H., Cao, J., & Zhao, F. 2016. System dynamics modeling of indium material flows under wide deployment of clean energy technologies. Resources, Conservation and Recycling, 114, 59-71.

[14] Feng, B., Ye, Q., & Collins, B. J. (2019). A dynamic model of electric vehicle adoption: The role of social commerce in new transportation. Information & Management, 56(2), 196-212.

[15] Jaroni, M. S., Friedrich, B., & Letmathe, P. (2019). Economical feasibility of rare earth mining outside China. Minerals, 9(10), 576.

[16] Werner, T. T., Mudd, G. M., & Jowitt, S. M. 2017a. The world's by-product and critical metal resources part II: A method for quantifying the resources of rarely reported metals. Ore Geology Reviews, 80, 658-675.

[17] Kavlak, G., McNerney, J., Jaffe, R. L., & Trancik, J. E. 2015. Metal production requirements for rapid photovoltaics deployment. Energy & Environmental Science, 8(6), 1651-1659.

[18] Ziemann, S., Müller, D. B., Schebek, L., & Weil, M. (2018). Modeling the potential impact of lithium recycling from EV batteries on lithium demand: a dynamic MFA approach. Resources, conservation and recycling, 133, 76-85.

[19] Qiu, Y., & Suh, S. (2019). Economic feasibility of recycling rare earth oxides from end-of-life lighting technologies. Resources, Conservation and Recycling, 150, 104432.

[20] Favot, M., & Massarutto, A. (2019). Rare-earth elements in the circular economy: The case of yttrium. Journal of environmental management, 240, 504-510.

[21] Rafiq, S., Bloch, H., & Salim, R. (2014). Determinants of renewable energy adoption in China and India: a comparative analysis. Applied Economics, 46(22), 2700-2710.

[22] Irfan, M., Zhao, Z. Y., Rehman, A., Ozturk, I., & Li, H. (2021). Consumers' intention-based influence factors of renewable energy adoption in Pakistan: a structural equation modeling approach. Environmental Science and Pollution Research, 28(1), 432-445.

[23] Choi, C. H., Kim, S. P., Lee, S., & Zhao, F. (2020). Game theoretic production decisions of by-product materials critical for clean energy technologies-Indium as a case study. Energy, 203, 117768.

[24] Lee, D. H. (2012). Toward the clean production of hydrogen: Competition among renewable energy sources and nuclear power. International Journal of Hydrogen Energy, 37(20), 15726-15735.

[25] Liu, H., Lei, M., Deng, H., Leong, G. K., & Huang, T. (2016). A dual channel, quality-based price competition model for the WEEE recycling market with government subsidy. Omega, 59, 290-302.

[26] Tang, Y., Zhang, Q., Li, Y., Wang, G., & Li, Y. (2018). Recycling mechanisms and policy suggestions for spent electric vehicles' power battery-A case of Beijing. Journal of Cleaner Production, 186, 388-406.

[27] Riddle, M., Macal, C. M., Conzelmann, G., Combs, T. E., Bauer, D., & Fields, F. (2015). Global critical materials markets: An agent-based modeling approach. Resources Policy, 45, 307-321.

[28] Riddle, M. E., Tatara, E., Olson, C. M., Graziano, D. J., Smith, B. J., & Bennett Irion, A. (2020). Argonne's global critical materials agent-based model (GCMat) (No. ANL-20/25). Argonne National Lab.(ANL), Argonne, IL (United States).

[29] Riddle, M. E., Tatara, E., Olson, C., Smith, B. J., Irion, A. B., Harker, B., ... & Graziano, D. J. (2021). Agent-based modeling of supply disruptions in the global rare earths market. Resources, Conservation and Recycling, 164, 105193.

[30] Wu, F., Zhong, S., & Qiao, C. (2008, April). Globally optimal channel assignment for non-cooperative wireless networks. In IEEE INFOCOM 2008-The 27th Conference on Computer Communications (pp. 1543-1551). IEEE.

[31] Deissenroth, M., Klein, M., Nienhaus, K., & Reeg, M. (2017). Assessing the plurality of actors and policy interactions: agent-based modeling of renewable energy market integration. Complexity, 2017.

[32] Krause, T., Beck, E. V., Cherkaoui, R., Germond, A., Andersson, G., & Ernst, D. (2006). A comparison of Nash equilibria analysis and agent-based modeling for power markets. International Journal of Electrical Power & Energy Systems, 28(9), 599-607.

[33] Bandara, H. D., Mantell, M. A., Darcy, J. W., & Emmert, M. H. (2015). Rare earth recycling: Forecast of recoverable Nd from shredder scrap and influence of recycling rates on price volatility. Journal of Sustainable Metallurgy, 1(3), 179-188.

[34] Bustamante, M. L., & Gaustad, G. (2015, June). Price volatility in pv-critical material markets: Perspectives for solar firms, consumers, and policy makers. In 2015 IEEE 42nd Photovoltaic Specialist Conference (PVSC) (pp. 1-6). IEEE.

[35] Li, G., & Shi, J. (2012). Agent-based modeling for trading wind power with uncertainty in the day-ahead wholesale electricity markets of single-sided auctions. Applied Energy, 99, 13-22.

[36] Stavrakas, V., Papadelis, S., & Flamos, A. (2019). An agent-based model to simulate technology adoption quantifying behavioural uncertainty of consumers. Applied Energy, 255, 113795.

[37] Gilbert, G. N. (2008). Agent-based models (No. 153). Sage.

[38] Lokanc, M., Eggert, R., & Redlinger, M. (2015). The Availability of Indium: The Present, Medium Term, and Long Term. No. NREL/SR-6A20-62409, National Renewable Energy Lab. (NREL): Golden, CO, USA.

[39] Anderson, C.S. (2019). Indium. In Minerals Yearbook—Metals and Minerals, Advance Release 2016, U.S. Geological Survey: Reston, VA, USA.

[40] Ciacci, L., Werner, T. T., Vassura, I., & Passarini, F. (2019). Backlighting the European indium recycling potentials. Journal of Industrial Ecology, 23(2), 426-437.

2. AGENT-BASED MODELING OF THE ADOPTION OF HIGH-EFFICIENCY LIGHTING IN THE RESIDENTIAL SECTOR

Due to the wide use of incandescent lighting, residential sector has much lower energy efficiency comparing to commercial sector. However, adoption of compact fluorescent (CFL) and light-emitting diode (LED) technology in residential sector has been slow because of several obstacles such as high price tag, poor public information, and additional cost to achieve favorable lighting features. A deep understanding on consumer's behavior is needed to support policy development in order to speed up the penetration of CFL and LED in the residential sector. Agent-based modeling (ABM) has been used to capture the dynamics of complex socio-technical systems, and represent a suitable tool. Previous work on ABM of consumer adoption of CFL and LED rely heavily on multi-criteria decision making of the agents. Since light bulbs are not a significant purchase for most households, it is highly possible that customers will not go through complex decision making mechanics. This research establishes an ABM of residential lighting purchase and usage within a hypothetical community and tries to illustrate possible adoption paths under different scenarios. Agents are divided into three groups with different simple decision heuristics when making purchase. Energy consumption and greenhouse gas (GHG) emission from each scenario are calculated and compared. Results of the simulation show that incandescent lamps will eventually fade out of the market even with no policy implemented. After 25 years, annual energy consumption can be reduced by roughly 30% compared to Year 2010. Under best case where incandescent bulbs are banned, the energy consumption reduction can be up to 70%. Among scenarios, incandescent ban and energy saving campaign yield best energy consumption and GHG emission reduction results. LED technology advancement can improve market penetration of LED lighting but has little effect on incandescent fade out. It is also shown that lighting technology retrofitting can achieve higher reduction on electricity consumption and GHG emission than electricity grid improvement.

2.1 Introduction

Residential and commercial lighting is an important contributor to total electricity consumption in U.S. According to U.S. Energy Information Administration [1], in 2014 about 412 billion kWh of electricity was consumed by residential and commercial sector in U.S., which is roughly 11% of total U.S. electricity consumption. Between them, residential lighting consumed 150 billion kWh, which is about half the amount of commercial sector consumption. However, a report published by U.S. Department of Energy characterizing the lighting market of 2010 pointed out that residential sector had similar lamp density and average lamp wattage comparing to commercial sector, whereas only 1/6 of average operating hours [2]. The main reason for the low energy efficiency in residential sector is the wide usage of incandescent lighting, including traditional incandescent lamps and halogen lamps.

Due to their low efficiency, incandescent lamps consume more electricity and generate more greenhouse gas (GHG) emission to deliver the same luminance comparing to other lighting technologies. Two types of lighting, compact fluorescent lamp (CFL) and light-emitting diode (LED) lamp are considered as "greener" alternatives to incandescent lighting due to their high energy efficiency. An estimate suggests that if incandescent lamps are banned globally by year 2016, up to 0.2 Gt CO2e of greenhouse gas emission can be reduced by 2020 [3], which is equivalent to the total carbon footprint of 10,000 cars with each one driving 100,000 km. To offer a comprehensive understanding on the environmental performance of the lighting technologies, several life-cycle assessments that compare incandescent lamp with CFL and LED to evaluate retrofitting benefits had been carried out recently [4] - [7]. U.S. Department of energy conducted a detailed LCA study [4], including a summary to previous studies and a new LCA result to compare incandescent, CFL and LED lighting. Shahzada et al. [5] estimated that to produce 20 million lumen-hours of light, CFL lighting will have 50% reduction on Sustainable Process Index (SPI) footprint and carbon footprint comparing to incandescent lighting, whereas LED lighting will have 75% reduction on these two impact categories. In another study, Bergesen et al. [6] suggests that CFL lighting will have 60% reduction in 13 of 14 impact categories considered including GHG emission comparing to incandescent lighting, while LED lighting will have 80% reduction. Franz et al. [7] compared environmental impact of incandescent lighting with several different assumptions of LED lighting and the worst case results in roughly 70% reduction of GHG emission. Despite these environmental advantages, the adoption of CFL and LED in residential section is much slower than commercial sector. A market report from National Electrical Manufacturers Association shows that during the first quarter of 2015, incandescent lighting, including halogen lamps, still accounts for 53.7% of the total consumer lamps market, whereas

CFL lighting claims 40% of the market share and LED lighting has only 6.3% [8]. For commercial buildings, CFL lighting already owned over 90% of market share.

This situation did not remain unnoticed. According to NEEA, over half of stores in northwest region of U.S. had promotional material on lighting replacements since 2013, and various promotions including advertisement flyers, brochures, demonstrations, and websites were conducted [9]. Efforts have been made to develop residential sector energy consumption model to provide insights on the problem. Richardson, I. et al. [10] presented a time-series based bottom-up model to estimate residential lighting energy demand. In their research, an active time series of occupancy was used to calculate the number and time of lighting equipment utilized, with consideration of outdoor irradiance level. The result was compared to historical data and proved to be with high accuracy. Johnson, B. J. et al. [11] used a Markov chain based approach to model residential energy consumption. The research established a statistical model to represent the activities of different types of occupants during a day and estimated energy consumption accordingly. Meanwhile, predictions of future residential market penetration and energy consumption level are made by several reports and researches. NEEA report [9] presented a residential lighting market share penetration based on expert opinion, predicting that CFL and LED lighting in total will have 49% of market share in year 2016, and 69% of market share in year 2018. DOE report [12] presented a top-down model to predict market penetration and energy consumption. In the model, consumers are cost conscious and the market penetration is calculated by logit regression models based on historical and predicted costs with consideration of technology diffusion curve. The result showed that energy consumption can be reduced by 37% at year 2020 and 67% at year 2030. However, it should be noted that consumers may consider factors other than cost when making decisions. To address the issue, two groups of researchers tried to characterize future residential lighting market with corresponding energy and environmental consequences with agent-based modeling (ABM) approach with consideration of different decision making criteria [13] - [14]. Residential lighting market consists of multiple parallel households exposed to market information and regulations, which are likely to have different criteria to make decision and change their decisions over time. Therefore, a self-evolving and bottom-up model is desired if one wants to study the long term evolution of the market. ABM adopts a bottom-up computational approach with “agents” imitating actors in real world events. Agents make interactions with each other and the “environment”, which is the representation of corresponding conditions, restrictions, and situations in the real world [15]. These features make ABM a suitable tool to simulate residential lighting market for its bottom-up nature and the ability to evolve through agent-to-agent and agent-to-environment interactions.

Among the two ABM studies on residential lighting, Chappin et al. [13] established a network-based agent based model to illustrate energy consumption and GHG emission reduction of residential lighting. In their model, agents made decisions by multi-criteria decision making process with different weights distribution. Agents will also adjust their weight by recent experience and social network information exchange. Detailed lighting products differences were considered with difference in technology, light color, slot type, etc. Several scenarios were explored to show the effect of possible policies. Their result indicated that incandescent lamps will still be the dominant technology after 40 years without policy support, and incandescent ban will be the most effective policy to reduce energy consumption and GSG emission. Hicks et al. [14] present a grid-based agent based model to illustrate possible rebound effects due to energy saving from adopting new technologies. In their model, agents first made random decisions based on a utility function coming from multi-criteria decision results. A survey was carried out to support the multi-criteria decision weighting data. Agents exchanged their opinion with their grid neighbors. Different rates of rebound effect and two possible scenarios were considered. Their result indicated that households will swiftly switch to new technologies, but with high rates of rebound effect, energy consumption may not be reduced.

It should be noted that both of the ABM studies on residential lighting (i.e., Chappin, E. J., et al. 2013; Hicks, A. L., et al. 2015) rely heavily on multi-criteria decision making from the agents. Early in 1979, Olshavsky et al. pointed out that such decision making process may not be realistic when facing a purchase that is not important [16]. Later, Hoyer made an experiment to show that most customers make very quick in-store choices by simple heuristics on a single criterion when purchasing common product like detergents [17]. Since lighting bulbs are not a significant purchase for most households, it is highly possible that customers will not go through complex decision making mechanics. Meanwhile, Chappin et al. did not consider use phase cost as a decision-making criterion. However, CFL and LED equipment is actually cheaper considering use phase cost and most CFL and LED lighting products will state this on their package. Also, since the research is conducted in Netherland, several parameters including number of lamps per household, average hours per lamp were different from U.S. situation. In model created by Hicks et al., although the agents make stochastic decisions, their utility function are pre-determined and cannot illustrate possible opinion changes of the public. To address these issues, this research aims to establish an ABM of residential lighting purchase and usage within a community and try to illustrate possible adoption paths under different scenarios. Agents, divided into groups, are applied with simple decision heuristics. The model provides market penetration and total energy consumption estimation of three types of lighting bulbs used in residential sector (i.e., incandescent lamp, CFL, and LED) over time.

2.2 Investigative Method

This research models residential lighting purchase choice within a hypothetical urban residential community with 500 households using network based ABM approach. To calculate electricity consumption and lifespan of lighting equipment while keeping reasonable simulation speed, the time step of the model is one day. The simulation starts at year 2010 and ends after 25 years (Year 2035, 9125 days), which allows model validation using historical data while capture the market penetration process of CFL and LED. The model is implemented under Repast Simphony 2.3.1 [18]

Each household is considered as an agent within a Watts Beta Small World network, which imitates social influence network [19]. Following the average data from USDOE [20], each agent will have a random number of lighting positions following a triangular distribution between 5 and 120 with mean 65, each in need of one light bulb. Also, for each specific lighting position, use time per day is assigned with a triangular distribution random number between 0 and 6 hours with a mean of 2 hours. The range of lighting positions follows the data from USDOE [20], and the range of use time per day is assumed to be the maximum range possible of triangular distribution.

To simplify the model, type of lighting is limited to traditional incandescent lamp, spiral CFL lamp, and LED lamp, with the assumption that these lamps are fully substitutable by each other when used for lighting. Each lighting bulb is treated as 60W equivalent and with average shelf price. The life span of each bulb is a random number following an exponential distribution with average corresponding to lighting type (1000 hours for incandescent, 10000 hours for CFL, and 25000 hours for LED). Further differences between lighting bulbs are excluded, such as colors, brands, and other features. Energy consumption during manufacture phase for the bulbs [4] is also included in the model to show the difference between total energy consumption and use phase energy consumption. Since the price and efficiency of incandescent and CFL bulbs are relevantly stable comparing to LED since 2010 (60W and $1.39 for traditional incandescent, 14W and $3.70 for CFL), these parameters are considered as constant for simplification [1], [9]. For LED equipment, USEIA report pointed out that both bulb cost and efficiency changed linearly (decreasing and increasing, respectively) during 2010-2014 [1]. At the beginning of the simulation (year 2010), LED bulbs cost $68.00 with a rating of 16W [4]. At year 5 (year 2014), LED bulbs cost $11.14 with a rating of 10W [9]. Both of these parameters are assumed to change linearly at an annual basis (-$11.374 and -1.2W, respectively) between 2010 and 2015. Price drop and energy efficiency increase of LED bulbs due to technology advancement after 2015 will be discussed in scenario analysis. Besides, average U.S. residential electricity price at year 2010 ($0.115 per kWh) and a linear increment from historical data ($0.002 per kWh) is applied over simulation period [21]. To calculate energy consumption other than use phase, U.S. DOE life cycle assessment data (0.53 kWh per incandescent bulb, 15.75 kWh per CFL bulb, 95.27 kWh per LED bulb) are used [4].

In order to address carbon footprint reduction from residential high-efficiency lighting adoption, use phase greenhouse gas (GHG) emission and total greenhouse gas emission including manufacturing, transport and disposal phase are calculated in a bottom-up manner. All use phase GHG emission (0.518 kg carbon dioxide equivalent (kgCO2e) per kWh) from electricity consumption is treated as U.S. average electricity grid emission and calculated from U.S. Environmental Protection Agency (EPA) electricity grid emission data [22] and all other GHG emission (0.968 kgCO2e per incandescent bulb, 9.167 kgCO2e per CFL bulb and 16.269 kgCO2e per LED bulb) is calculated from U.S. DOE life cycle assessment data [4]. All GHG emission is assessed using 100-year GWP.

Whenever a bulb burned out, the agent will replace it with a new bulb at the beginning of the following day (since time step is one day). When facing the option to choose a bulb, either at the beginning of the simulation or when a bulb burns out, agents are divided into three groups: cost heuristic (CH), self attitude heuristic (SAH) and network attitude heuristic (NAH). The actions an agent takes during each time step is summarized in Figure 2.1.

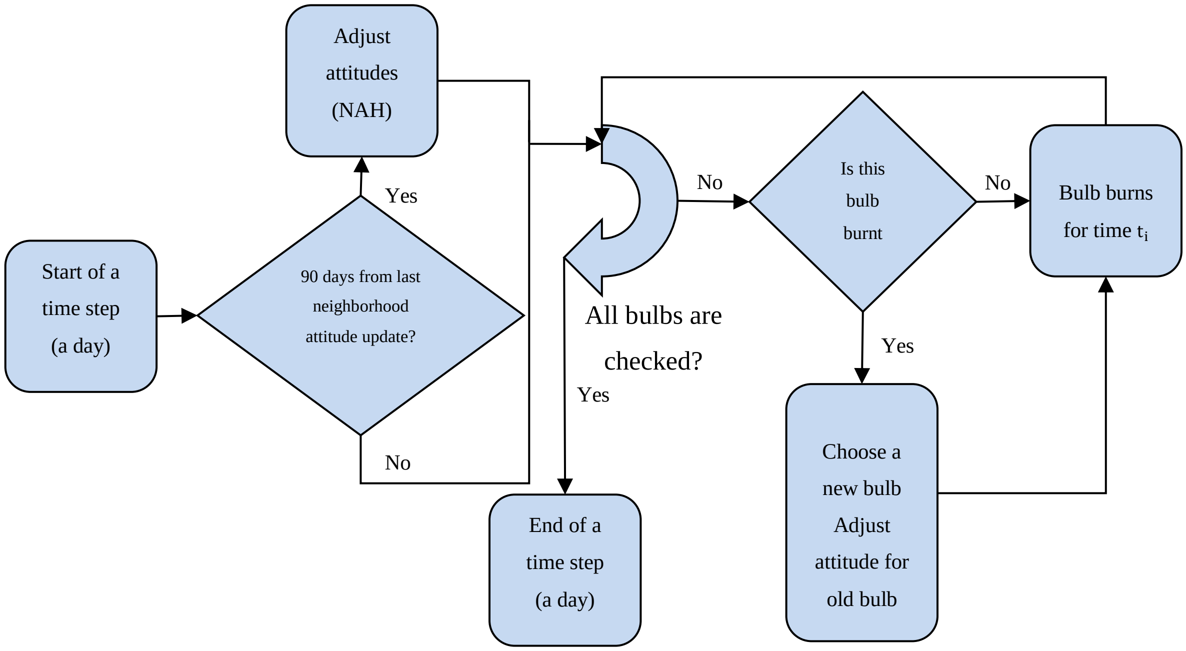

Figure 2.1. Agent flow chart

CH agents calculate the costs for each lighting position with different bulbs considering only a limited period of time from now. A predetermined random number y_c following a triangle distribution between 0 and 20 with mean 10 represents the time period to calculate the costs. Taking current electricity price p_e, current bulb price p_j (j=1 for incandicent, j=2 for CFL, and j=3 for LED), current bulb efficiency e_j, average bulb life span l_j, and usage per day for position i t_i, the calculated cost for lighting position i with bulb type j is:

$$c_{ij} = p_j \times \lceil y_c \times 365 \times t_i \div l_j \rceil + p_e \times y_c \times 365 \times t_i \quad (1)$$

To choose a new bulb, a CH agent compares calculated cost of three different lighting types for the lighting position and chooses the cheapest one. For a small purchase like this, households are unlikely to carry out a more complicated calculation involving the time value of money. Thus, discount rate and other possible cost adjustments are not included.

SAH and NAH agents choose new bulb based on their attitude towards three different lighting types, representing their overall feelings (satisfaction, familiarity, etc.) towards them. SAH agents determine their attitudes solely based on their own experience, while NAH agents are also influenced by their neighbors. At the beginning of the simulation, each agent (including CH agents) is assumed to have an attitude level of 10 to incandescent bulbs, 1 to CFL bulbs and 0 to LED bulbs, reflecting the fact that at year 2010, incandescent bulbs were most well-known and LED bulbs were still unknown to most households. Every time an agent has a burnt-out bulb, the agent will adjust its attitude of that lighting type. It should be noted that CH agents will also adjust their attitudes in order to provide information for NAH agents. NEEA report includes a survey regarding satisfactory of CFL and LED customers [9]. Based on this, each time an agent adjusts their attitude towards CFL or LED bulbs and the adjustment value is randomly determined with probability shown in Table 2.1. For incandescent bulbs, the adjustment value is assumed to always be 2, as incandescent bulbs have more pleasant features available like various size and shape selection, excellent color rendition, and instant turn-on time. Also, this adjustment is divided by the number of same-type bulbs currently used by the agent. This is to reflect the fact that the more bulbs an agent owns, the more unlikely the agent's opinion will be built on a single bulb. When adjusting attitudes, if an agent with attitude 0 towards LED lighting finds a neighbor using LED bulbs, the agent will change its attitude to 1, representing that the agent receives information about LED from the neighbor. For NAH agents, an additional adjustment happens every 90 days. For each lighting type, an NAH agent adds attitudes from all neighbors together and find out the type with highest total neighbor attitude. The agent then adds 1 rank to its attitude towards that type.

Table 2.1. Probability table of attitude adjustments

Adjustment Value	**Incandescent**	**CFL**	**LED**
+2 (Very satisfying)	100%	40%	63%
+1 (Satisfying)	0%	34%	25%
0 (Somewhat satisfying)	0%	16%	10%
-1 (Unsatisfying)	0%	10%	2%

To choose a new bulb, both SAH and NAH agents make stochastic decisions. Suppose a SAH or NAH agent has an attitude of a_1, a_2, and a_3 towards incandescent, CFL, and LED bulbs respectively, the probability for the agent to choose type i as the new bulb is:

$$p_i = a_i/(a_1 + a_2 + a_3) \tag{2}$$

Since this model is stochastic, multiple runs are required to reduce the effect of randomness. To do so, 10 runs are made first to construct a 95% confidence interval and additional runs will be made if relative error of the interval is greater than 0.05. The details of simulation technique can be found in [23].

By default, each agent will be assigned to a heuristic group with equal probability, resulting roughly equal population for the three heuristic groups. This in conjunction with all parameters mentioned above forms the base case of the model. In order to illustrate more possibilities of future and explore the effect of several possible policies, 5 scenarios are explored as below:

1. Cost-conscious community: In this scenario, we start with 60% CH agents and 20% for both SAH and NAH agents. This is to show how the model will perform when a different population base is provided.
2. Incandescent lamp ban: Starting from the 10th year (year 2020, 3650 days), no new incandescent bulbs can be bought. However, incandescent bulbs already installed can still be used until they burn out.
3. LED technology advancement: According to DOE projection, LED lighting efficiency will increase to 200 lumens per watt (4W LED as 60W incandescent equivalent) and price will fall to $3.34 at year 2030. In addition to existing adjustment to LED price and efficiency, starting from year 5, LED lighting efficiency and price will adjust on an annual basis (at the rate of -$0.52 per year for price, and -0.4W per year for wattage) until year 20 [1]. Also, a more conservative scenario where LED only advances at half speed (-$0.26 and -0.2W per year until year 20) is explored to show the impact of slow technology advancement.
4. Energy-saving campaign: In this scenario, all agents are influenced by a campaign to improve their attitude towards CFL and LED bulbs. The campaign will increase their

attitudes towards CFL and LED by 1 every year starting in year 5. A more effective scenario is also explored where agents' attitudes increase by 1 every 90 days.

5. Energy efficient incandescent: According to The Energy Independence and Security Act (EISA), 60W equivalent incandescent lamps should improve their efficiency to 43W by the start of 2014. In response to this act, incandescent bulb rate in this scenario will be reduced to 43W at year 5.
6. Cleaner electricity grid: To compare the GHG emission reduction effects of residential lighting retrofitting and electricity grid retrofitting, this scenario uses projected GHG emission data from electricity sector and compares GHG emission with base case. The projected GHG emission per kWhr in 2035 of electricity grid is 88% of 2012 data [24].
7. Mercury issues with CFL lighting: It is highly possible that mercury content of CFL lighting will become a public concern. In this scenario, a $3 CFL mercury tax will be in effect and attitude towards CFL will decrease by 1 at year 5.
8. Rebound effect: As Hicks, A. L., et al pointed out, households may tend to extend their lighting hours or increase number of lighting after they switch into a more efficient option. In this scenario, after an agent switch to a more cost-efficient option for a lighting position, they will extend lighting hours of that position by 10%. Also, they have a 10% probability to have a new lighting position.

2.3 Model Verification and Validation

Several verification and validation techniques proposed for ABM are employed here to verify the model [25]. First, tracing technique is applied by observing the behavior of one single agent throughout a test run. This ensures that the model runs as designed. For each heuristic group, an agent is followed and no abnormal behavior is found. Secondly, 10 test runs are made with arbitrary random seed. The results are used for two purposes. An internal validity is made by observing the data range. The result is shown in Table 2.2. Besides, historical data, including EIA estimation and DOE estimation are applied to compare with test run results [1] [20]. The results, including critical parameters applied, are shown in Table 2.3.

From the internal validity test, it is apparent to see that the model itself is consistent. For the 10 test runs on the base case, no extreme results are observed and standard deviation of the output is smaller than 5% of mean value. When compare with historical data, base case results give an average lamp power close to DOE and EIA data at the beginning of the simulation. From data provided by EIA, it is also possible to estimate annual average energy consumption per household for year 2014. The result is presented as average lamp wattage. The model gives slightly lower energy consumption at the beginning but slower energy consumption reduction than EIA data. Still, the average wattage power is close to the historical data.

Table 2.2. Internal validity test

Test data		**Base case**
2010 Use Phase Energy Consumption (kWh)	Min	959331
	Max	1034983
	Average	997785
	stdev	28518.51
2014 Use Phase Energy Consumption (kWh)	Min	852776
	Max	923704
	Average	888965
	stdev	25771.21
2034 Use Phase Energy Consumption (kWh)	Min	683557
	Max	753723
	Average	718692
	stdev	21213.67

Table 2.3. Comparison with historical data

Result	**Average Number of Lamps**	**Average Hour of Use Per Day (h)**	**Average Energy Consumption Per Day Per Household 2010(Wh)**	**Average Lamp Power 2010(W)**	**Average Lamp Power 2014(W)**
Base case	65	2	5467	42.1	37.2
DOE data	67	1.6	4679	47.7	N/A
EIA data	51	1.8	4223	46	39

Finally, to address parameter variability, sensitivity analysis is conducted. To begin with, a selection of parameters coming from assumption and rough estimation are chosen, as shown in Figure 2.2. Each parameter will be modified by ±10%. To compare the sensitivity of parameters on the same basis, one run of each possible parameter setting with the same random seed is conducted and sensitivity of parameter is measured by changes on use phase annual energy consumption in year 2034 (final output). The result of sensitivity analysis shows that the model is reasonably robust. Most sensitive parameters are wattage of incandescent lamps, average hour of use per lamp, and average number of lamps per household.

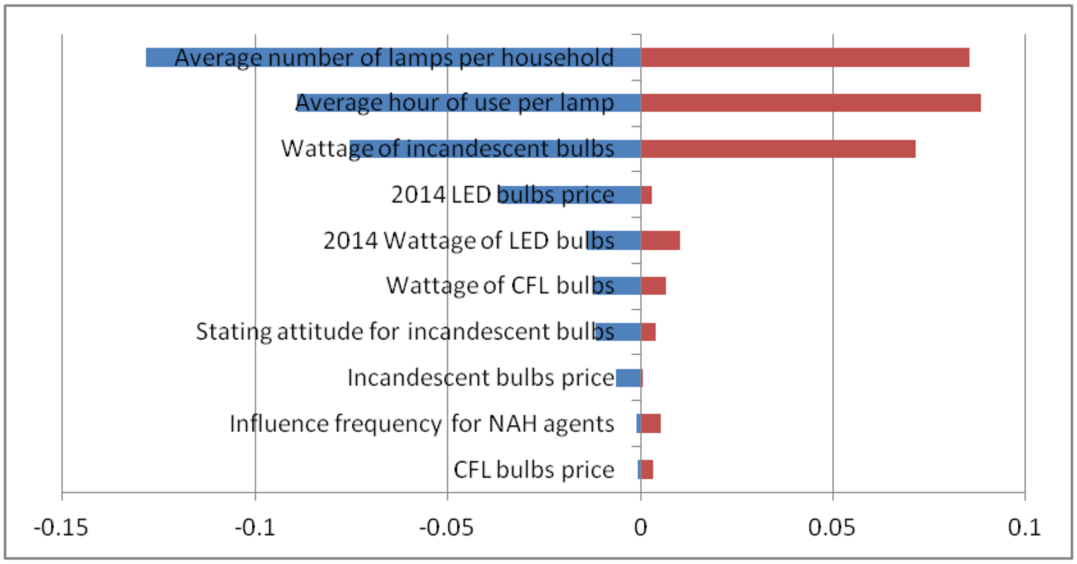

Figure 2.2. Tornado graph

2.4 Results and Discussion

The results for energy consumption, GHG emission, and shares of bulbs by technology of base case and each scenario are shown below. Since random effect in this model is relatively small, calculation result shows that relative error of confidence interval is smaller than 0.05. Therefore, no additional runs are made. Also, the confidence interval is very tight (with half width less than 5% of the value). Therefore, to better illustrate the result, only mean value is plotted in the graph.

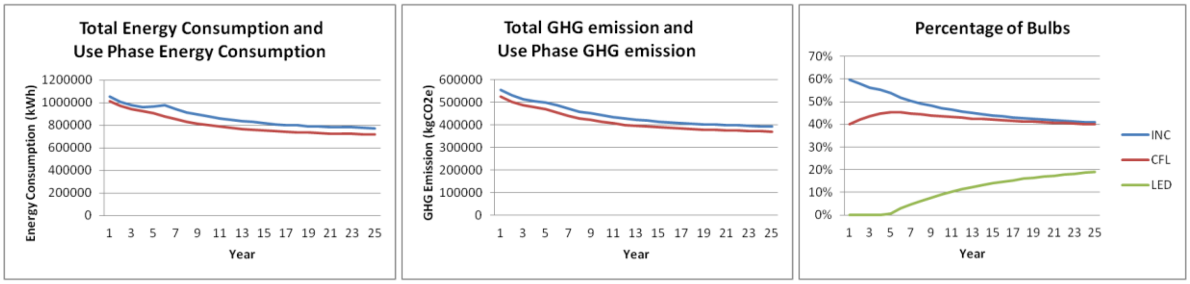

Figure 2.3. Base case results

For the base case result in Figure 2.3, annual total energy consumption is reduced by 27% and annual use phase energy consumption is reduced by 30% at the end of simulation. Meanwhile, annual total GHG emission is reduced by 30%. Incandescent bulbs are reduced to 70% of starting number, whereas the number of CFL bulbs remains roughly the same level for the whole simulation period. LED bulbs grow rapidly, holding 20% of market share at the end of simulation. The result shows that households are slowly adapting to high-efficiency lighting. However, without any interference, incandescent will remain the major technology at year 2035. Also, for total energy consumption, a spike can be observed around year 6. This is due to much higher manufacturing energy consumption from CFL and LED lighting. When incandescent lighting is replaced by CFL and LED lighting intensively at year 6, manufacturing energy consumption that year will increase greatly, which result in higher total energy consumption that year.

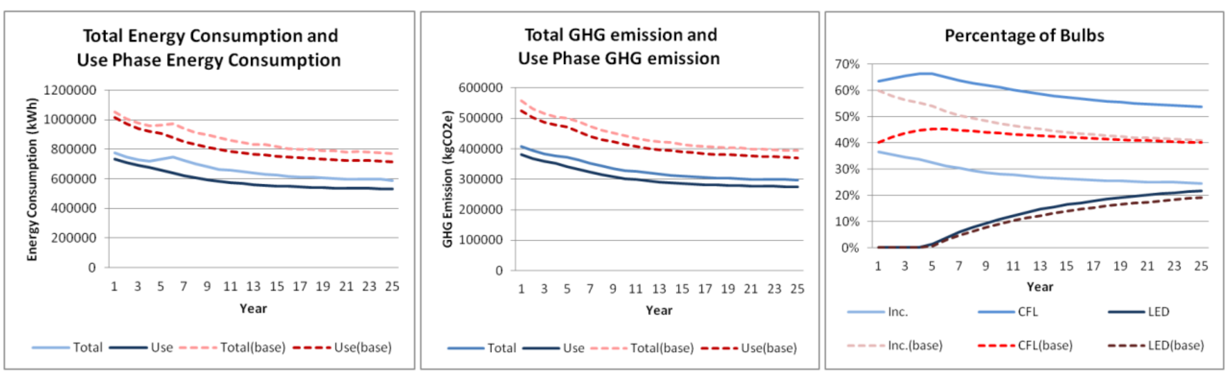

Figure 2.4. Cost conscious community

When the community has higher portion of cost heuristic households, CFL lighting becomes the leading technology at the beginning of simulation, as it is the most cost-effective under most situation. As a result shown in Figure 2.4, the starting energy consumption and GHG emission are roughly 72% of the base case. The trend of energy consumption and GHG emission reduction is similar to the base case. At year 2035, total energy consumption is reduced by 24% and total GHG emission is reduced by 28%. Reduction rate is slightly smaller than the base case due to the fact that fewer inefficient lighting bulbs are installed at the beginning of simulation. It is apparent to draw the conclusion that cost-efficient households tend to choose energy-saving technologies just like users in commercial sector.

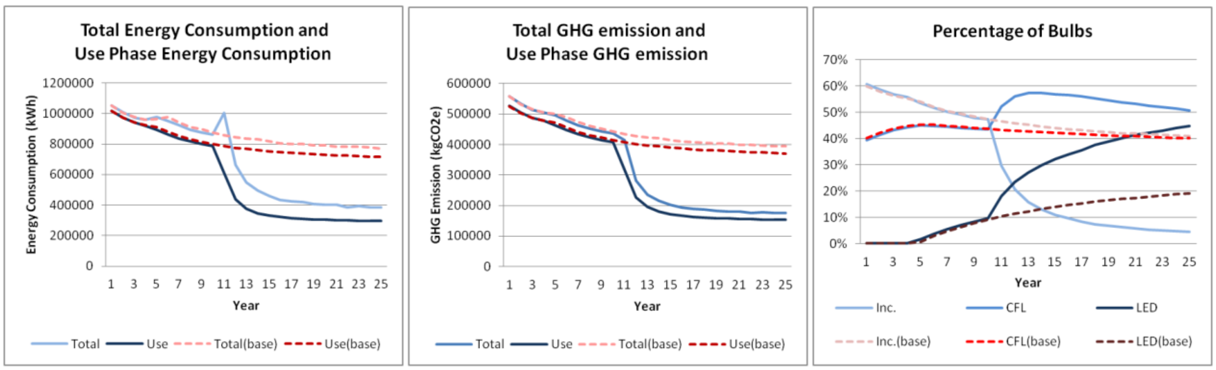

Figure 2.5. Incandescent lamp ban

Under incandescent lamp ban scenario in Figure 2.5, a sharp change in trend can be observed when ban comes into effect. Annual use phase energy consumption, annual total GHG emission and annual use phase GHG emission drastically fall, whereas a spike happens in annual total energy consumption. This is due to that fact that manufacturing CFL and LED bulbs is more energy intensive than incandescent bulbs. Besides, both CFL and LED bulbs have s-shape curve market share increase after incandescent bulbs are banned, but CFL bulbs are replaced by LED bulbs afterwards. Under this scenario, total energy consumption in year 2035 is reduced by 65%, while use phase energy consumption is reduced by 72%. Meanwhile, total GHG emission is reduced by 70%. At the year of incandescent ban, a sudden increase of total energy consumption can be observed. As stated before, this is caused by higher manufacturing energy consumption of CFL and LED bulbs. However, with longer lifespan and higher use phase efficiency of these technologies, total energy consumption quickly falls afterwards.

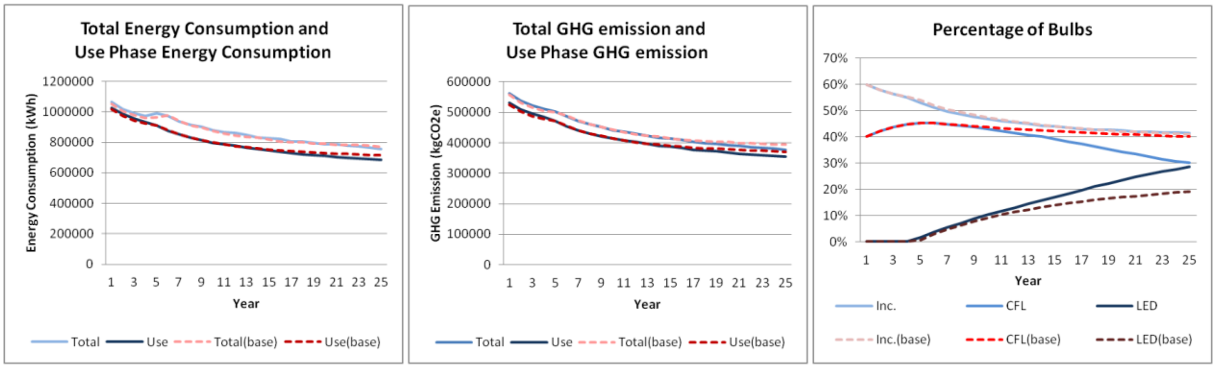

Figure 2.6. LED advancement (EIA case)

If LED technology continues to develop as EIA estimated, as shown in Figure 2.6, LED lighting will have 29% market share at year 2035, which is roughly 50% higher than base case. However, as most replacement comes from CFL lighting, the total number of incandescent bulbs at year 2035 remains the same level with base case. Therefore, only slight improvements on energy consumption and GHG emission reduction are observed. Under this scenario, annual total energy consumption is reduced by 29%, and use phase energy consumption is reduced by 34%. For annual total GHG emission the reduction rate is 33%.

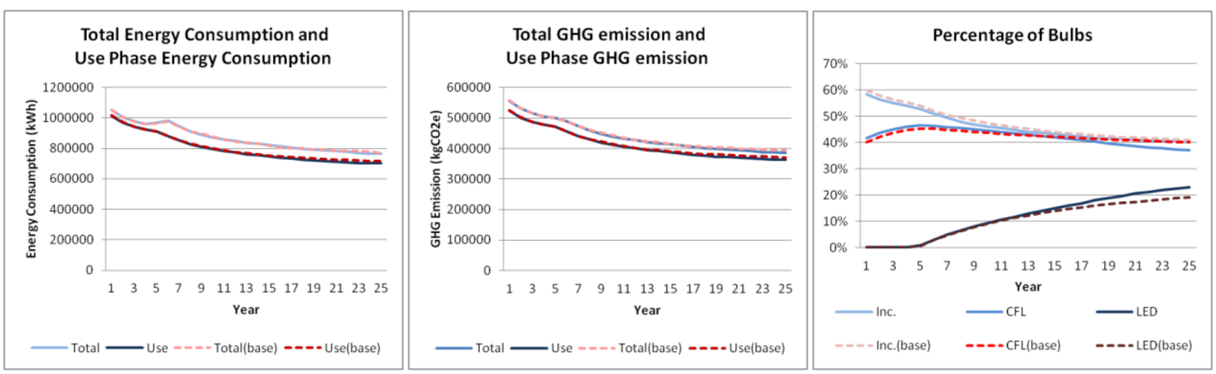

Figure 2.7. LED advancement (conservative case)

For a more conservative LED technology advancement scenario, the result shown in Figure 2.7 is very close to the base case. At year 2035, LED lighting will have 23% market share, which is 15% better than base case. However, energy consumption and GHG emission reduction rates are nearly the same as the base case. Comparing with EIA case, it is apparent to see that the advancement of LED technology still has a positive effect in increasing the market share of LED lighting. However, it is not able to push the fade out of incandescent, since in this model most incandescent users are not cost sensitive.

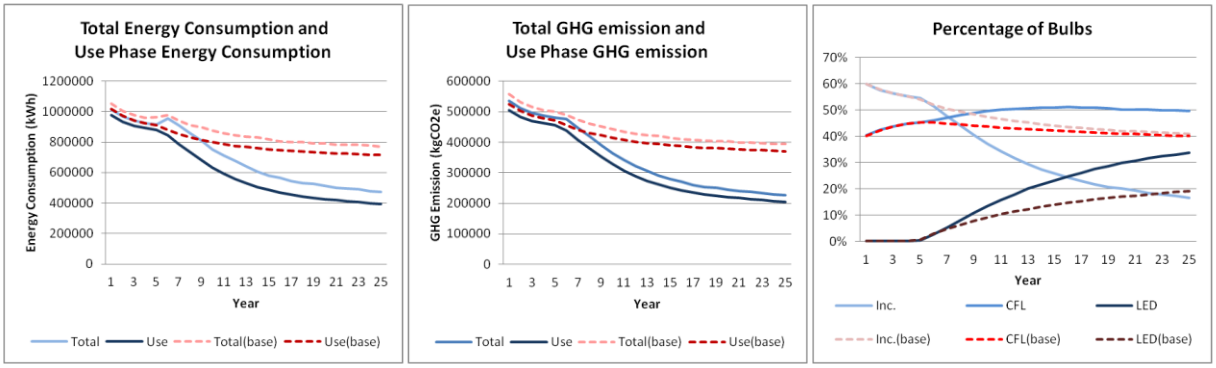

Figure 2.8. Energy saving campaign (slower case)

Under energy saving campaign scenario, the constant increase of attitudes toward high-efficiency lightings causes incandescent lamps to fade out, as shown in Figure 2.8. At Year 2035, annual total energy consumption is reduced by 53% and annual use phase energy consumption is reduced by 60%. Also, annual total GHG emission is reduced by 58%. Although in reality, it is very hard to directly improve public opinion steady and fast like this, the scenario still shows that information plays a key role in residential lighting retrofitting process and further study should be focused on this.

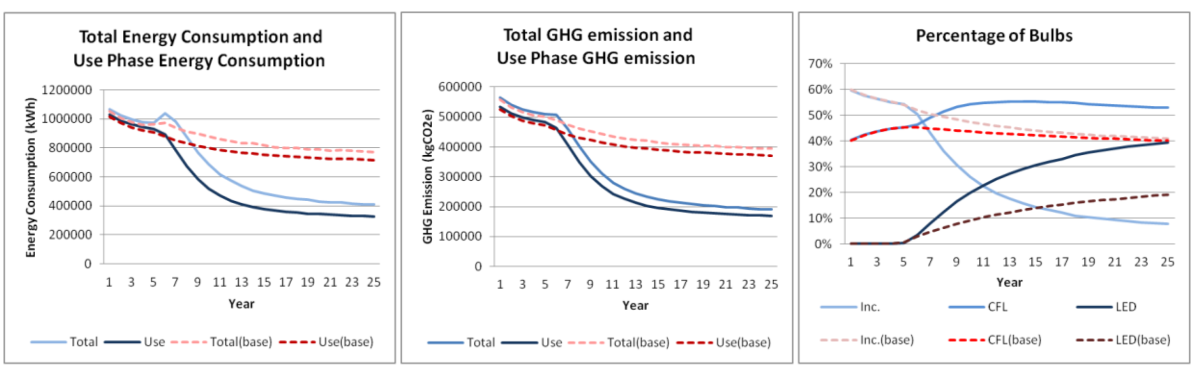

Figure 2.9. Energy saving campaign (faster case)

Under faster attitudes changes favoring high-efficiency lightings, the fade-out of incandescent becomes faster and more thoroughly, as shown in Figure 2.9. At year 2035, total energy consumption is reduced by 62% and use phase energy consumption is reduced by 68%.

Similarly, annual total GHG consumption is reduced by 66%. With even faster improvements of households' attitude towards CFL and LED lighting, the result is very close to incandescent ban scenario.

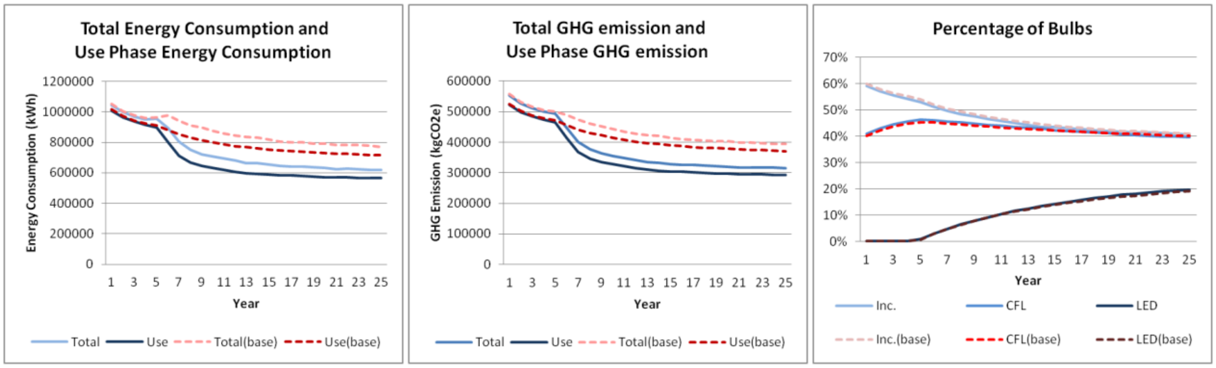

Figure 2.10. Energy efficient incandescent

With energy efficient incandescent, although market share is similar with base case scenario, the reduction rates of energy consumption and GHG emission are higher. At year 2035, Total energy consumption is reduced by 41% and use phase energy consumption is reduced by 44% as shown in Figure 2.10. Besides, annual total GHG emission is reduced by 43%. Although energy efficient incandescent still consume much more energy than CFL and LED lighting, such policy can reduce a significant amount of energy consumption and GHG emission provided that incandescent fade out is slow.

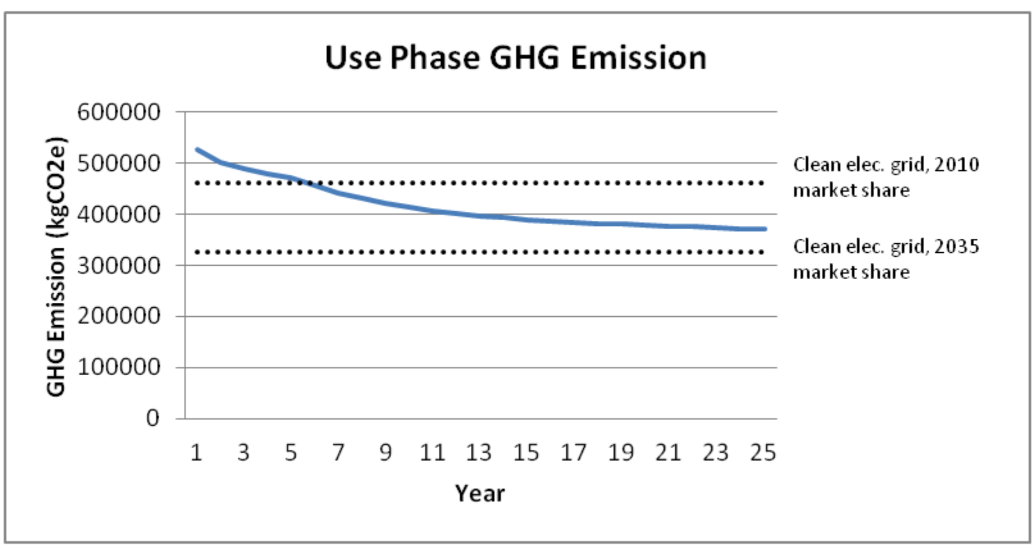

Figure 2.11. Base case GHG emission vs. cleaner electricity grid

The annual GHG Emission with cleaner electricity grid is shown in Figure 2.11 as reference line. The line is calculated by combining cleaner electricity grid emission data (2035 projection) with lighting market share data from corresponding year. As stated above, when applying market share data from year 2010, cleaner electricity grid alone can reduce GHG emission by 12%. With base case, the reduction from high-efficiency lighting technologies will exceed this after 5 years. The result shows that high-efficiency lighting retrofitting plays an important role in reducing GHG emission from residential lighting sector. GHG emission reduction from incandescent fade out is greater than the reduction from electricity grid improvement.

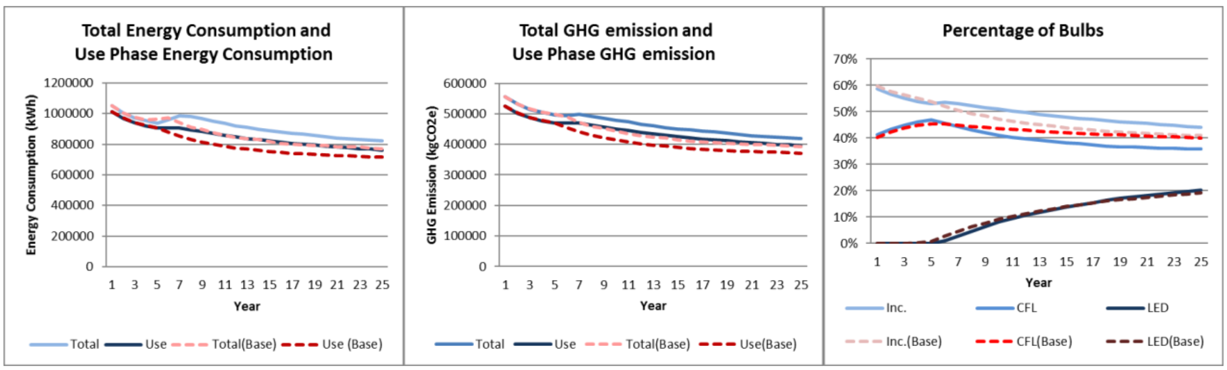

Figure 2.12. Mercury tax

If mercury tax is applied and the public become more concern about mercury in CFL lighting, more households will stay with incandescent lamps, as shown in Figure 2.12. In this scenario, incandescent lamps stay with 5% more market share at year 2035. Meanwhile, only 25% reduction of energy consumption and GHG emission is observed.

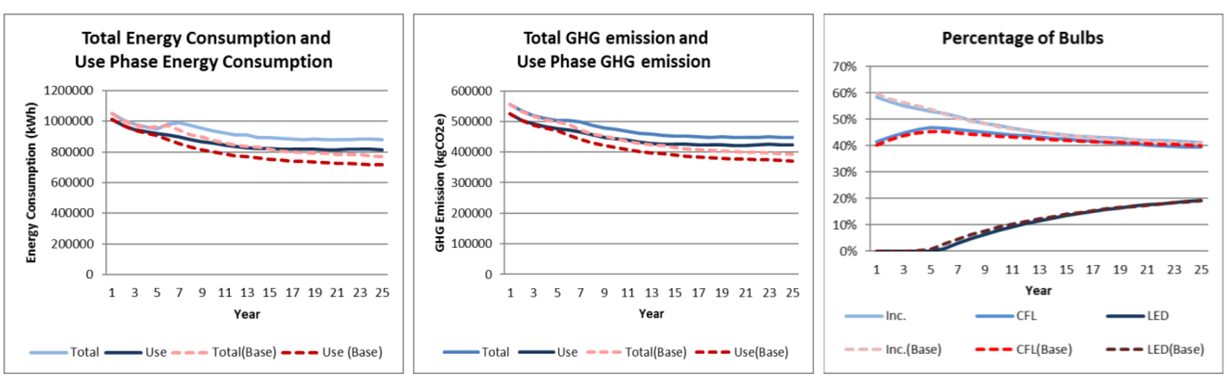

Figure 2.13. Rebound effect

If rebound effect is considered, it is apparent to see that both energy consumption reduction and GHG emission reduction will be hindered. The result shows the same market penetration with the base case along the simulation. However, due to increased lighting time and lighting position, only 20% reduction can be observed on energy consumption and GHG emission. Therefore, if rebound effect happens in residential lighting market, it should be considered as an important negative factor to affect energy and GHG emission reduction.

2.5 Conclusion and Future Work

In this study, an agent-based model is implemented to simulate the adoption of high-efficient lighting in a residential community. The result shows that a 30% of energy consumption and GHG emission reduction can be achieved by year 2035 with no policy applied. Furthermore, if there is an incandescent ban, the model projects 65% reduction of energy consumption and 70% reduction of GHG emission, which is the best among all scenarios. The result also shows that aside from direct ban of incandescent, it is more important to improve market share of high-efficiency lighting than improve the efficiency of them. Therefore, proper way of marketing campaign can accelerate the reduction of energy consumption and GHG emission. Also, some factors, including health concerns and rebound effects, may have a negative effect in energy and GHG emission reduction. Finally, the model shows the importance of residential lighting retrofitting. There is a significant potential of energy saving and GHG emission reduction and the efficiency is better than mere improvement of electricity grid.

This model is very crude in the aspect of agent classification and behaviors. In fact, several possible factors can be detailed to improve model design. New smartphone applications will help households to calculate total lighting cost more precisely and may increase the number of rational users. CFL and LED lighting may have health issues, like emitting more blue light that is harmful before bedtime. Also, more cultural and political factors should be considered, as households with different backgrounds may response differently to new technology or government policies. Further study of the topic requires survey data on the customers, such as the one carried out by Hicks, A. L. et al. Deeper understanding of customer behavior can help improving the model and increasing its validity. Also, the model can be expanded in several ways. Commercial sectors can be integrated into the model and may affect the adoption process with its influence towards residential customers. Critical material consumption of the adoption process can be analyzed with expansion of the model. More detailed classification of lighting equipment, like the inclusion of halogen lamps and linear fluorescent bulbs can also be considered.

2.6 References

[1] U.S. Energy Information Administration. (2014). Annual Energy Outlook 2014. United States Department of Energy.

[2] Navigant. (2012). 2010 U.S. Lighting Market Characterization. United States Department of Energy.

[3] Blok, K., Höhne, N., van der Leun, K., & Harrison, N. (2012). Bridging the greenhouse-gas emissions gap. Nature Climate Change, 2(7), 471-474.

[4] Navigant. (2012). Life-Cycle Assessment of Energy and Environmental Impacts of LED Lighting Products. United States Department of Energy.

[5] Shahzada, K., Rehana, M., Ismaila, I. M., Sagirb, M., Tahirb, M. S., Bertokc, B., & Nizami, A. S. (2015). Comparative Life Cycle Analysis of Different Lighting Devices. CHEMICAL ENGINEERING, 45.

[6] Bergesen, J. D., Tähkämö, L., Gibon, T., & Suh, S. (2015). Potential Long-Term Global Environmental Implications of Efficient Light-Source Technologies. Journal of Industrial Ecology.

[7] Franz, M., & Nicolics, J. (2015). Environmental aspects of white LED lighting systems: Energy statistics, study parameters, rare earths. In Electronics Technology (ISSE), 2015 38th International Spring Seminar on (pp. 396-401). IEEE.

[8] Cullen, T. (2015). First Quarter Proves to be a Mixed Bag for Consumer Lamp Indexes. National Electrical Manufacturers Association http://www.nema.org/news/Pages/First-Quarter-Proves-to-be-a-Mixed-Bag-for-Consumer-Lamp-Indexes.aspx

[9] DNV GL. (2015). 2014–2015 Northwest Residential Lighting Long-Term Market Tracking Study. Northwest Energy Efficiency Alliance

[10] Richardson, I., Thomson, M., Infield, D., & Delahunty, A. (2009). Domestic lighting: A high-resolution energy demand model. Energy and Buildings, 41(7), 781-789.

[11] Johnson, B. J., Starke, M. R., Abdelaziz, O. A., Jackson, R. K., & Tolbert, L. M. (2014, February). A method for modeling household occupant behavior to simulate residential energy consumption. In Innovative Smart Grid Technologies Conference (ISGT), 2014 IEEE PES (pp. 1-5). IEEE.

[12] Navigant. (2012). Energy Savings Potential of Solid-State Lighting in General Illumination Applications. United States Department of Energy.

[13] Chappin, E. J., & Afman, M. R. (2013). An agent-based model of transitions in consumer lighting: Policy impacts from the EU phase-out of incandescents. Environmental Innovation and Societal Transitions, 7, 16-36.

[14] Hicks, A. L., Theis, T. L., & Zellner, M. L. (2015). Emergent effects of residential lighting choices: Prospects for energy savings. Journal of Industrial Ecology, 19(2), 285-295.

[15] Gilbert, G. N. (2008). Agent-based models (No. 153). Sage.

[16] Olshavsky, R. W., & Granbois, D. H. (1979). Consumer decision making-fact or fiction?. Journal of Consumer Research, 93-100.

[17] Hoyer, W. D. (1984). An examination of consumer decision making for a common repeat purchase product. Journal of consumer research, 822-829.

[18] North, M. J., Collier, N. T., Ozik, J., Tatara, E. R., Macal, C. M., Bragen, M., & Sydelko, P. (2013). Complex adaptive systems modeling with Repast Simphony. Complex adaptive systems modeling, 1(1), 1-26.

[19] Watts, D. J. (1999). Small worlds: the dynamics of networks between order and randomness. Princeton university press.

[20] DNV KEMA (2012). Residential Lighting End-Use Consumption Study: Estimation Framework and Initial Estimates

[21] U.S. Energy Information Administration. (2016). Electric Power Annual, DOE/EIA-0348. United States Department of Energy.

[22] U.S. Environmental Protection Agency (2015) The Emissions & Generation Resource Integrated Database https://www.epa.gov/energy/egrid

[23] Kelton, W. D., & Law, A. M. (2000). Simulation modeling and analysis. Boston: McGraw Hill.

[24] U.S. Department of State, (2014). 2014 U.S. Climate Action Report http://www.state.gov/documents/organization/219038.pdf

[25] Xiang, X., Kennedy, R., Madey, G., & Cabaniss, S. (2005). Verification and validation of agent-based scientific simulation models. In Agent-Directed Simulation Conference (pp. 47-55).

3. AGENT-BASED MODELING FOR BY-PRODUCT METAL SUPPLY—A CASE STUDY ON INDIUM

With rapid development and deployment of clean energy technology, demand for certain minor metals has increased significantly. However, many such metals are by-products of various host metals and are economically infeasible to extract independently. Meanwhile, by-product metals present in the mined ores may not be extracted even if they are sent to smelters along with host metal concentrates if it is not economically favorable for the producers. This dependency poses potential supply risks to by-product metals. Indium is a typical by-product metal, mainly from zinc mining and refining, and is important for flat panel displays, high efficiency lighting, and emerging thin-film solar panel production. Current indium supply–demand forecast models tend to overlook the volatile and competitive nature of minor metal market and are mostly based on top-down approaches. Therefore, a bottom-up agent-based model can shed new light on the market dynamics and possible outcome of future indium supply–demand relationship. A multi-layered model would also be helpful for identifying possible bottlenecks of indium supply and finding solutions. This work takes indium as an example of minor metal market and sets up an agent-based model to predict future market situation and supply－demand balance. The market is modeled as a Cournot competition oligopolistic market by refineries with capacity restriction based on host metal production. The model maintains active Nash equilibrium each year to simulate competitions between suppliers. The model is validated and verified by historical data and sensitivity analysis. Several scenarios are also explored to illustrate possible uncertainties of the market.

3.1 Introduction

Energy is a fundamental element of economic growth. Global primary energy consumption has increased by 2.9% in 2018, which is the fastest for the decade [1]. To avoid dependency on fossil fuels, which still count for 64% of world energy generation [1], non-fossil resources, especially renewable energy from wind and solar power, have been heavily promoted by governments. Between 2005 and 2015, the US government spent $51.2 billion US dollars on incentives to solar and wind power industries, including tax, credit, and R&D grants [2]. As a result, renewable energy consumption has increased by four times between 2008 and 2018, to a total of 561.3 million tons oil equivalent [1]. With an imminent need for renewable energy development and technology advancement, minor metals have become increasingly important. The US Department of Energy has identified 14 materials as critical to the clean energy economy [3]. Meanwhile, Joint Research Centre of European Commission addressed 32 significant materials toward clean energy sector [4]. One major issue for these materials is the potential supply risk caused by the increasing demands.

Many of the so-called critical materials are by-product metals. By-product metals are those minor metals that are mined mostly or solely as companion of other major metals [5]. For example, only 15% of cobalt is mined and produced as primary product, whereas the rest is a by-product of nickel and copper; indium is a secondary product mostly from zinc processing [6]. Other by-product metals that are critical to renewable energy include cadmium, gallium, germanium, selenium, and tellurium [6]. To satisfy the increasing demands of such metals, it is usually not economically feasible to directly mine them due to their scarcity. Instead, further supplies may be found through increased host metal production, additional processing circuits to recover by-product metals, improved recovery efficiency, and recycling [5,6].

Again, these measurements are only implementable if they are economically profitable for related mines and smelters. According to Indium Corporation, only indium with 100 ppm or higher concentration in zinc ore is recovered as a by-product. The final amount of indium metal produced by the smelters only counts for roughly 30% of total indium mined [7]. The unit production cost for by-product indium was assessed to be 1549.55 CNY per kg by a Chinese smelter during 2006 [8]. Meanwhile, NREL deducted that the average production cost for indium from the proposed Mount Pleasant, Canada, mining project would be $288 USD/kg with an extra capital cost of $90 USD/kg per year over a 10-year production period [9]. Therefore, to address the issue of by-product metal supply, it is crucial to not only consider by-product metal production capacity but also economical concerns of individual suppliers.

Since each of the by-product metals has its own dependency and criticality, rather than creating a generalized model, this research focuses its efforts on indium. The indium market is a typical by-product metal market with volatile price and relatively low global consumption level compared to the host metal market. During 2016, global indium consumption is estimated to be 1430 t [10], and the leading consumption is the production of indium-tin oxide (ITO). Indium is also used for alloys, semiconductor materials, and CIGS solar cells. Since indium has a small market, the price of indium is easily impacted by supply–demand balance. Before 2003, indium price stayed low at $200 USD/kg due to cheap supply from China matching the demand of ITO production [3]. However, as Chinese mines and smelters reduced their production due to new environmental regulations, indium price was pushed to 1000 $/kg during the 2005. The market is also fragile in regard to investment operations. Beginning in 2011, Fanya Metal Exchange tried to manipulate indium prices by stocking large amounts of indium [10]. This resulted in increases of both indium price and indium supply [11]. However, after Fanya's collapse, a stock of roughly 3,600t indium metal was obtained by the Chinese government, and the international indium price collapsed from $705 to $345 USD/kg, and the price has remained low since then [11].

Meanwhile, with the rapid development of solar cells, CIGS thin film had become a noticeable source of indium consumption. USGS suggested that a total of 40 t indium was used for CIGS production in 2016 and the total CIGS market size was 1.5 GW [12]. Although CIGS accounts for only 2% of the global PV module market share, the annual addition of solar PV is projected to be 360 GW in 2050 by IRENA [13]. Even if CIGS maintains its current market share, the annual indium demand would be 200 t under such projection. Thus, CIGS production would induce new indium demand in addition to the ITO industry.

Such a situation certainly draws the attention of various researchers. A brief literature review is provided in the following chapter to summarize existing efforts and identify research gaps.

3.2 Literature Review

To illustrate the nature of indium market, research was conducted focusing on market of by-product metals. Several efforts were made to understand price change trends of by-product metal markets [14,15,16,17]. Fizaine et al. discussed the relationship between by-product metal and host-metal production using regression and various statistical test tools. Afflerbach et al. established a two-stage competition market model for various host metals and by-product minor metals. Redlinger et al. discussed by-product metal price velocities using a regression model. Fu et al. established an ARDL regression model for indium and other minor metals to link indium supply with various economic parameters. These reports provided insights on the behaviors of by-product metal prices using various optimization or regression models and linked them with various factors, especially with production and price of primary metals. The NREL indium report also provided economic assessments of indium production cost, price, and supply curve based on the Monte Carlo method [9].

Some researchers also dealt with minor metal reserves. Both USGS and NREL reports provided estimations on indium reserves of roughly 15,000 t [9,12]. A three-part research report summarized current assessment of minor metal reserves and specifically applied a new investigative method to assess indium reserves [18,19,20]. The research estimated total indium reserves to be as much as 356,000 t (without assessing economic feasibility).

Meanwhile, research was conducted to assess the impact of photovoltaics technology on by-product metal demand. Several reports focused on projections of by-product metal demands induced by CIGS solar panels [21,22,23]. Kavlak et al. discussed indium demand projection for CIGS indium consumption based on least square regression over historical growth rate. Nassar et al. discussed projected U.S. CIGS demand for indium based on future parameter estimation. Stamp et al. discussed different indium demands under various energy scenarios using system dynamics modeling. Moreover, to deal with the price change caused by possible supply deficit, the price impact of indium on both ITO and solar PV industries was reported. It is reported that flat panel industry is unlikely to be impacted by Indium price increase [24]. Candelise et al. discussed critical metal price impact on thin-film solar panels using cost analysis [25]. A system dynamics model with price elasticities and a mixed integer linear programming model that optimized global production cost were also employed to analyze the indium supply–demand balance [26,27].

Currently, end-of-life recycling of indium is not feasible due to economic constraints. Research has been conducted to explore the possibility of recovering indium from waste LCDs [28,29,30]; however, economic assessments performed on indium recycling from LCDs show that the result is not favorable under current indium price and recycling cost [31,32].

The recycling of thin-film photovoltaic wastes was also discussed by several researchers. Marwede et al. discussed the potential cost of CIGS thin-film recycling [33]. McDonald et al. discussed the possibility of offsetting recycling cost by charging the waste handling cost to producers or end users [34]. Liu et al. discussed the cost–benefit analysis to recycle photovoltaic model in China including CIGS model [35]. Several recent lab phase indium end-of-life recycling methods are also being developed [36,37,38].

It should be noted that most of the works mentioned analyzing indium supply–demand balance are conducted from a top-down point of view. However, the by-product metal market is in fact a competing market, and individual supplier decision may impact the overall by-product metal supply and price [14]. Thus, a bottom-up approach to model indium market competition sheds new light on the supply–demand balance of the material.

Additionally, although research has been conducted on indium supply potential, few works are driven by cost–benefit analysis. In fact, the current primary indium recovery efficiency is projected to be 17%, as large portions of indium material were either not sent to smelters or not refined by smelters due to economic considerations [9]. Therefore, research focused on the profit-driven behavior of indium producers would help to better understand the market and the supply of indium under different price and demand conditions.

3.3 Model Description

3.3.1 Model Objective and Implementation

This model aims at simulating a competitive oligopolistic indium metal market based on Cournot equilibrium between 2008 and 2050 with dynamic indium demand inputs. To demonstrate the heterogeneous nature of indium producers in the market, this research employs agent-based modeling as a tool. Agent-based modeling is comprised of autonomous, interreacting agents that act under certain environmental setting [39]. Numerous studies have already adopted the method to investigate similar cases, such as metal networks [40], electricity markets [41], and rare earth markets [42].

The time step for the simulation model is 1 year. During the simulation, while ITO still remains a major demand of indium, the emerging demand from CIGS solar PV technology requires additional indium supply. This model presents simulation result of dynamic supply–demand balance under different assumptions of future market and possible uncertainty factors. The result demonstrate potentials for possible bottleneck of indium supply and identify whether the economic considerations of producers are the key factor for such a supply shortage. For this purpose, global model boundary and assumptions are first determined. Then, the behavior of agents, including multiple supply agents imitating indium smelters and a demand agent deriving future demands, are defined. After that, the necessary parameters are either derived from historical data or calibrated to fit the model to historical results. Meanwhile, verification and validation of the model are conducted. Finally, different scenarios are implemented to illustrate uncertainties of the future. The Repast Simphony toolkit based on JAVA was used to implement the model [43].

3.3.2 Assumptions and Boundary of the Model

Although agent-based modeling is by nature microscopic, it is not possible to include all details of system and agents. Therefore, it is vital to define a proper boundary for the model.

The model defines each time step of the indium metal supply market as a competitive oligopolistic market with complete information. Each agent in the model resembles a primary indium metal producer and is rational for determining the production. The model assumes that all agents are also myopic and determine their production only based on maximum profit of current time step. Meanwhile, it is assumed that all production exceeding demand is sold at current price to a global dealer and is stocked for possible future demand. Secondary production of indium metal, mostly coming from in-process recycling of off-target ITO, is considered as a reduction of primary indium demand as per the opinion from Lokanc et al. [9]. At the same time, the model assumes that each zinc metal producer retains their market share for the duration of simulation.

For the demand side, this model considers ITO as a major consumer, which currently accounts for 83% of global indium consumption [44]. CIGS thin-film solar PV, although accounting for only 1% of current global indium consumption, is projected to have a major growth in the future and is modeled as a potential source of indium demand.

It should be noted that two rapid growing markets involving indium consumption, LED, and InP semiconductors are not modeled in detail by this model. Based on reports from USGS, total global LED production in 2014 consumed 85 kg of indium [45]. According to DOE forecast, the total of LED lighting systems installed in U.S. during 2014 was 215 million and will be roughly 7500 million by 2035 [46,47]. Based on both estimations, indium consumption by LED will be roughly 3 t by 2035, assuming that LED global production growth is on par with U.S. LED lighting market. Meanwhile, although InP wafer market is projected to grow from $77m to $162m between 2018 and 2024 [48], the amount of indium consumed by the semiconductor is estimated to be less than 1 t [49]. Therefore, together with other applications of indium, these portions of indium consumption are modeled as a constant.

3.3.3 Model Formulation

A total of 25 supply agents representing active indium metal producers listed by USGS indium minerals yearbook are included in the model [12]. A global demand agent is also created to manage demand, stock, and price changes. This agent represents a centralized indium market that adjusts global indium price based on supply–demand balance at each time step and exchanges decision-critical information with the rest of the model. The data dependency chart is shown in Figure 3.1.

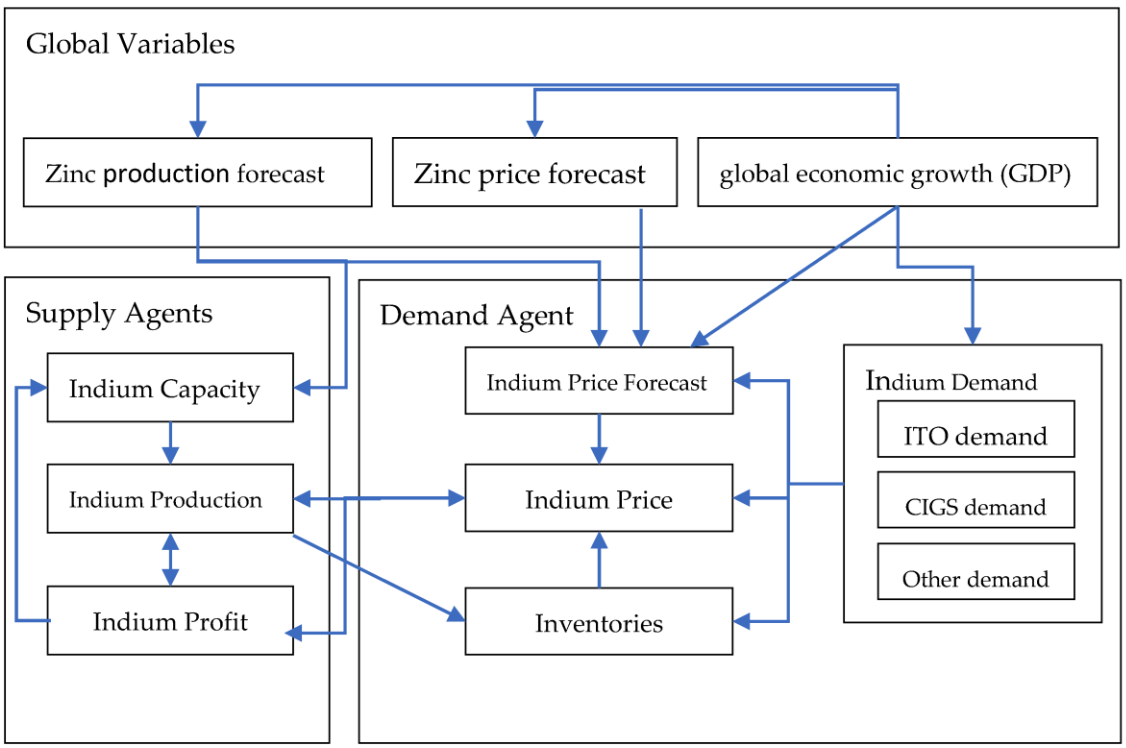

Figure 3.1. Data dependency chart

The simulation starts at 2008, and the first 11 years are used as a warm-up period and for model validation. Since minimum resolution of indium data available is at annual level, the simulation time step is set to 1 year. The simulation ends by 2050. Specific agent behaviors and parameter setting are discussed in the following sections.

For each time step, global agent follows processes shown in Figure 3.2. Variables are first generated based on input data including zinc total production, projected zinc price, and GDP growth rate. After that, indium demand of current time step is generated, and a long-term indium price forecast is made based on zinc production, zinc price, indium demand, and economic growth rate. Indium capacity is also adjusted if a supply agent is zinc based and its zinc production changes. After that, a Cournot market competition problem for current time step is generated based on given data.

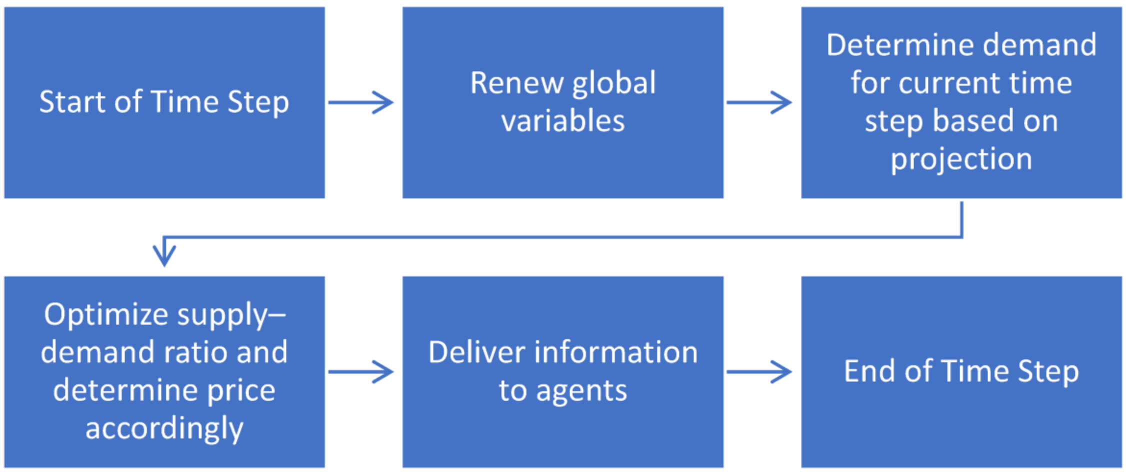

Figure 3.2. Model flow chart

To ensure the existence of the Nash equilibrium, the model assumed a decreasing marginal revenue and an increasing marginal cost for all agents. The formulation for time step t is shown below:

$$\max P_t(q_{-i_t} + q_{i_t})q_{i_t} - C_{i_t}(q_{i_t}) \quad for\ i = 1,2, \dots, n$$
$$such\ that:$$
$$0 \le q_{i_t} \le k_{i_t} \quad for\ i = 1,2, \dots, n$$

where q_{i_t} is the production of agent i at time t; q−it is the total production of all other agents at time t; $P_t(q_{-i_t} + q_{i_t})$ is the global price function at time t; $C_{i_t}(q_{i_t})$ is the cost function for agent i at time t; and k_{i_t} is the production capacity for agent i at time t. This model assumes a quadratic production cost function and a fixed unit capital cost. Detailed parameter setting is listed in Appendix: Detailed Model Formulation.

It is assumed that indium price is both influenced by long-term predictions and short-term supply–demand ratio. The price function can be formulated as follows:

$$P_t(q_{-i_t} + q_{i_t}) = e^{-\beta ln r_t} p_{f_t}$$
$$where\ r_t = \frac{q_{-i_t} + q_{i_t} + i_{t-1}}{d_t}$$

where p_{f_t} is the long-term predicted price and r is the current supply–demand ratio calculated by current production level $q_{-i_t} + q_{i_t}$ inventory level i_{t-1}, and demand d_t at time t. $\beta > 0$ is the impact parameter of supply–demand ratio over the price and is calibrated based on historical data. Long-term predicted price is based on input from historical data utilizing ARDL regression. The predicted price is determined by zinc production, zinc price, current indium demand, GDP growth, and indium price from previous years.

Once the Nash equilibrium problem is solved, the model calculates current global inventory level based on total production and demand, which is:

$$i_t = \max(i_{t-1} + q_{total_t} - d_t, 0)$$

The model then continues to the next time step after agent behaviors are determined.

3.3.4 Indium Demand Projection

The demand projection is divided into three parts: ITO, CIGS, and others. ITO demand projection is assumed to follow a logistic curve based on year-wise deduction after 2018:

$$d_{ito\_total}(t) = \frac{K}{1 + e^{-G(t-t_0)}}$$

where the curve parameters K, G, and t_0 are determined by non-linear regression from existing ITO production and projection data between years 2011 and 2020 [50]. Since the USGS report estimated ITO production has remained the same in recent years [12], the model assumes that the market is near a saturation state.

Meanwhile, a large amount of secondary indium is reclaimed by recycling ITO off target during the spurring process and is returned into ITO production loop. USGS assumed that a total of 1200 t/year of secondary indium was recovered from ITO recycling during 2016 [12]. However, based on the opinion from NREL, this number contains indium recovered from multiple loops [9]. Thus, calculation is conducted to determine the percentage of primary indium needed, which utilizes the same approach from NREL report. The ITO spurring loop data is shown in Table 3.1. A 30% efficiency for the spurring process and a 90% efficiency for the recovery process are assumed here [51].

As a result, to recover 1200 t of indium, 705.45 t of primary indium should be fed into the loop. Thus, a deduction factor of 2.70 is applied to total indium demand from ITO, indicating that only 37% of total indium consumption by ITO comes from primary production.

Table 3.1. ITO Loop Table

Cycle	**1**	**2**	**3**	**4**	**5**	**6**	**7**	**8**	**9**	**10**	**11**	**12**	**13**	**14**	**15**	**Total**
Units available (t)	705.45	444.43	279.99	176.40	111.13	70.01	44.11	27.79	17.51	11.03	6.95	4.38	2.76	1.74	1.09	1904.76
Units deposited (t)	211.64	133.33	84.00	52.92	33.34	21.00	13.23	8.34	5.25	3.31	2.08	1.31	0.83	0.52	0.33	571.43
Units for recycling (t)	493.82	311.10	196.00	123.48	77.79	49.01	30.88	19.45	12.25	7.72	4.86	3.06	1.93	1.22	0.77	1333.33
Units recycled (t)	444.43	279.99	176.40	111.13	70.01	44.11	27.79	17.51	11.03	6.95	4.38	2.76	1.74	1.09	0.69	1200.00
Units lost (t)	49.38	31.11	19.60	12.35	7.78	4.90	3.09	1.95	1.23	0.77	0.49	0.31	0.19	0.12	0.08	133.33

For CIGS demand, three different parameter sets are generated to represent different projections on thin-film solar PV market [52,53]. Historical data are then fed into the three scenarios to generate separate logistic demand curves similar to ITO demand. The parameters are listed in Table 3.2.

Table 3.2. CIGS Scenarios

Parameter	**Pessimistic**	**Base**	**Optimistic**
Layer thickness by 2020 (μm)	1.2	1.0	0.8
Layer thickness by 2050 (μm)	0.8	0.8	0.8
Annual production by 2050 (GW)	17	54	105
Efficiency by 2020	14%	15.9%	16.8%
Efficiency by 2050	22.9%	22.9%	22.9%

A layer thickness of 1.6 μm and efficiency at 11.2% in 2008 were previously reported [52]. The model assumes that these two parameters will shift linearly toward the 2020 assumption listed in the table under three different scenarios and then shift toward 2050 assumption under different rates. The report also gave an indium consumption estimate of 83 kg per GW of CIGS manufactured in 2008, which decreases accordingly due to reduce layer thickness and improve efficiency.

For other demands of indium, the simulation assumes that the demand remains constant at 2012 level as reported by NREL [9].

3.3.5 Supply Agent Behaviors

The supply agents include 25 primary indium producers listed by USGS, except for producers who have already terminated their operations [12]. Agents are assigned with several attributes. Detailed discussion on the value and deduction of such attributes is presented in the Appendix. Based on USGS information, there are three types of indium producers. Out of the 25 producers in the model, three agents produce indium based on primary metal other than zinc. Five agents produce indium from secondary source (mine residues, primary metal refinery residues, etc.) and purchase indium-containing materials from a third party. The remaining seventeen agents are zinc based.

For each time step, supply agents make several decisions following the flow chart in Figure 3.3. First, the agents calculate any production cost and capital cost changes, either due to inflation or expansion. After that, zinc-based agents decide their zinc production of the current step. The total amount of zinc capacity taken into consideration by this study is only 1/3 of global primary zinc capacity [54]. The zinc market is therefore treated as a market with perfect competition and optimized accordingly [15]. The formulation of the optimization problem is listed as below:

$$\max p_{z_t} q_{zj_t} - \left(c_{zj_t} {q_{zj_t}}^{a_z}\right) q_{zj_t} \quad for\ j = 1,2,\dots,17$$

$$such\ that:$$

$$0 \le q_{zj_t} \le k_{zj_t} \quad for\ j = 1,2,\dots,17$$

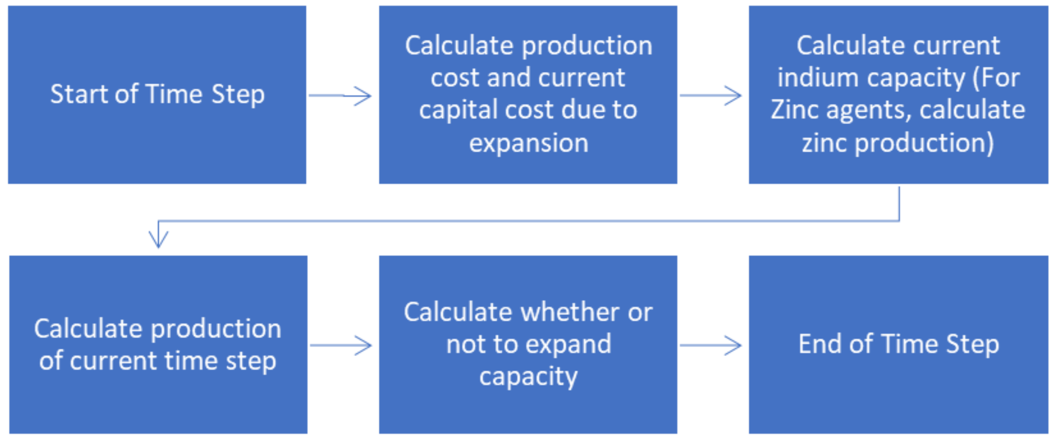

Figure 3.3. Supply agent flow chart

Each agent calculates its actual indium capacity for each time step based on both facility capacity and indium content delivered to the facility. Non-zinc-based primary producers have their available indium raw material increasing each year in accordance with GDP growth. Zinc-based primary producers calculate their indium content based on zinc production and unit indium content of zinc-concentrate. Secondary producers have no indium content limit as they can always adjust the amount of raw material they bought.

The agents then decide whether they want to expand their indium production capacity by comparing possible profit against capital cost. The agent only expands their capacity if they have already utilized 90% of their current capacity. Total projected profit is calculated using a moving average of price in 3 years (pavg) and a deduction rate (rdiscount) of 8% [58] over a 10 year period. The agent solves the following local optimization problem:

$$\max \sum_{i=1}^{10} \frac{p_{avg} q_{i_t} - C_{i_t}(q_{i_t})}{(1 - \mathrm{r}_{discount})^i} - c_{ei_t} k_{i_t}^* \quad for\ i = 1,2, \dots, n$$

$$such\ that:$$

$$0 \le q_{i_t} \le k_{i_t} + k_{i_t}^*$$

$$0 \le k_{i_t}^* \le k_{i,max_t} - k_{i_t} \quad for\ i = 1,2, \dots, n$$

where q_{i_t} is the projected production, $C_{i_t}(q_{i_t})$ is the cost function, and one year of construction period is assumed based on refinery report [58]. c_{ei_t} is the unit expansion cost, k_{i,max_t} is the maximum possible capacity calculated based on indium content, and $k_{i_t}^*$ is the capacity expanded. After an expansion, the expansion cost is averaged to a 10 year period as an increased fixed cost, and the indium capacity is increased after the construction period to reflect the expansion.

3.3.6 Validation and Verification

The verification and validation of agent-based model is vital [59]. Verification is to prove that the model itself is valid and correctly runs as intended, and validation is to prove that the model correctly and robustly reflects situations in the real world.

To verify the model, each subsystem of the model is tested individually to ensure that they work as proposed. Codes are carefully examined to ensure they work as intended. A dynamic test of the whole system with a different set of parameters is also conducted, which also serves as a sensitivity analysis for validation of the model.

To validate the model, several approaches are made. First, the model runs under a real-world dataset between 2007 and 2018, and several outputs are compared with the corresponding historical data. The result is shown in Table 3.3.

Table 3.3. Historical data validation

Output	Historical Data	Modeled Result	Reference
Stock after investment (t)	3629.6	3200.4	[44]
Price between 2016 and 2019 ($/kg)	240,225,291,210	283,268,267,276	[60]
Production between 2016 and 2019 (t)	759,680,714,741	851,694,598,646	[60]

The model also runs under a set of extreme parameters, including large demand, zero demand, and a large stock. The extreme test was used to ensure that the model reflects correctly under such conditions.

Finally, a sensitivity analysis is conducted to ensure the robustness of the model. The tornado graph of such analysis is shown in Figure 3.4

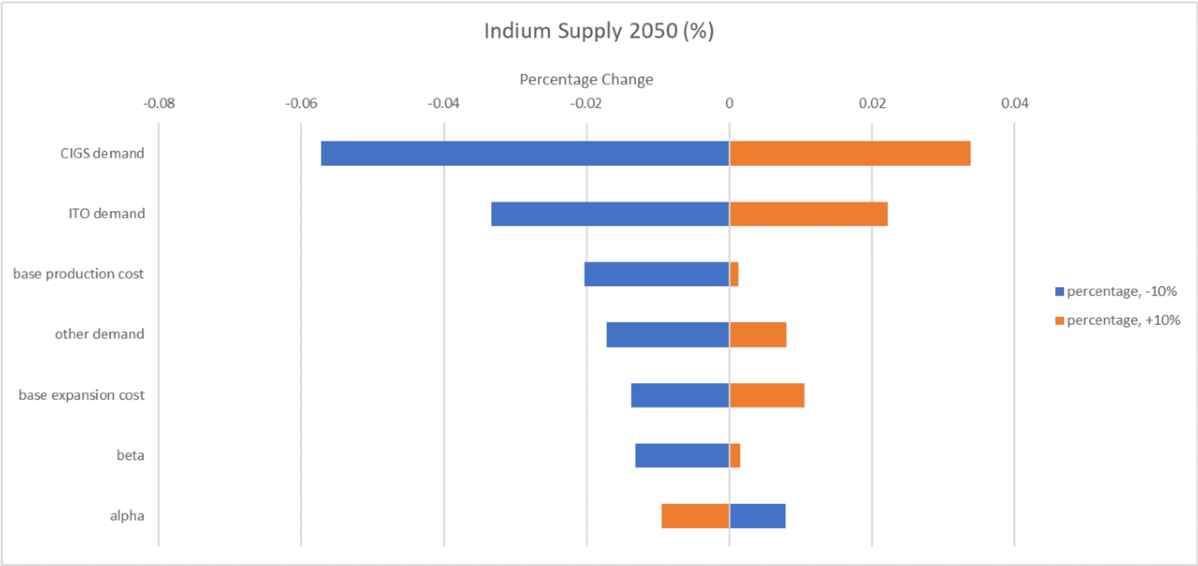

Figure 3.4. Sensitivity analysis

Overall, the model correctly reflects historical production and price trends, while maintaining a good robustness considering parameter inaccuracy.

3.4 Results and Discussions

The result under the base case is shown in Figure 3.5, Figure 3.6 and Figure 3.7. Under the base case, the smelters are able to provide enough supply for future primary indium demand in a competitive market. With enough demand, the existing stock is gradually decreased to the level of annual indium production. Indium price is mostly pushed by the inflation rate, as the final price is equivalent to 452 $/kg in 2016 dollar. Although usually increasing, indium capacity decrease between years can be observed mainly due to decreased zinc primary production.

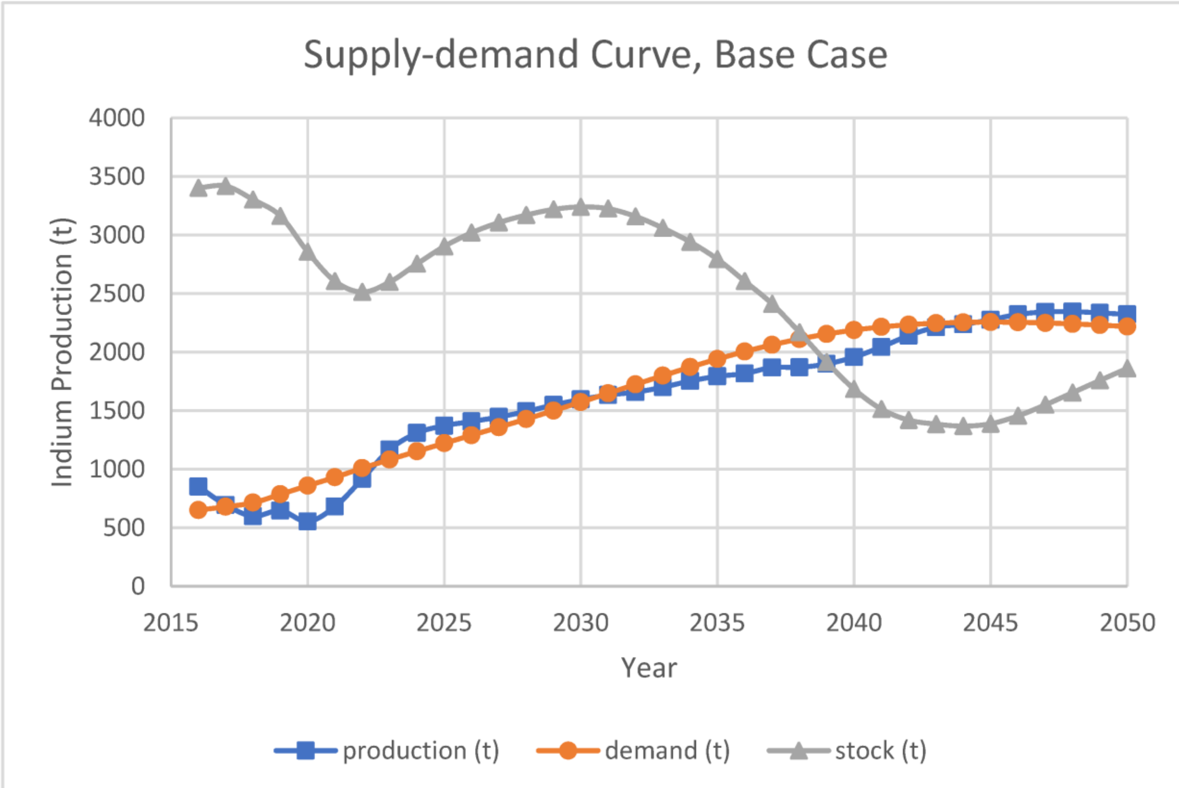

Figure 3.5. Supply–demand balance, base case

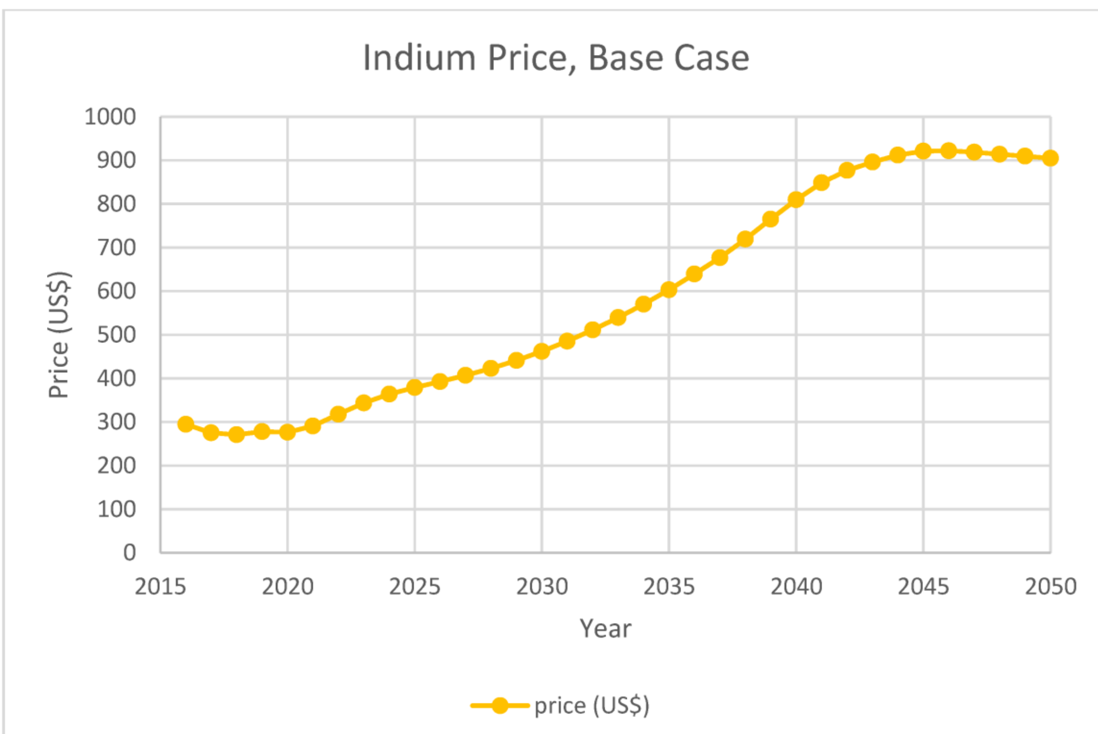

Figure 3.6. Indium price, base case

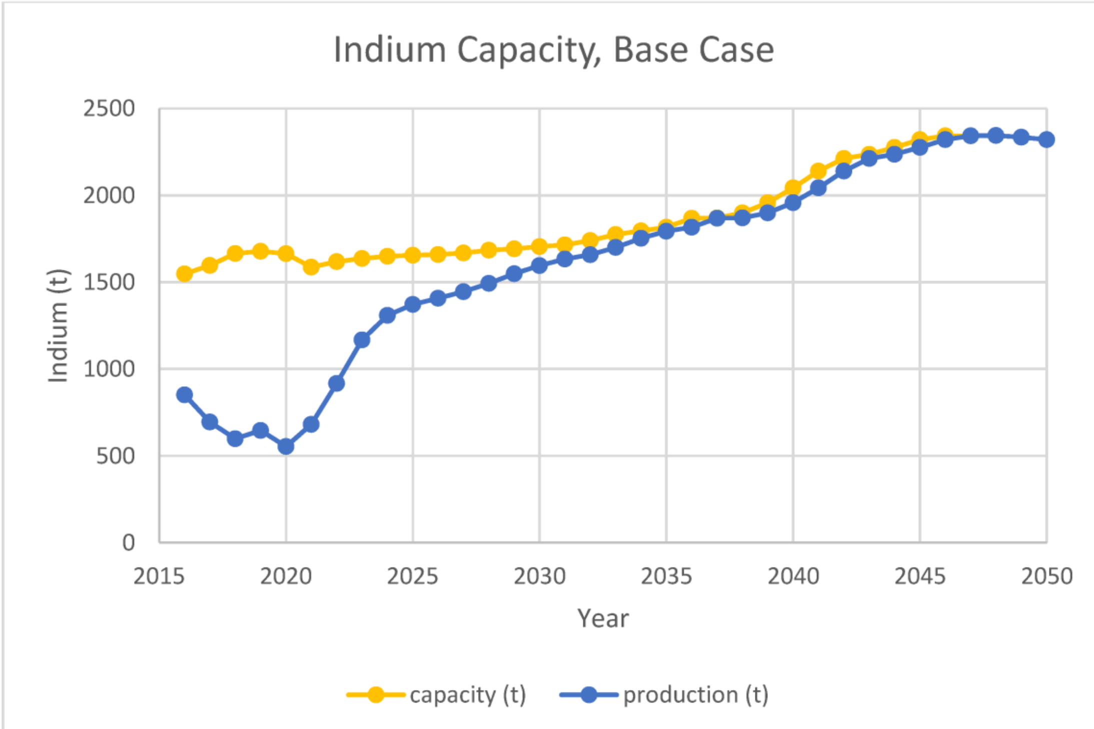

Figure 3.7. Indium production capacity, base case

For pessimistic and optimistic CIGS projection scenarios, the results are shown in Figure 3.8, Figure 3.9, Figure 3.10, Figure 3.11, Figure 3.12 and Figure 3.13, respectively. The lack of demand increase in the pessimistic case makes it difficult for the high stock level to be consumed. As a result, indium price remains low. In addition, the capacity of indium smelters is not expanded as indium demand can already be satisfied. For the optimistic case, a supply deficiency is predicted after 2040. Although indium price is high, the expansion of current facilities is at their limit under current indium recovery rate.

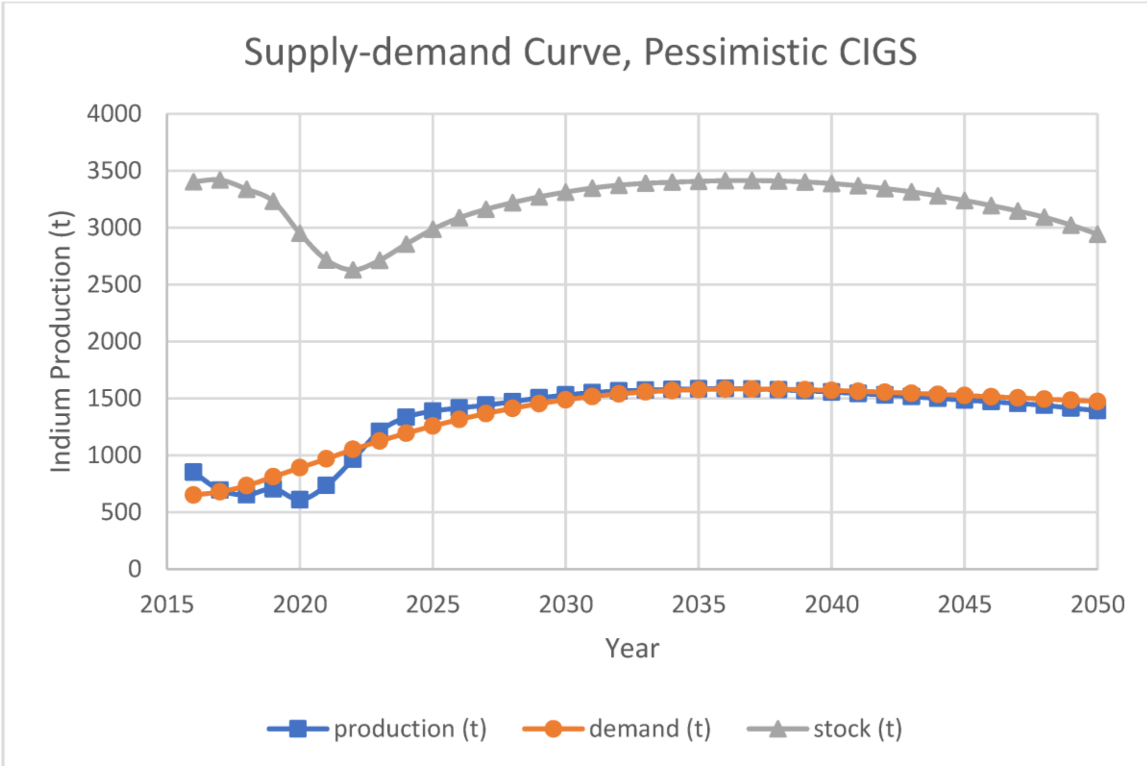

Figure 3.8. Supply–demand balance, pessimistic CIGS

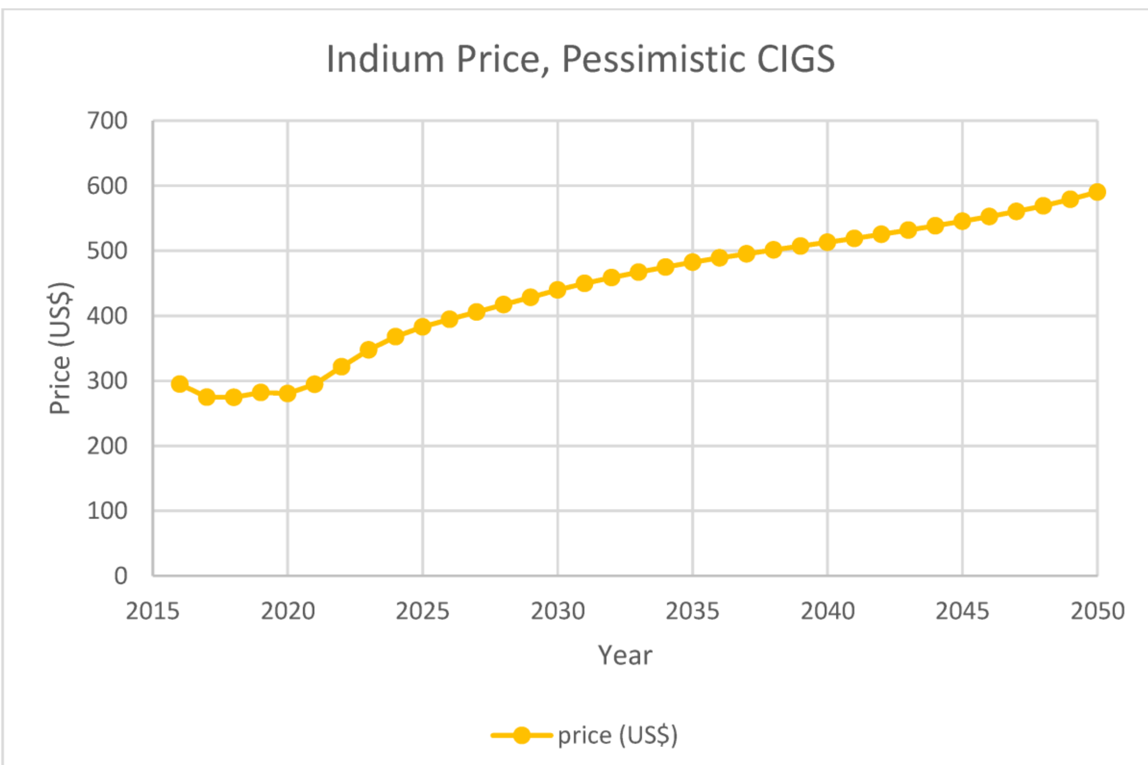

Figure 3.9. Indium capacity, pessimistic CIGS

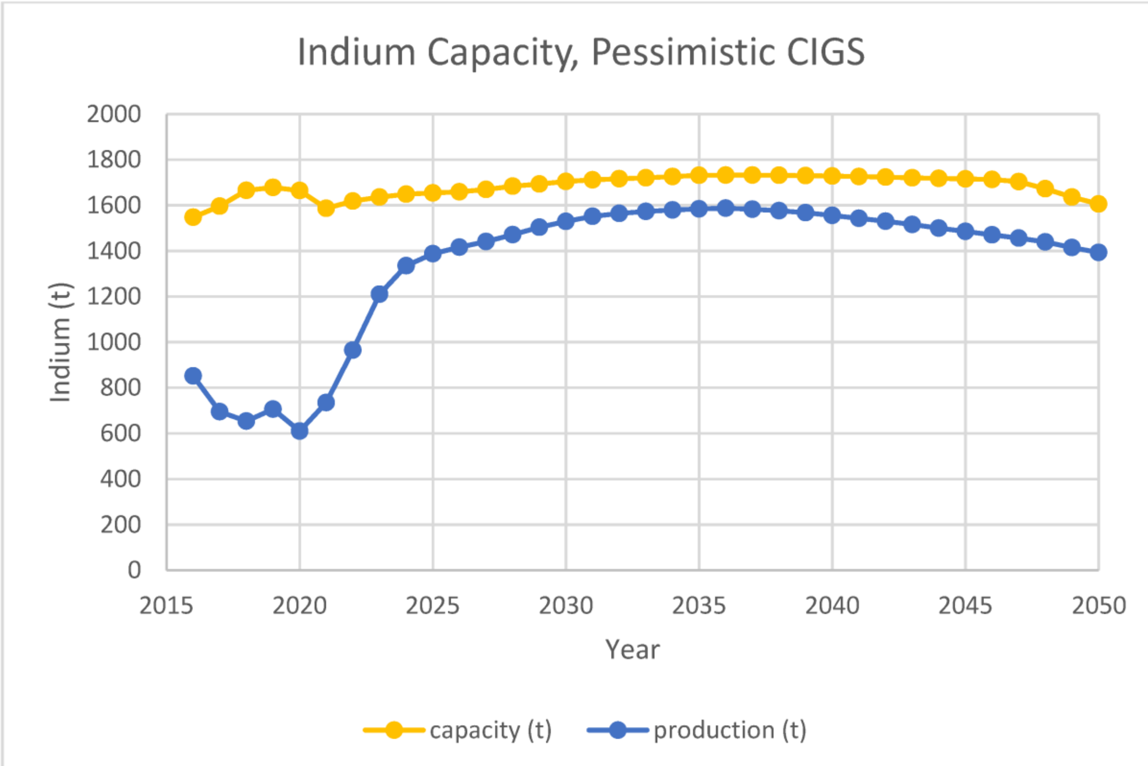

Figure 3.10. Indium capacity, pessimistic CIGS

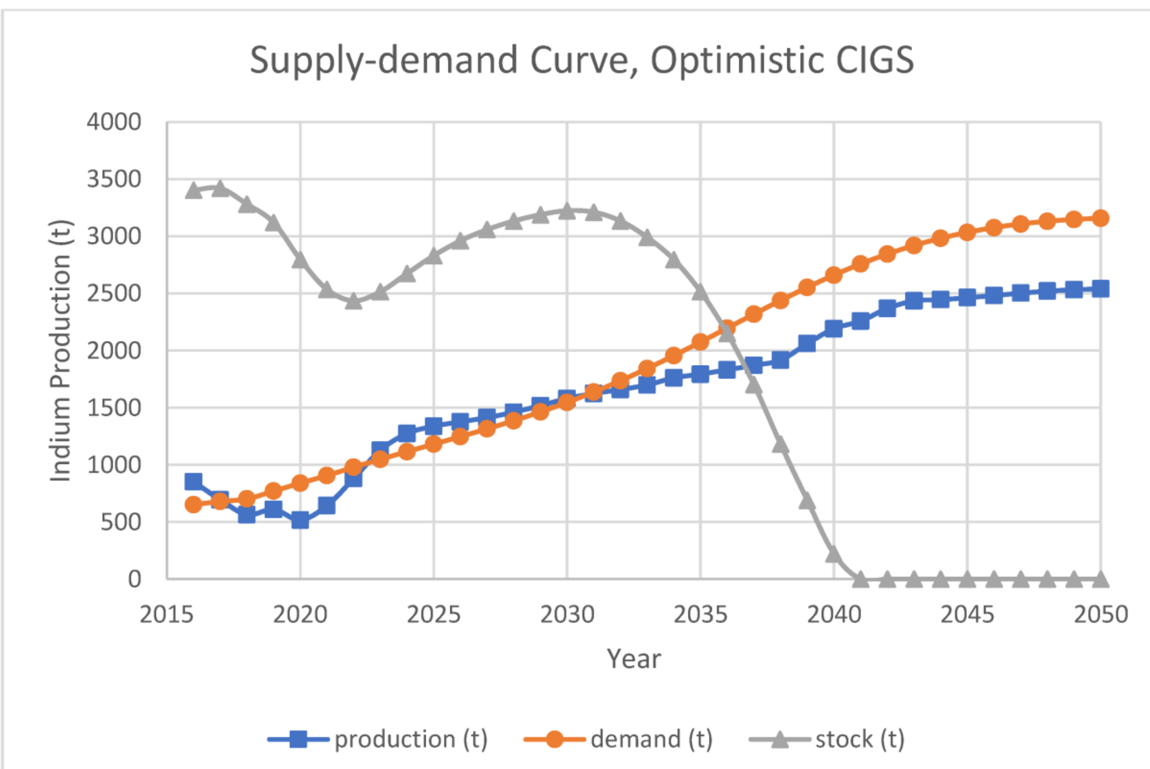

Figure 3.11. Supply–demand balance, optimistic CIGS

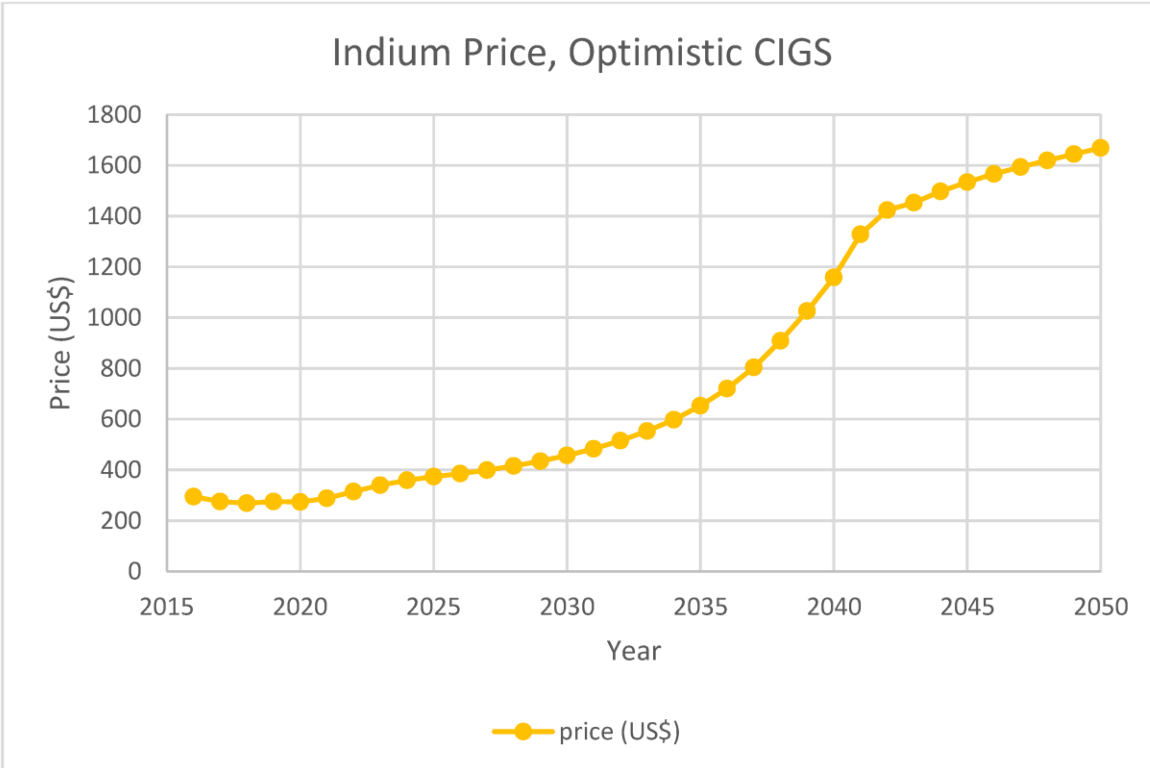

Figure 3.12. Indium price, optimistic CIGS

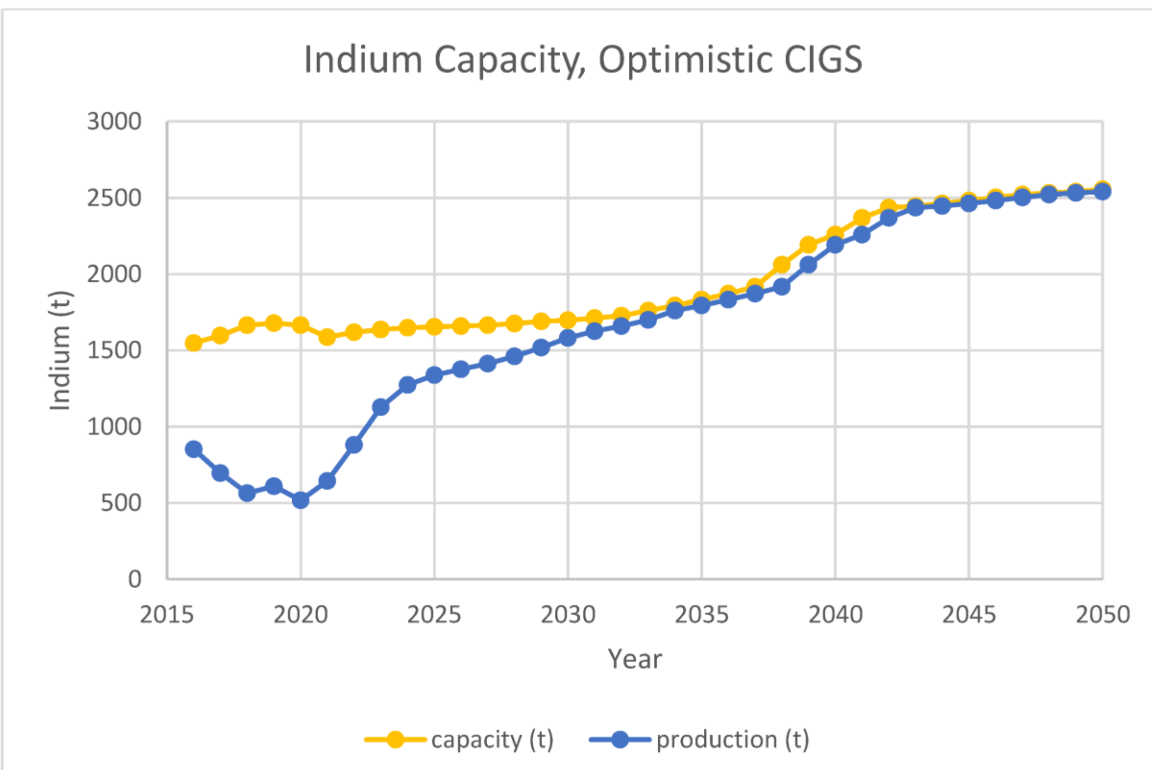

Figure 3.13. Indium capacity, optimistic CIGS

It is also interesting to see how indium extracting efficiency affects the supply. Two scenarios are set up to study such situations. The first scenario assumes that indium concentration in delivered ores starts to deteriorate over time. This scenario is established on the basis of the base-case scenario. This assumption follows Werner's indium reserve assessment [20]. The assessment includes many indium-containing resources with low indium ppm. Thus, in this scenario, after the proposed current reported deposits of 76,000 t is consumed, the average indium ppm deteriorates linearly to 100 (reported minimum economic feasible value) until a total 356,000 t of indium is mined. This reduces the maximum indium capacities for smelters and raises unit production cost. An overall indium ore-to-metal efficiency of 17% is assumed following Lokanc et al.'s estimation [9].

Another scenario assumes a possible indium recovery efficiency increase. This can include improved technology to recover more indium from ores into host-metal concentrates at mines, better recovery rate at smelters, or higher percentage of indium-containing concentrates sent to indium smelters. For the scenario setup, an efficiency of 68% is achieved at the end of simulation [9]. The efficiency increases linearly from 17% over time for each smelter after 2020. This increases the maximum indium capacity for smelters. The unit production costs for the smelters are also reduced. To better reflect the result, this scenario is set up based on optimistic CIGS scenario, where a supply shortage happens.

The results for both scenarios are shown in Figure 3.14, Figure 3.15, Figure 3.16 and Figure 3.17, respectively. It is apparent that efficiency of smelters is vital to indium supply. If the primary supply of indium-containing ore could not maintain current quality, supply shortage occurs. Meanwhile, improvements on indium overall efficiency are extremely effective, and indium supply with improved efficiency is sufficient to meet the optimistic CIGS projection demand.

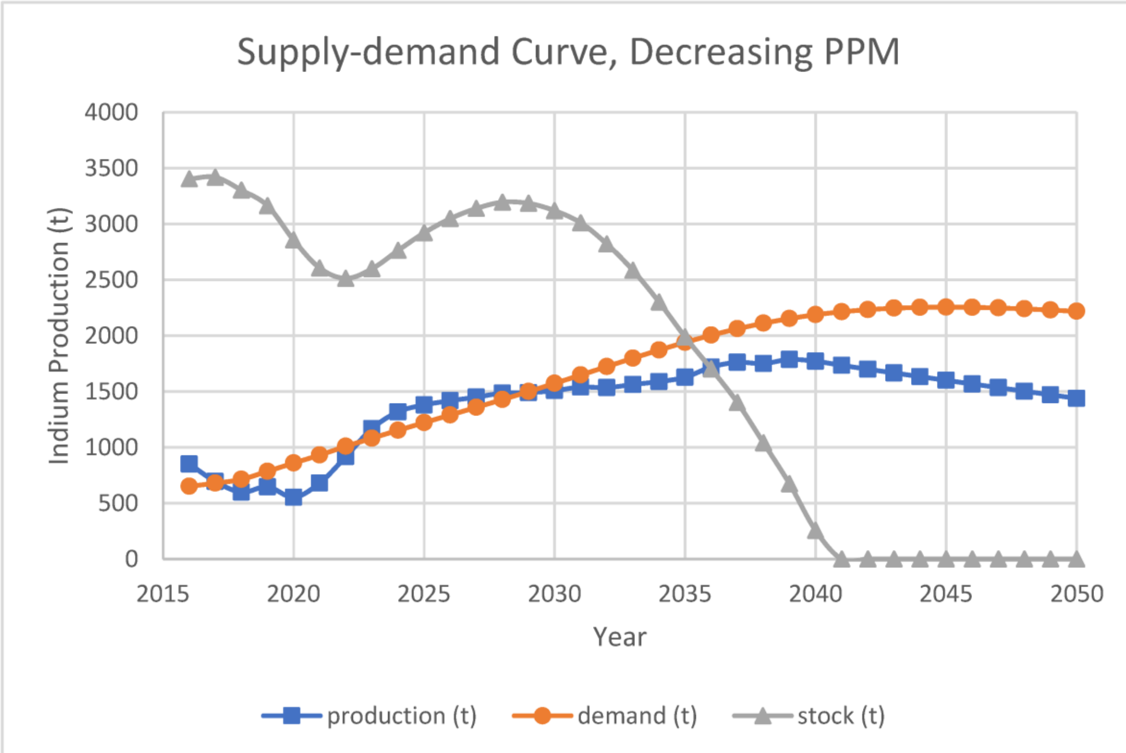

Figure 3.14. Supply–demand balance, decreased indium concentration

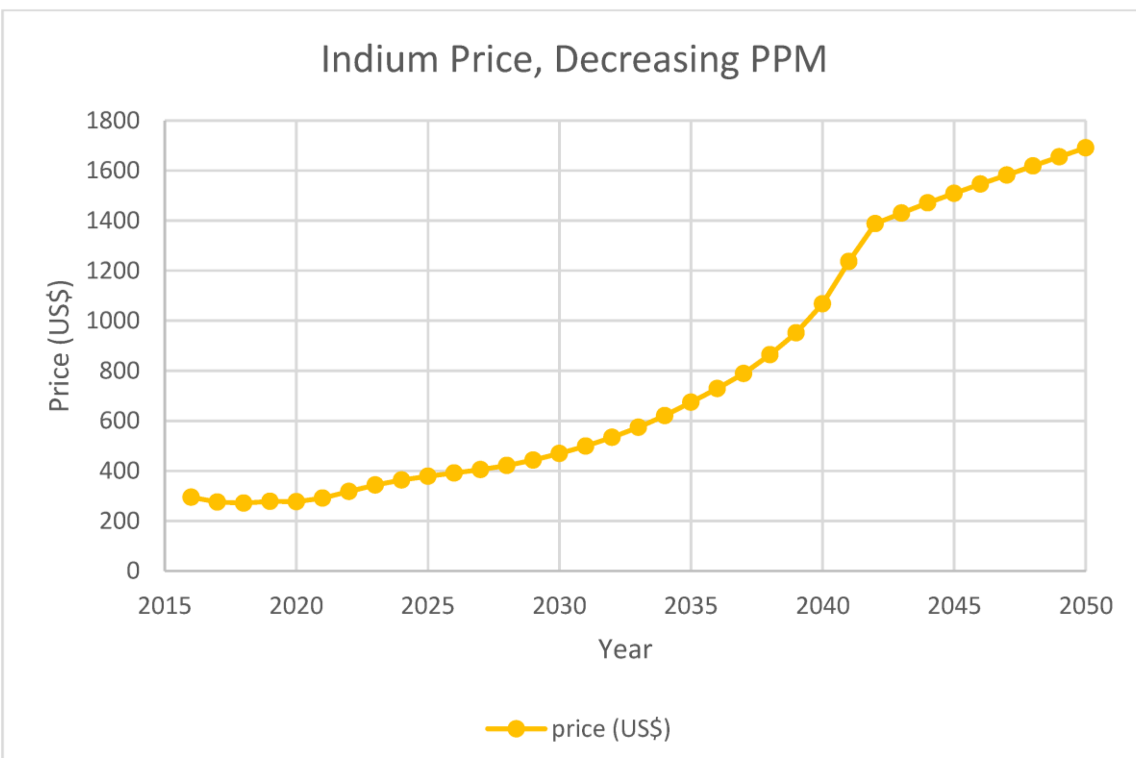

Figure 3.15.Indium price, decreased indium concentration

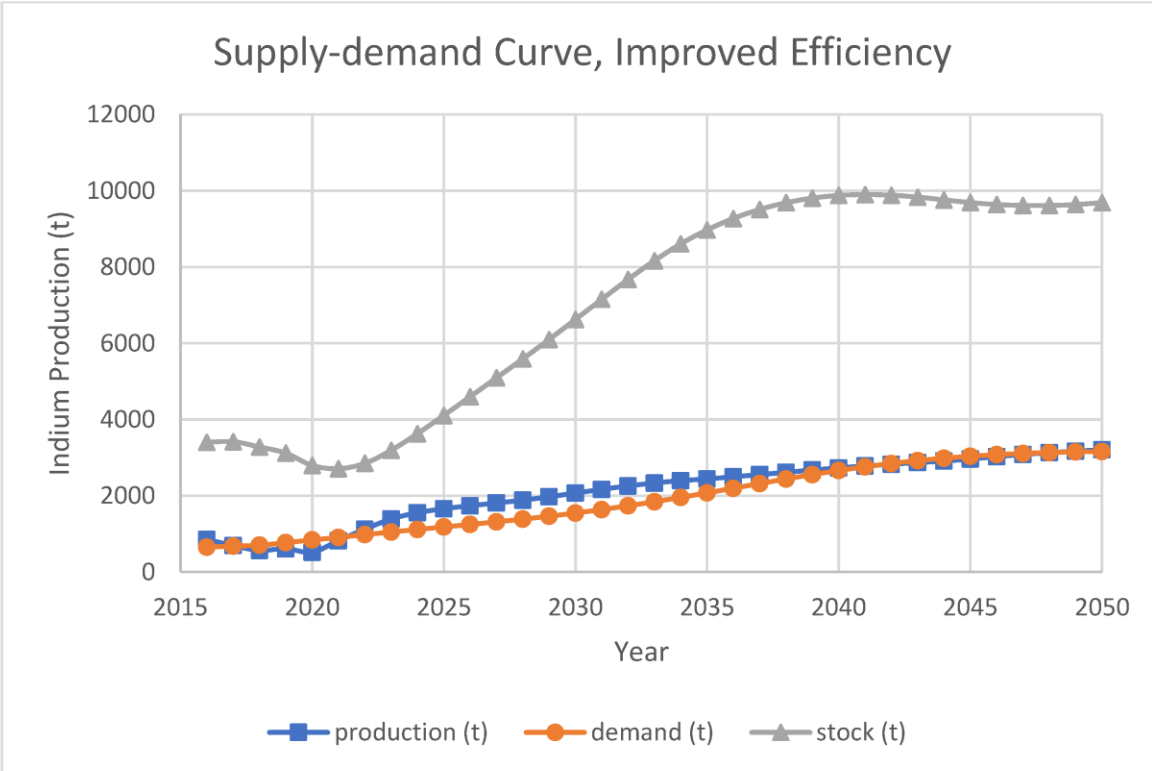

Figure 3.16. Supply–demand balance, improved indium efficiency

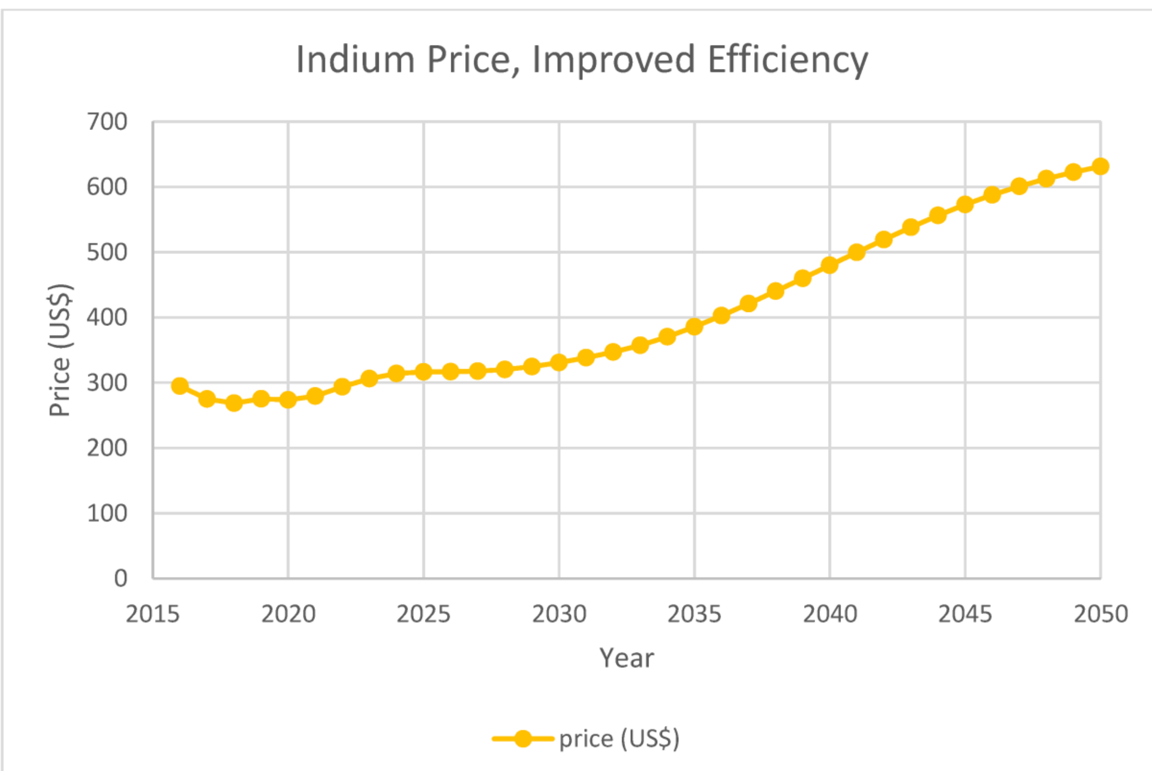

Figure 3.17. Indium price, improved indium efficiency.

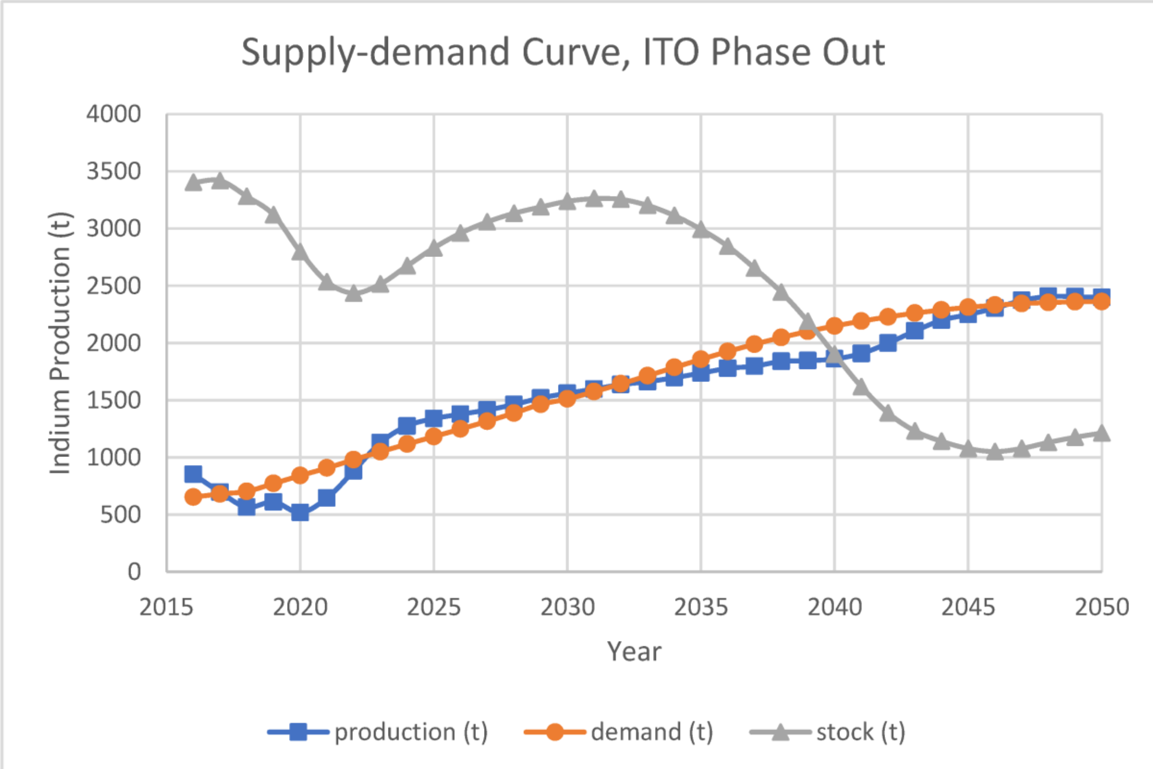

Figure 3.18. Supply–demand balance, ITO phase out

Another possible scenario would be the phase out of ITO technology. Since ITO might be substituted with carbon nanotube and graphene (Bernhardt, 2019), in this scenario, an ITO phase out will start happening at 2025 following a reversed S-curve. The result based on optimistic CIGS case is shown in Figure 3.18. A more apparent supply shortage is observed around 2040. Due to the phase out of ITO, the producers are not fully expanding their capacities until more demand from CIGS emerges, which causes temporary shortage before indium price is raised to attract facility expansion.

The above simulation result shows several interesting trends. The competition between producers helps to stabilize indium price at the cost of supply–demand gaps. The producers are unwilling to utilize full indium production capacities at a lower price even if there is surplus demand. Meanwhile, when the market is relatively stable, the production roughly meets the demand. Moreover, it may not be profitable for producers to continually expand indium production due to increasing marginal cost for indium production under this model.

The primary supply result from this research is also compared with previous predictions on indium demand, as shown in Figure 3.19. The demand outlooks from different research vary mainly because of different CIGS market penetrations. Under most cases, there is a gap between primary indium supply predicted by this model and predicted indium demands from other research. Part of the gap can be filled with secondary indium supply, mainly from in-process ITO production, which is roughly 1400 t by the end of simulation. However, for even higher indium demand penetration, as shown in the optimistic CIGS case from this research, it may be difficult to fulfill the gap solely with primary indium production.

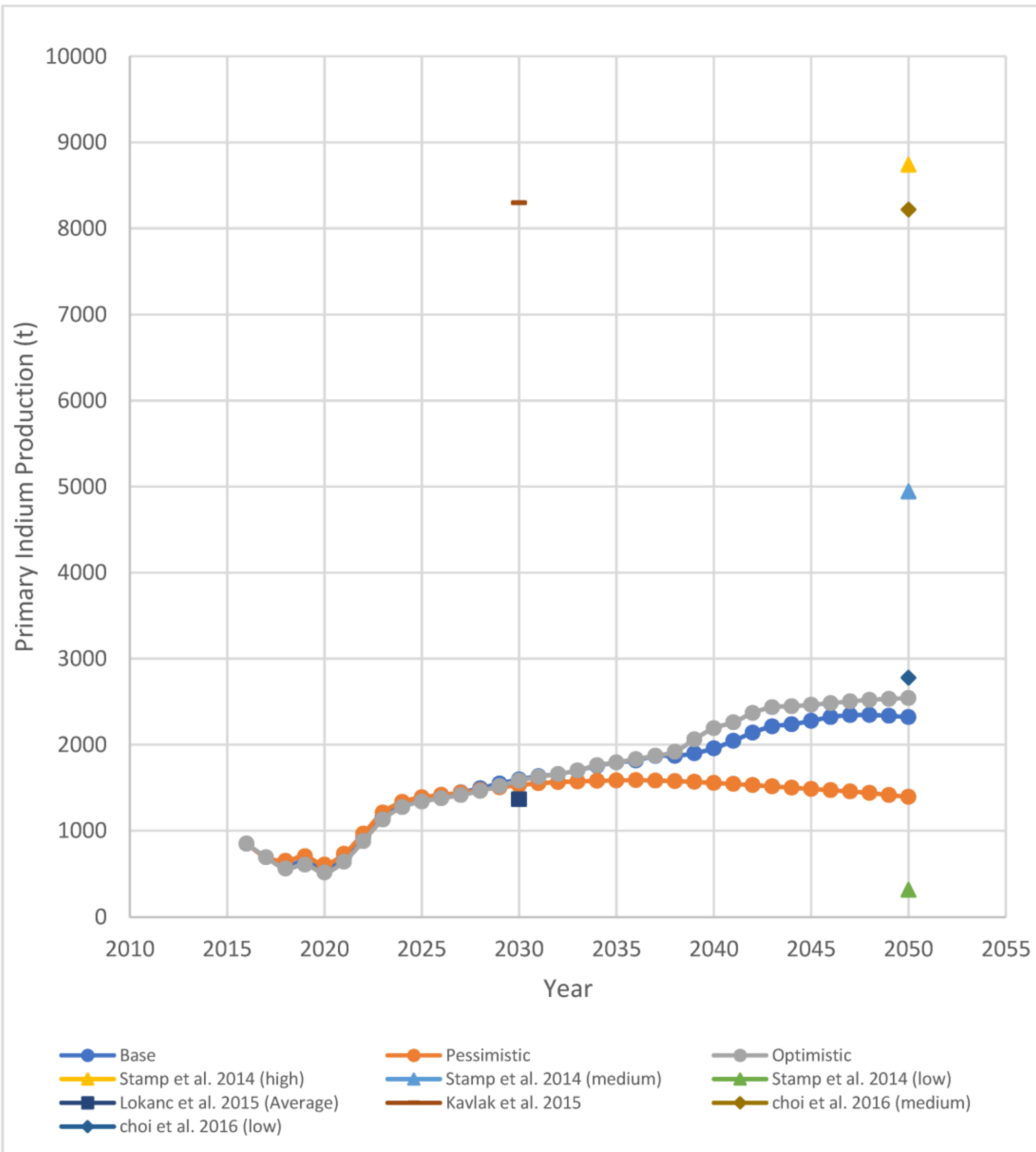

Figure 3.19. Primary indium supply vs. total demands

3.5 Conclusions and Future Research

Overall, this work established a competitive oligopolistic indium metal market model based on Cournot equilibrium using agent-based modeling method. Under base-case and low CIGS demand case of the model, supply–demand balance can be maintained by current market suppliers. However, if faced with higher demand from CIGS manufacturing, current suppliers are not willing to continue expanding their indium production due to increased marginal cost even with a supply shortage. There is also a delay between increased demand and increased indium capacities. The suppliers often wait until indium price is high enough before they expand their indium capacities. This can also cause temporary supply shortage. As a conclusion, the economic concerns of indium producers largely influence the indium supply–demand balance.

On the other hand, the availability of raw material with high indium concentration is vital to indium supply. If unit indium production costs increase due to the deterioration of raw material, the producers would not be willing to expand their production but rather try to maintain a high indium price to compensate the increased cost. A way to reduce such costs is to increase overall indium recovering efficiency, but it may require additional research and capital costs, which is not modeled in this work.

Current base model assumes that smelters can always acquire sufficient raw materials. However, this may not be true. As reported by Werner et al., current indium primary resource inferred is 356,000 t [20]. Although this seems sufficient to support demand described by the model, economic feasibility of each site for indium remains questionable.

Current work did not include other layers of indium supply chain. Important questions regarding indium-containing ores—if they hold sufficient indium, economic feasibility in their recovery, and complementary sources of indium supply—are still left unanswered.

Another possible source of indium supply is the recycling of end-of-life indium products. Currently, recycling mainly happens within the ITO production cycle. For end-of-life recycling, flat panel display is projected to be the largest source, for which cost-effective recycling methods are currently being developed [61]. According to the current literature review, ITRI technology developed a pilot recycling system with a cost of $2000 per ton of e-scrap processed [62]. However, only 750 grams of indium can be extracted from 1 ton of waste flat panel display, and the profit of indium is the lowest comparing to other products. Thus, indium is still a by-product in the end-of-life recycling process. As discussed prior, CIGS waste flow will become significant in the future since the average lifespan of current product is about 10–15 years [63].

3.6 Appendix: Detailed Model Formulation

3.6.1 Global Parameters and Variables

Global parameters are input parameters from outside of the model and are applied to each agent including demand agent and indium producer agents. Detailed description of each parameter is listed in Table 3.4. Average CPI and GDP growth are assumed based on respective values for recent years [64,65]. Indium primary production cost quadratic factor and indium price elasticity are calibrated by running the model from 2008 to 2018 with different parameter pairs ($\alpha \in [0,0.02]$ $(step = 0.001), \beta \in [0,1]$ $(step = 0.1)$). Modeled indium primary production and modeled indium price are compared with historical production and price data. Parameter pairs with least normalized squared error are selected as final model parameters.

Table 3.4. Global parameters

Parameter Name	Description	Data source
Indium primary production cost quadratic factor (α)	Quadratic factor for indium primary production cost function. $\alpha = 0.005$	Calibrated [8,44,58]
Indium price elasticity (β)	Indium price change factor in response to supply–demand ratio $\beta = 0.6$	Calibrated. [44]
GDP (GDP)	Global GDP annual nominated growth. (Data before 2020 are historical growth) $GDP = 3\%$	[64] Assumption
Inflation (CPI)	Most cost increases proportionally by inflation rate each time step. $CPI = 2\%$	[65] Assumption
Predicted zinc production ($q_{z,total_t}$)	Predicted total annual primary zinc production. (Data before 2020 are historical data)	[56,57]
Predicted zinc price (p_{z_t})	Predicted zinc price. (Data before 2020 are historical data, prediction extended from 2030 to 2050)	[55]

Global variables are variables aggregated among agents each time step. Detailed description of each variable is listed in Table 3.5. Global inventory each step is calculated by the following equation:

$$i_t = \max(i_{t-1} + q_{total_t} - d_t, 0)$$

Table 3.5. Global variables

Variable Name	Description	Data source
Inventory (i_t)	Global indium inventory level at time t. Initial value equals to 2008's total primary production capacity.	[12]
Indium primary production (q_{total_t})	Annual total indium primary production at time t. Initial value equals to 2008's total primary production capacity.	[12]
Indium predicted price (p_{f_t})	Long-term prediction of indium price based on ARDL regression at time t.	[44,55,57,60]
Indium price (p_t)	Modeled indium price after competition at time t. Initial value equals to 2008's historical price.	[60]
Indium demand (d_t)	Modeled indium primary demand at time t. Initial value equals to 2008's historical primary demand.	[44]
Supply–demand ratio (r_t)	Modeled supply–demand ratio at time t.	Calculated

Indium primary production at time step t is calculated by the sum of primary production from all indium supply agents:

$$q_{total_t} = \sum_{i=1}^{n} q_{i_t}$$

Indium demand at time step t is calculated by the sum of ITO demand, CIGS demand, and other demand:

$$d_t = d_{ITO,t} + d_{CIGS,t} + d_{other}$$

Indium long-term predicted price p_{f_t} at time step t is calculated by the following regressed equation:

$$lnp_{f_t} = 0.8lnp_{t-1} - 0.392lnp_{t-2} + 0.3416lnp_{z_t} - 0.0038q_{z,total_t} + 0.194lnd_t + 0.051GDP$$

The long-term predicted price is regressed using corresponding data between year 1974 and 2017 with ARDL regression [17]. The long-term predicted price explains most variance of the data (R-squared 0.74). Short -term supply-–demand ratio is also an important factor to the market price [42]. Due to lack of data, it is not possible to include supply-–demand ratio into long-term regression. Instead, the model calibrated the impact factor β as mentioned before. Final indium market price is calculated as a function of total production and supply-–demand ratio:

$$P_t\left(q_{total_t}, r_t\right) = e^{-\beta lnr_t} p_{f_t}$$

where supply-–demand ratio r_t is calculated by:

$$r_t = \frac{q_{total_t} + i_{t-1}}{d_t}$$

3.6.2 Demand Agent Parameters and Variables

Input parameters for indium demand prediction is listed in Table 3.6.

Table 3.6. Demand agent parameters

Parameter Name	Details	Data source
ITO recycling factor (rec)	Ratio between total ITO demand and ITO primary production $rec = 2.7$	Calculated [9]
ITO indium content factor (w_{ito})	Indium content in ITO $w_{ito} = 0.74$	Calculated by molecular weight. [66]
ITO demand logistic parameters ($K_{ito}, G_{ito},\ t_{0_{ito}}$)	Logistic curve parameters regressed using historical and prediction data $(K_{ito}, G_{ito},\ t_{0_{ito}}) = (3000, -0.298, 6.722)$	Assumption [12,50]
CIGS efficiency 2008 (e_{cigs_0})	Known CIGS module energy efficiency by 2008 $e_{cigs_0} = 11.2\%$	[52]
CIGS indium layer thickness 2008 (μm) (l_{cigs_0})	Known CIGS module indium-contained layer thickness by 2008 $l_{cigs_0} = 1.6$	[52]
CIGS indium content (w_{cigs})	Indium content (t) per MW of CIGS installation, with indium layer thickness of 1.6 μm $w_{cigs} = 0.083$	[6,13,52,53]
CIGS scenarios parameters	See table A1-4 Logistic curve parameters regressed using historical and prediction data	
Other indium demand (d_{others})	Demand from other minor indium applications $d_{others} = 269.12$	[9,12,44]

ITO recycling factor is calculated as described in the Model Formulation section of the article. ITO demand logistic parameters are the parameters of the logistic growth function, defined as:

$$d_{ito\_total}(t) = \frac{K_{ito}}{1 + e^{-G_{ito}(t - t_{0_{ito}})}}$$

where $d_{ito\_total}(t)$ is the total ITO demand at time t. The parameter K_{ito}, which is the saturated market size of ITO, is assumed based on the prediction from USGS and ResearchInChina [12,50], with an additional 20% relaxation for a higher estimation of ITO demand. The other two parameters are then regressed based on historical ITO demand data calculated from historical primary indium demand data for ITO, with the recycling factor and indium content factor taken into consideration. Thus, total ITO demand projection each year can be generated by the function.

Meanwhile, since CIGS is an evolving technology, its material efficiency and energy efficiency will be improved over time. The decrease in indium-contained layer thickness and increased photovoltaic efficiency results in decreased indium consumption per GW of CIGS installation. To reflect this fact, based on the prediction from DOE and recent CIGS photovoltaic development information on market share and lab energy efficiency, three scenarios based on different technology projection are developed [6,52,53]. Here, final technological advancement by year 2050 on layer thickness and energy efficiency for all scenarios are the same. Layer thickness follows the data from DOE projection, and energy efficiency follows the latest reported lab efficiency. On the other hand, different advancement speed and market projection are selected for each scenario. Advancement speed is based on the scenarios provided by DOE projection [13,52]. Market size projection by year 2050 are calculated from market share projection from latest photovoltaic report and total solar power generation market size [13,53]. Similarly, a logistic growth function is then regressed based on historical CIGS production and final CIGS market size for each scenario, from which CIGS annual installation projection for each scenario is generated.

Finally, indium consumption from other minor usages is modeled as constant either because the application is a long-existing one with a saturated market, or the application does not consume significant amount of indium, as discussed in the article.

Demand agent variables are described in detail in Table 3.7. Demand agent variables. Primary indium demand from ITO at time t is calculated based on logistic function for annual total ITO demand as:

$$d_{ito_t} = \frac{w_{ito}}{rec} \times d_{ito_{total}}(t) = \frac{w_{ito}}{rec} \times \frac{K_{ito}}{1 + e^{-G_{ito}(t - t_{0_{ito}})}}$$

where total ITO demand is firstly deducted by recycling factor to determine ITO produced from primary indium, and primary indium consumption is then calculated by applying ITO indium content factor.

Table 3.7. Demand agent variables

Variable Name	Details	Data source
ITO indium demand (d_{ito_t})	Predicted primary indium demand from ITO at time t.	Logistic curve parameters regressed
CIGS efficiency (e_{cigs_t})	Linearized yearly result for CIGS efficiency under corresponding scenario	Calculated
CIGS indium layer thickness (l_{cigs_t})	Linearized yearly result for indium-contained layer thickness in CIGS under corresponding scenario	Calculated
CIGS indium demand (d_{cigs_t})	Predicted primary indium demand from CIGS at time t. d_{cigs_t}	Logistic curve parameters regressed
Total indium demand (d_t)	$\mathrm{d}_t = d_{ito_t} + d_{cigs_t} + d_{others}$	

The model assumed that CIGS technology advancement is linear between scenario-wise checkpoints. For example, under the base case, layer thickness changes linearly between 2008 and 2020, from 1.6 to 1.0 µm and then follows another linear change between 2020 and 2050, from 1.0 to 0.8 µm. Primary indium demand from CIGS at time t is similarly calculated based on logistic function for annual CIGS installation in GW as:

$$d_{cigs_t} = w_{cigs} \times \frac{l_{cigs_t}}{l_{cigs_0}} \times \frac{e_{cigs_0}}{e_{cigs_t}} \times \frac{K_{cigs}}{1 + e^{-G_{cigs}(t - t_{0_{cigs}})}}$$

Finally, total indium demand is calculated by:

$$\mathrm{d}_t = d_{ito_t} + d_{cigs_t} + d_{others}$$

To ensure that the uncertainties of model data and assumption do not impact model result too much, an uncertainty analysis has been conducted, as described in the Validation and Verification section of the article.

3.6.3 Supply Agent Parameters and Variables

Input parameters for each supply agent is listed in Table 3.8

Table 3.8. Supply agent parameters

Parameter Name	Details	Data source
Indium capacity, 2016 ($k_{ref,i}$)	Indium capacity for supply agent i at 2016	[12]
Initial indium capacity factor ($w_{capacity}$)	Factor converting indium capacity of 2016 into 2008 $w_{capacity} = \frac{p_{2008}}{p_{2016}} = 0.487$	Assumption [60]
Average indium content in respect of host metal content (ppm) (ppm_{avg})	Average indium content in zinc concentrates that are processed by indium refineries $ppm_{avg} = 243$	[9]
Manufacturing cost index (MCI)	Relative manufacturing cost between different countries, US=100	[67]
Discount rate ($r_{discount}$)	$r_{discount} = 0.08$	[58]
Indium reference variable cost ($c_{v,ref}$)	Indium production unit variable cost from refinery report $c_{p,ref} = 190.43$	
Indium reference fixed cost ($c_{f,ref}$)	Indium production unit fixed cost from refinery report $c_{f,ref} = 36.48$	[8] Converted to 2008 dollar
Indium reference expansion cost ($c_{e,ref}$)	Indium production unit capital cost over 10 years from refinery report, used as unit expansion cost $c_{e,ref} = 36.18$	
Indium refinery efficiency (e_{indium})	Overall indium refinery efficiency to recover indium metal from zinc concentrates $e_{indium} = 60.65\%$	[8]
Zinc refinery efficiency (Zinc agents only) (e_{zinc})	Zinc refinery efficiency to recover zinc metal from zinc concentrates $e_{zinc} = 79.42\%$	[58]
Zinc market factor (Zinc agents only) (a_z)	The marginal cost factor of increased zinc production. Calculated from two refinery reports $a_z = -0.15$	Calculated [8,14,58]
Zinc reference cost (Zinc agents only) ($c_{z,ref}$)	Zinc production base cost, calculated from two refinery reports $c_{z,ref} = 6838.19$	
Indium residue price factor (w_{raw})	Indium-containing residue material cost, modeled as percentage of current indium price $w_{raw} = 15\%$	[58]

Indium capacity for each agent at the beginning of simulation is assumed to have same proportion as 2016, thus the initial capacity for agent i can be calculated as:

$$k_{i_0} = k_{ref,i} \times \mathrm{w}_{capacity}$$

As described in the article, zinc market is formulated as a perfect market. Based on two known refinery reports from Canada and China with different zinc production capacity and cost, marginal cost factor and base cost are assessed by exponential regression with marginal cost formulation as:

$$C_z(q_z) = c_{z,ref} {q_z}^{a_z}$$

Here, all cost data are normalized into U.S. dollar 2008 with MCI of 96 (China).

Indium supply agents are divided into three categories. Three agents produce indium based on host metal other than zinc. Five agents produce indium from secondary sources (mine residues, primary metal refinery residues, etc.) and purchase indium-containing raw materials. The remaining seventeen agents are zinc based. Detailed information is provided in Table 3.9. Several smelters listed by USGS are already terminated, thus excluded from the model.

All variables used to model supply agents are presented in

Table 3.10. For each time step, current indium maximum capacity is firstly calculated. This represents maximum possible indium-containing raw material available to each agent and is calculated as:

$$k_{i,max_t} = \begin{cases} \infty, if\ agent\ i\ is\ secondary \\ k_{i,max_{t-1}} \times GDP, if\ agent\ i\ is\ non\ zinc\ based\ primary \\ k_{i,max_{t-1}} \times \dfrac{k_{zj_t}}{k_{zj_{t-1}}}, if\ agent\ i\ is\ zinc\ based \end{cases}$$

The initial value of k_{i,max_t} for non-zinc-based primary agents are equal to their initial capacity k_{i_0}. The initial value of k_{i,max_t} for zinc-based primary agent j is calculated as:

$$k_{j,max_0} = \max(k_{j_0}, \mathrm{ppm}_{avg} \cdot k_{zj_0})$$

For zinc-based agents, current zinc production capacity is modeled as:

$$k_{zj_t} = \frac{q_{z_t}}{q_{z_{t-1}}} k_{zj_{t-1}}$$

Table 3.9. Supply agent details

Agent	Location and MCI	Initial indium Capacity 2016 (t)	Type or Zinc production Capacity	Reference (All links last accessed on Nov. 17, 2020)
1	Belgium 123	50	Lead based	https://pmr.umicore.com/en/metals-products/minor-metals/
2	Canada 115	75	295000	https://www.teck.com/products/zinc/
3	China 96	85	Secondary	http://www.atk.com.cn/enterprise/index.shtml?id=199044
4	Do.	7	Antimony based	http://www.hksts.com/about.asp
5	Do.	60	290000	http://pdf.dfcfw.com/pdf/H2_AN201904221321181861_1.pdf
6	Do.	40	10000	http://www.chinaindium.org/2013/0117/13142.html
7	Do.	80	60000	http://www.camining.org/index.php?homepage=user010&file=introduce
8	Do.	20	110000	https://liuxingx.company.lookchem.cn/about/
9	Do.	150	Secondary	http://cnge.com.cn/product.aspx
10	Do.	50	Secondary	https://www.tianyancha.com/company/2350518552
11	Do.	25	165000	http://www.nonfemet.com/about/gsyw.php?aid=13
12	Do.	75	Secondary	http://www.114best.com/gs43/433136689.html
13	Do.	40	Secondary	http://www.intaitech.com/gywm
14	Do.	20	250000	http://www.ygzn.com.cn/cn/about.aspx?TypeId=10718
15	Do.	10	Tin based	http://www.yhtin.cn/intro/1.html
16	Do.	60	102184	http://www.ynhlxy.com/
17	Do.	20	93000	http://vip.stock.finance.sina.com.cn/corp/view/vCB_AllBulletinDetail.php?stockid=002114&id=5156491
18	Do.	60	70000	http://218.63.105.198/ch/About.asp
19	Do.	60	550000	http://www.torchcn.com/
20	France 124	48	155000	https://www.nyrstar.com/
21	Japan 111	70	200000	https://www.dowa.co.jp/en/products_service/metalmine.html
22	Korea 102	160	656000	https://www.koreazinc.co.kr/english/product/page/productMain.aspx
23	Do.	35	400000	http://www.ypzinc.co.kr/eng/company/menu_05.html
24	Peru 92.5	50	610600	http://relatoriovmetais.com.br/2016/en/performance/
25	Russia 99	15	180000	https://www.marketscreener.com/CHELYABINSKIY-TSINKOVYI-Z-4006531/news/PJSC-Chelyabinsk-Zinc-Plant-Final-Results-26232821/

Table 3.10. Supply agent variables

Variable Name	Details	Data source
Indium capacity (k_{i_t})	Indium capacity for supply agent i at time t	Initial value k_{i_0}
Indium maximum capacity (k_{i,max_t})	Maximum possible indium capacity for supply agent i at time t	
Indium production (q_{i_t})	Indium production decision variable for supply agent i at time t	
Indium production expansion ($k_{i_t}^*$)	Indium production capacity expansion decision variable for supply agent i at time t	
Indium variable cost (c_{v,i_t})	Indium production variable cost parameter for supply agent i at time t	
Indium fixed cost (c_{f,i_t})	Indium production unit fixed cost for supply agent i at time t	
Indium expansion cost (c_{e,i_t})	Indium production unit capital cost for supply agent i at time t over 10 years	
Indium total expansion cost (c_{e_total,i_t})	Indium total expansion cost for supply agent i at time t, formulated as additional fixed cost $c_{e\_total,i_t} = \sum_{s=t-10}^{t-1} c_{e,i_s} \cdot k_{i_s}^* \cdot CPI^{t-s}$	
Zinc production base cost (Zinc agents only) (c_{zj_t})	Zinc marginal cost parameter for zinc-based supply agent j at time t	
Zinc production (Zinc agents only) (q_{zj_t})	Zinc production decision variable for zinc-based supply agent j at time t	
Zinc capacity (Zinc agents only) (k_{zj_t})	Zinc capacity for zinc-based supply agent j at time t	
Indium content in respect of zinc content (Zinc agents only) (ppm_{j_t})	Indium content density in respect of zinc content for zinc-based supply agent j at time t	

Based on perfect market competition [14], each zinc-based agent j can be optimized separately by the following optimization problem:

$$\max p_{z_t} q_{zj_t} - \left(c_{zj_t} q_{zj_t}{}^{a_z} \right) q_{zj_t} \quad for\ j = 1,2, \dots, 17$$

$$such\ that:$$

$$0 \le q_{zj_t} \le k_{zj_t} \quad for\ j = 1,2, \dots, 17$$

Here, $c_{zj_t} = c_{zj_{t-1}} \cdot CPI$, and $c_{zj_0} = \mathrm{c}_{z,ref} \cdot \frac{MCI_j}{MCI_{China}}$

Once solved, current indium capacity for agent i can be represented as:

$$k_{i_t} = \min(k_{i_{t-1}}, k_{i,max_t})$$

Meanwhile, the cost function of agent i at time t is modeled as:

$$C_{i_t}(q_{i_t}) = \alpha q_{i_t}{}^2 + \left(\mathrm{c}_{v,i_t} - 20\alpha \right) q_{i_t} + \mathrm{c}_{f,i_t} + \mathrm{c}_{e\_total,i_t}$$

The quadratic function is formulated so that it fits the known production cost from refinery report (Gu, 2006) with 20 t of annual indium production.

Here, $\mathrm{c}_{v,i_t} = \mathrm{c}_{v,i_{t-1}} \times CPI$, $\mathrm{c}_{f,i_t} = \mathrm{c}_{f,i_{t-1}} \times CPI$,
$\mathrm{c}_{v,i_0} = \mathrm{c}_{v,ref} \times \frac{MCI_i}{MCI_{China}}$, and $\mathrm{c}_{f,i_0} = \mathrm{c}_{f,ref} \times \frac{MCI_i}{MCI_{China}}$

c_{e_total,i_t} is the total expansion cost for current time step t, which is formulated as:

$$\mathrm{c}_{e\_total,i_t} = \sum_{s=t-10}^{t-1} \mathrm{c}_{e,i_s} \times k_{i_s}^{*} \times CPI^{t-s}$$

After all parameters are determined, the Nash equilibrium problem can be formulated as:

$$\max P_t(q_{-i_t} + q_{i_t}) q_{i_t} - C_{i_t}(q_{i_t}) \quad for\ i = 1,2, \dots, n$$

$$such\ that:$$

$$0 \le q_{i_t} \le k_{i_t} \quad for\ i = 1,2, \dots, n$$

Here,

$$P_t(q_{-i_t} + q_{i_t}) = e^{-\beta ln\frac{q_{-i_t}+q_{i_t}+i_{t-1}}{d_t}} p_{f_t}$$

This is a potential game and can be solved using the best-response scheme.

Finally, each agent needs to consider about indium capacity expansion if they utilize up 90% of current capacity. This process is conducted via solving the following heuristic local optimization problem for $k_{i_t}^*$ from Canada refinery report [58]:

$$\max \sum_{i=1}^{10} \frac{p_{avg} q_{i_t} - C_{i_t}(q_{i_t})}{(1 - \mathrm{r}_{discount})^i} - 10 c_{ei_t} k_{i_t}^* \quad for\ i = 1,2,\dots,n$$

$$such\ that:$$

$$0 \le q_{i_t} \le k_{i_t} + k_{i_t}^*$$

$$0 \le k_{i_t}^* \le k_{i,max_t} - k_{i_t} \quad for\ i = 1,2,\dots,n$$

Here, p_{avg} is the indium price average in the recent 3 years,

$c_{ei_t} = c_{ei_{t-1}} \cdot CPI$ and $\mathrm{c}_{e,i_0} = \mathrm{c}_{e,ref} \cdot \frac{MCI_i}{MCI_{China}}$.

3.7 References

[1] Dudley, B. (2019). BP Statistical Review of World Energy. BP Statistical Review: London, UK.

[2] Kutak, R. (2018). Examination of Federal Financial Assistance in the Renewable Energy Market. Office of Nuclear Energy: Washington, DC, USA.

[3] Chu, S. (Ed.) (2011). Critical Materials Strategy. DIANE Publishing: Darby, PA, USA.

[4] Moss, R.L. Tzimas, E., Willis, P., Arendorf, J., Thompson, P., Chapman, A., Morley, N., Sims, E., Bryson, & R., Peason, J. (2013). Critical Metals in the Path towards the Decarbonisation of the EU Energy Sector. Assessing Rare Metals as Supply-Chain Bottlenecks in Low-Carbon Energy Technologies. JRC Report EUR, European Commission: Brussels, Belgium, 2013, p. 25994.

[5] Nassar, N.T., Graedel, T.E., & Harper, E.M. (2015). By-product metals are technologically essential but have problematic supply. Sci. Adv. 2015, 1, e1400180.

[6] Bleiwas, D.I. (2010). Byproduct Mineral Commodities Used for the Production of Photovoltaic Cells. US Department of the Interior, US Geological Survey: Reston, VA, USA.

[7] Mikolajczak, C. (2009). Availability of Indium and Gallium. Indium Corporation of America: Clinton, NY, USA.

[8] Gu, C., Huang, S., Cao, H., Tan, H., Liang, X., & Jiang, Z. (2006). Nandan Country Jilang Indium Manufacturing Co., Ltd. Integrated Indium and Zinc Recovery Project Environmental Impact Statement. Scientific Research Academy of Guangxi Environmental Protection: Guangxi, China.

[9] Lokanc, M., Eggert, R., & Redlinger, M. (2015). The Availability of Indium: The Present, Medium Term, and Long Term. No. NREL/SR-6A20-62409, National Renewable Energy Lab. (NREL): Golden, CO, USA.

[10] Bernhardt, D., & Reilly, J.F., II. (2019). Mineral Commodity Summaries 2019, US Geological Survey: Reston, VA, USA, 2019.

[11] Du, Y., Hu, Y., & Lei, X. (2016). Analysis of the supply and demand trend of indium and recommended management strategies. China Min. Mag. 2016, 25, 33–34, 64.

[12] Anderson, C.S. (2019). Indium. In Minerals Yearbook—Metals and Minerals, Advance Release 2016, U.S. Geological Survey: Reston, VA, USA.

[13] Dhabi, A. (2019). Global Energy Transformation: A Roadmap to 2050, 2019th ed., International Renewable Energy Agency, IRENA: Abu Dhabi, United Arab Emirates.

[14] Fizaine, F. (2013). Byproduct production of minor metals: Threat or opportunity for the development of clean technologies? The PV sector as an illustration. Resour. Policy 2013, 38, 373–383.

[15] Afflerbach, P., Fridgen, G., Keller, R., Rathgeber, A.W., & Strobel, F. (2014). The by-product effect on metal markets–new insights to the price behavior of minor metals. Resour. Policy 2014, 42, 35–44.

[16] Redlinger, M., & Eggert, R. (2016). Volatility of by-product metal and mineral prices. Resour. Policy 2016, 47, 69–77.

[17] Fu, X., Polli, A., & Olivetti, E. (2019). High-Resolution Insight into Materials Criticality: Quantifying Risk for By-Product Metals from Primary Production. J. Ind. Ecol. 2019, 23, 452–465.

[18] Mudd, G.M., Jowitt, S.M., & Werner, T.T. (2017). The world's by-product and critical metal resources part I: Uncertainties, current reporting practices, implications and grounds for optimism. Ore Geol. Rev. 2017, 86, 924–938.

[19] Werner, T.T., Mudd, G.M., & Jowitt, S.M. (2017). The world's by-product and critical metal resources part II: A method for quantifying the resources of rarely reported metals. Ore Geol. Rev. 2017, 80, 658–675.

[20] Werner, T.T., Mudd, G.M., & Jowitt, S.M. (2017). The world's by-product and critical metal resources part III: A global assessment of indium. Ore Geol. Rev. 2017, 86, 939–956.

[21] Kavlak, G., McNerney, J., Jaffe, R.L., & Trancik, J.E. (2015). Metal production requirements for rapid photovoltaics deployment. Energy Environ. Sci. 2015, 8, 1651–1659.

[22] Nassar, N.T., Wilburn, D.R., & Goonan, T.G. (2016). Byproduct metal requirements for US wind and solar photovoltaic electricity generation up to the year 2040 under various Clean Power Plan scenarios. Appl. Energy 2016, 183, 1209–1226.

[23] Stamp, A., Wäger, P.A., & Hellweg, S. (2014). Linking energy scenarios with metal demand modeling—The case of indium in CIGS solar cells. Resour. Conserv. Recycl. 2014, 93, 156–167.

[24] Jackson, W., Director, T.F., & Unit, S.B. (2012). The Future of Indium Supply and ITO, Indium Corporation: Clinton, NY, USA.

[25] Candelise, C., Winskel, M., & Gross, R. (2012). Implications for CdTe and CIGS technologies production costs of indium and tellurium scarcity. Progress Photovolt. Res. Appl. 2012, 20, 816–831.

[26] Choi, C.H., Cao, J., & Zhao, F. (2016). System dynamics modeling of indium material flows under wide deployment of clean energy technologies. Resour. Conserv. Recycl. 2016, 114, 59–71.

[27] Choi, C.H., Eun, J., Cao, J., Lee, S., & Zhao, F. (2016). Global strategic level supply planning of materials critical to clean energy technologies–A case study on indium. Energy 2018, 147, 950–964.

[28] Zhang, K., Wu, Y., Wang, W., Li, B., Zhang, Y., & Zuo, T. (2015). Recycling indium from waste LCDs: A review. Resour. Conserv. Recycl. 2015, 104, 276–290.

[29] He, Y., Ma, E., & Xu, Z. (2014). Recycling indium from waste liquid crystal display panel by vacuum carbon-reduction. J. Hazard. Mater. 2014, 268, 185–190. [PubMed]

[30] Zeng, X., Wang, F., Sun, X., & Li, J. (2015). Recycling indium from scraped glass of liquid crystal display: Process optimizing and mechanism exploring. ACS Sustain. Chem. Eng. 2015, 3, 1306–1312.

[31] Cucchiella, F., D'Adamo, I., Koh, S.L., & Rosa, P. (2015). Recycling of WEEEs: An economic assessment of present and future e-waste streams. Renew. Sustain. Energy Rev. 2015, 51, 263–272.

[32] D'Adamo, I., Ferella, F., & Rosa, P. (2019). Wasted liquid crystal displays as a source of value for e-waste treatment centers: A techno-economic analysis. Curr. Opin. Green Sustain. Chem. 2019, 19, 37–44.

[33] Marwede, M., Berger, W., Schlummer, M., Mäurer, A., & Reller, A. (2013). Recycling paths for thin-film chalcogenide photovoltaic waste–Current feasible processes. Renew. Energy 2013, 55, 220–229.

[34] McDonald, N.C., & Pearce, J.M. (2010). Producer responsibility and recycling solar photovoltaic modules. Energy Policy 2010, 38, 7041–7047.

[35] Liu, C., Zhang, Q., & Wang, H. (2020). Cost-benefit analysis of waste photovoltaic module recycling in China. Waste Manag. 2020, 118, 491–500.

[36] Gu, S., Fu, B., Dodbiba, G., Fujita, T., & Fang, B. (2018). Promising approach for recycling of spent CIGS targets by combining electrochemical techniques with dehydration and distillation. ACS Sustain. Chem. Eng. 2018, 6, 6950–6956.

[37] Marchetti, B., Corvaro, F., Giacchetta, G., Polonara, F., Cocci Grifoni, R., & Leporini, M. (2018). Double Green Process: A low environmental impact method for recycling of CdTe, a-Si and CIS/CIGS thin-film photovoltaic modules. Int. J. Sustain. Eng. 2018, 11, 173–185.

[38] Dimitrijević, S., Rajčić-Vujasinović, M., Stević, Z., Kamberović, Ž., Korać, M., & Dimitrijević, S. (2018). Metal Extraction and Separation Processes in Recycling of CIGS Based Thin Film Pv Modules. In Zbornik Međunarodne Konferencije o Obnovljivim Izvorima Električne Energije–MKOIEE, Proceedings of the 6th International Conference on Renewable Electrical Power Sources, Belgrade, Serbia, 11–12 October 2018, Savez Mašinskih i Elektrotehničkih Inženjera i Tehničara Srbije—SMEITS: Belgrade, Serbia, 2018, Volume 2, pp. 1–8.

[39] Macal, C.M., & North, M.J. (2005). Tutorial on agent-based modeling and simulation. In Proceedings of the Winter Simulation Conference, Orlando, FL, USA, 4 December 2005, p. 14.

[40] Nikolic, I., Bollinger, A., & Davis, C. (2010). Agent Based Modeling of Large-Scale Socio-Technical Metal Eetworks, Proceedings of the TMS 2010 Annual Meeting & Exhibition, Seattle, WA, USA, 14–18 February 2010, Minerals, Metals and Materials Society/AIME: Warrendale, PA, USA, 2010.

[41] Young, D., Poletti, S., & Browne, O. (2014). Can agent-based models forecast spot prices in electricity markets? Evidence from the New Zealand electricity market. Energy Econ. 2014, 45, 419–434.

[42] Riddle, M., Macal, C.M., Conzelmann, G., Combs, T.E., Bauer, D., & Fields, F. (2015). Global critical materials markets: An agent-based modeling approach. Resour. Policy 2015, 45, 307–321.

[43] North, M.J., Collier, N.T., Ozik, J., Tatara, E., Altaweel, M., Macal, C.M., Bragen, M., & Sydelko, P. (2013). Complex Adaptive Systems Modeling with Repast Simphony. In Complex Adaptive Systems Modeling, Springer: Berlin/Heidelberg, Germany.

[44] Zhao, K. (2018). Review and Analysis of Indium Market Detailed Comparison of Data between China, the United States, Japan and South Korea. Available online: https://news.metal.com/newscontent/100896637/zhao-kefeng:-review-and-analysis-of-indium-market-detailed-comparison-of-data-between-china-the-united-states-japan-and-south-korea/ (accessed on 17 November 2020).

[45] Wilburn, D.R. (2012). Byproduct Metals and Rare-Earth Elements Used in the Production of Light-Emitting Diodes—Overview of Principal Sources of Supply and Material Requirements for Selected Markets, U.S. Geological Survey Scientific Investigations Report 2012–5215, U.S. Geological Survey: Reston, VA, USA, 2012, 15p. Available online: http://pubs.usgs.gov/sir/2012/5215/ (accessed on 17 November 2020).

[46] Ashe, M., Chwastyk, D., de Monasterio, C., Gupta, M., & Pegors, M. (2010). US Lighting Market Characterization, US Department of Energy, Office of Energy Efficiency and Renewable Energy: Washington, DC, USA.

[47] Elliott, C. (2019). Energy Savings Forecast of Solid-State Lighting in General Illumination Applications, No. DOE/EERE 2001, Navigant Consulting: Chicago, IL, USA.

[48] Dogmus, E., & Hong, L (2019). InP Wafer and Epiwafer Market—Photonic and RF Applications Report, Yole Développement: Lyon, France.

[49] Öko-Institut (2019). Substance Assessment of Indium Phosphide. RoHS, Öko-Institut: Freiburg, Germany.

[50] ResearchInChina (2016). Global and China ITO Sputtering Targets Industry Report, 2016–2020, ResearchInChina: Beijing, China.

[51] Gu, S., Fu, B., Dodbiba, G., Fujita, T., & Fang, B. (2017). A sustainable approach to separate and recover indium and tin from spent indium–tin oxide targets. RSC Adv. 2017, 7, 52017–52023.

[52] Fthenakis, V. (2009). Sustainability of photovoltaics: The case for thin-film solar cells. Renew. Sustain. Energy Rev. 2009, 13, 2746–2750.

[53] Philipps, S. (2019). Photovoltaics Report, Fraunhofer ISE and Werner Warmuth, PSE Conferences & Consulting GmbH: Freiburg, Germany.

[54] Thomas, C.L. (2019). Zinc. In Minerals Yearbook—Metals and Minerals, Advance Release 2016, U.S. Geological Survey: Reston, VA, USA, 2019.

[55] The World Bank (2020). Commodity Markets Outlook, Quaterly Report, April, The World Bank: Washington, DC, USA.

[56] Mohr, S., Giurco, D., Retamal, M., Mason, L., & Mudd, G. (2018). Global projection of lead-zinc supply from known resources. Resources 2018, 7, 17.

[57] USGS (2020). Zinc Data Sheet—Mineral Commodity Summaries 2020. Available online: https://pubs.usgs.gov/periodicals/mcs2020/mcs2020-zinc.pdf (accessed on 17 November 2020).

[58] Thibault, J., Dean, T.R., McKeen, S.M., Scott, T.B., & Hara, A. (2010). NI 43–101 Independent Technical Report: Mount Pleasant North Zone. Preliminary Economic Assessment, Thibault & Associates Inc.: Toronto, ON, Canada, 2010, Published on behalf of Adex Mining.

[59] Sargent, R.G. (2010). Verification and validation of simulation models. In Proceedings of the 2010 Winter Simulation Conference, Baltimore, MD, USA, 5–8 December 2010, IEEE: Hoboken, NJ, USA.

[60] USGS (2020). Indium Data Sheet—Mineral Commodity Summaries 2020. Available online: https://pubs.usgs.gov/periodicals/mcs2020/mcs2020-indium.pdf (accessed on 17 November 2020).

[61] Fontana, D., Forte, F., Pietrantonio, M., & Pucciarmati, S. (2020). Recent developments on recycling end-of-life flat panel displays: A comprehensive review focused on indium. Crit. Rev. Environ. Sci. Technol. 2020, 51, 1–28.

[62] Rimbach, R. (2017). Liquid Crystal Display (LCD) Recycling System Developed by the Industrial Technology Research Institute of Taiwan. Available online: https://www.pollutionequipmentnews.com/liquid-crystal-display-lcd-recycling-system-developed-by-the-industrial-technology-research-institute-of-taiwan (accessed on 17 November 2020).

[63] Patel, K. (2018). Solar Panel Efficiency and Lifespan. Available online: https://solarenergyforus.com/solar-panel-efficiency-lifespan/ (accessed on 17 November 2020).

[64] The World Bank (2020). GDP Growth (Annual %). Available online: https://data.worldbank.org/indicator/NY.GDP.MKTP.KD.ZG (accessed on 17 November 2020).

[65] The World Bank (2020). Inflation, Consumer Prices (Annual %). Available online: https://data.worldbank.org/indicator/FP.CPI.TOTL.ZG (accessed on 17 November 2020).

[66] Indium Corporation (2018). Product Data Sheet Indium Tin Oxide (ITO). Available online: https://www.indium.com/technical-documents/product-data-sheets/download/540/ (accessed on 17 November 2020).

[67] Sirkin, H.L., Zinser, & M., Rose, J.R. (2014). The Shifting Economics of Global Manufacturing, The Boston Consulting Group: Boston, MA, USA, 2014.

4. AGENT-BASED MODELING FOR ELECTRIC VEHICLE BATTERIES RECYCLING IN CHINA

Accompanied with the rapid growth of electric vehicles (EV) market in China, management of end-of-life (EOL) EV batteries has raised serious concerns as most EV batteries will last less than ten years. Due to relative high material values, most EV batteries have the potential to be recycled economically. Meanwhile, EOL EV batteries are in general still functional but at reduced capacity, thus can be repurposed into other applications, especially stationary energy storage. As a result, EOL EV batteries are usually sold to the recyclers by EV consumers, which forms a recycling market. The Chinese government had made efforts to impose policies and regulations on the market, as well as introduce entry permit to enforce environmental and safety requirements. However, many illegal recyclers still exist and dominate the market due to cost advantage coming from lack of environmental and safety protection.

To better understand the situation and identify possible policies that can be utilized by the government, this work sets up an agent-based model for EOL EV battery market. The core mechanism of the model is a cost-benefit based bidding competition between legal and illegal recyclers. This bottom-up approach attempts to elaborate the advantages of illegal recyclers and explore several scenarios to find possible solutions to the situation.

4.1 Introduction

An electric vehicle (EV) is a vehicle that uses one or more electric motors for propulsion. It can be powered by a collector system, with electricity from extravehicular sources, or it can be powered autonomously by a battery (sometimes charged by solar panels, or by converting fuel to electricity using fuel cells or a generator) [1]. Battery-based electric vehicles have a long history in China. During 1990s, low-speed electricity-propelled scooters and electrical power supplemented bicycles grew rapidly due to the ban of gasoline powered motorcycles in urban areas by the government [2]. Chinese government started an 863 project to invest in domestic production of electric cars during 2000s, providing funding of 880 million RMB to the industry during the tenth Five-year Plan period and another 1.2 billion RMB during the eleventh plan [3] [4]. As a result, China had become the leading producer as well as consumer for EVs [5].

Currently, battery electric vehicles, hybrid electric vehicles and plug-in hybrid electric vehicles are most commercialized types and these EVs rely heavily on different types of electric vehicle batteries to operate [6]. According to several research reports [7] [8], battery chemistry for BEV battery cathode is constantly changing and largely different in different regions. While lithium iron phosphate (LFP) battery is fading out in US [7], it still counts for 38% of total EV battery market share in China [8]. Meanwhile, lithium nickel manganese cobalt oxide (NMC) is the dominating EV battery chemistry in China, occupying another 54% of market share [8].

Since EV batteries have a limited lifespan of around 5-10 years [7] [8], it is projected that a large amount of EV batteries will reach end of life (EOL) during the next five years. Assuming that LFP batteries have a 5-year life span and NMC batteries have a 6-year lifespan, Tan et al. predicts that the total EOL EV batteries in China will reach 26.3 GWh by year 2021 and 126.0 GWh by year 2025[8]. Due to the relatively high material value and the possibility to reuse these batteries on other energy storage application, EOL EV battery recycling can be economically viable which in turn could lessen the demand of critical materials such as Lithium and Cobalt. As EV batteries generate multiple potential environmental risks during EOL disposal or recycling phase [9], Chinese government started to enforce EOL regulations and establish an entry permit system for EV battery recycling industry [10]. Currently, a total of 22 companies are officially permitted to recycle or repurpose EOL EV batteries [11].

However, as reported by Xinhua News Agency, many illegal recyclers for EV batteries exists due to high material values of used EV batteries and they often offer higher buying price, taking their advantages of low operating cost due to lack of necessary environmental protection measures [12]. Meanwhile, legal recyclers tend to collect EOL EV batteries from local dealers and transport these batteries to centralized recycling facilities, whereas illegal recyclers are mostly local. Since legal recyclers are less cost competitive, it is vital for the government to support legal recyclers by regulations and policies such as subsidy. Event with these measures, it is still not clear if these companies are profitable and willing to compete with each other on recycling EOL EV batteries.

Research have been conducted on methodology, environmental impact, cost-profit analysis, and policy making of EOL EV batteries recycling. Detailed literature review will be provided in the next section. Meanwhile, few research considered EOL batteries market where competition exists among multiple recyclers by an agent-based model simulation. This research aims at setting up a competitional EOL EV batteries market between legal and illegal recyclers. Governments can utilize several policies to intervene the competition and target at increasing overall battery recycling rate of legal recyclers. This model will shed light on the market dynamics and help the government to make further policy decisions.

4.2 Literature Review

Research had been focused on various EOL EV batteries recycling processes. An overview from Melin at al. discussed the overall number of research available on EV batteries, including recycling processes, reuse processes, and battery types [13]. For recycling processes, most studies and reviews focus on hydrometallurgical processes with mechanical or mechanochemical methods working as pre-process steps [14] [15] [16] [17]. Other recycling processes, such as pyrometallurgy processes [18], regeneration and direct recycling of cathode [19] [20] are also discussed. These studies show high recycling rate (over 90%) of cathode materials. For EV batteries reuse, many studies focus on EOL batteries status assessment [21] [22].

Economic performance of EOL EV batteries recycling and reuse are also discussed. Pagliaro et al. and Richa et al. assessed EV batteries recycling and reuse from a circular economy point of view [23] [24]. Several reports focused on providing a cost and profit analysis of various EV battery types [7] [25] [26]. NREL developed a cost assessment tool for EV batteries reuse in 2015 [27]. Dai et al. from Argonne National Lab (ANL) developed a closed-loop battery recycling model to assess recycling cost as well as environmental impacts [28].

Environmental impacts of EOL EV batteries recycling and reuse are addressed by several studies. Several studies assessed environmental impacts of EOL EV batteries along with economic benefits [26] [28] [29]. Life cycle assessment have been utilized to analyze environmental impact and benefits comparing to the original production process [30] [31] [32].

Meanwhile, several studies utilized dynamic modeling tools to provide more insights on EOL EV batteries collection market. Ziemann et al. utilized dynamic material flow analysis technique to discuss the impacts of EV batteries recycling on lithium supply-demand balance [33]. Blumberga et al. and Li et al. created system dynamics model to provide a temporal view of the market [34] [35]. Liu et al. created an agent-based model to analyze the importance of EV batteries recycling based on battery life and technology renovation [36].

To address the nature of a competing recycling market, either game-theory-based models or simulation-based models can be utilized. Tang et al. modeled EV batteries recycling market as a Stackelberg game and discussed different collection mechanisms [37]. Liu et al. discussed WEEE recycling with a dual channel model where competitors can choose to stay legal and receive subsidy form the government or become illegal and have reduced costs [38]. Murata et al. created a simulation model for global EV batteries reuse [39].

EOL EV batteries recycling market in China have some notable characteristics. First, two major types of EOL EV batteries exist (LFP and NMC) along with different recycling processes and costs, as well as potential profit from recycled materials [8]. Secondly, most recyclers are operating far under their capacities and the recycling market is a seller's market [40]. Finally, the geological distribution of EOL EV batteries impose an increased cost on battery collection and recycling, as EOL batteries are considered hazardous by regulation and need to be transported by special vehicles [41]. Besides, due to the difference on processes of EV battery recycling and reuse, recyclers may not be able to handle all battery types for recycling and reuse [11]. Meanwhile, it is vital to understand how policy makers can influence the market. To establish a market model based on these conditions, agent-based modeling (ABM) is a promising tool to address the heterogenicity and uncertainty of the system. Various studies based on this technique had been applied to competing markets, including electricity grids [42], e-waste recycling [43], and Freight transport markets [44]. Although Liu et al. [36] have already established an agent-based model on EV recycling, their model was purely based on demand of EV batteries and did not consider economic factors of EOL EV recycling process.

4.3 Model Description

4.3.1 Model Objectives and Implementation

This work is dedicated to creating a bottom-up model for EOL EV batteries recycling market using ABM as a tool and provides insight to the market nature and possible government measurements to increase recycling rate. The model simulated EOL EV batteries recycling collection market, where potential recyclers compete for spent EV batteries as raw material of recycling or reuse.

The model simulated the market between Jan. 2021 and Dec. 2025 in a monthly time step basis. Recyclers, modeled as agents, repeatedly receive spent EV battery offers and bids for them. Bidding model is commonly used in seller's market and had already been utilized to describe similar recycling market [45] [46]. Meanwhile, policy makers can utilize several tools to influence the market, such as regulations and subsidies. Recycled material and reused battery pack prices can also influence the willingness of recyclers. These uncertainties are modeled as different scenarios.

The following sections will first introduce general assumptions and system boundaries of the model, then goes into details about agent behaviors and parameter settings. Finally, details on possible scenarios are introduced, as well as validation and verification process. The Repast Simphony toolkit based on JAVA was used to implement the model [47].

4.3.2 Model assumptions and boundaries

Due to model scope and data availability, it is not possible to include every detail of the market into the model. Therefore, it is important to define the model properly so that it can properly imitates real world activities without being too complicated.

This model includes the recycling and reuse market of two major battery types in China, LFP and NMC. These two types of batteries cover more than 92% of current installed EV batteries in China [11]. Currently, NMC batteries are usually recycled due to relatively low EOL reuse value and high recycled material value [48]. Meanwhile, LFP batteries have relatively low material value, and can be reproposed into other applications based on EOL battery health [49] [50]. Therefore, this model did not include possibilities of NMC reuse nor the recycling and reuse of battery types other than LFP and NMC.

Legal recyclers from Chinese government list are modeled as agents [11]. The model assumes that each agent collects all batteries they acquired nationwide and transport them to one centralized processing facilities at their registered province. To simplify the model, the model assumes that the transportation distance for each EOL battery equals to the road distance between the capitals of two provinces. Meanwhile, an agent representing illegal recyclers is created to compete for EOL batteries. This agent resembles the collection of all local illegal recyclers. As this model assumes that all illegal recyclers have homogeneous recycling cost without considering transportation cost, only local illegal recyclers are most cost effective in the competition. Therefore, one agent is enough to resemble the behavior of illegal recyclers as it always represents a local illegal recycler in the competition.

The amount of EOL EV batteries and types available each time step (month) are direct input data from the report [50]. Meanwhile, following the survey result from Tang et al. [26], the model assumes that each EOL battery seller has a personal preference on the choice of recyclers and are not purely profit-driven. This preference is determined stochastically during the simulation.

4.3.3 Model Formulation

The model included 20 legal recyclers as agents following the list from Chinese government [11]. The original list contained two pairs of recyclers belonging to a same company, but with different recycling technologies or methods (recycling or reuse). Thus, they are combined into one agent correspondingly. Meanwhile, an illegal recycler agent is created to imitate all local illegal recyclers in the market. A seller agent is also created to provide EOL EV batteries for recycler agents to bid. The model flow chart is shown in Figure 4.1 to demonstrate model scheme.

During each time step, global variables such as subsidy amount and recycled material prices are first updated if necessary. After that the amount and types of available EOL EV batteries are determined from report data [50]. The model then started its auction process, first determine battery location and seller type stochastically based on known probability distribution [26] [51]. To simplify the process, spent batteries are auctioned in one ton unit and independence of probability distribution is assumed. Since this market is an open price competition, the winner need only to pay more than all its competitors. Therefore, the model assumed that second-price auction is used in the market, and each agent reserves a portion of their revenue as minimum gross margin based on historical data [50] [52]. For each auction, the recycler with highest bidding price wins the bid, and pays the seller with second-highest price. If no recyclers are willing to pay, the unit of battery will not be recycled. After all batteries are auctioned, the time step ends.

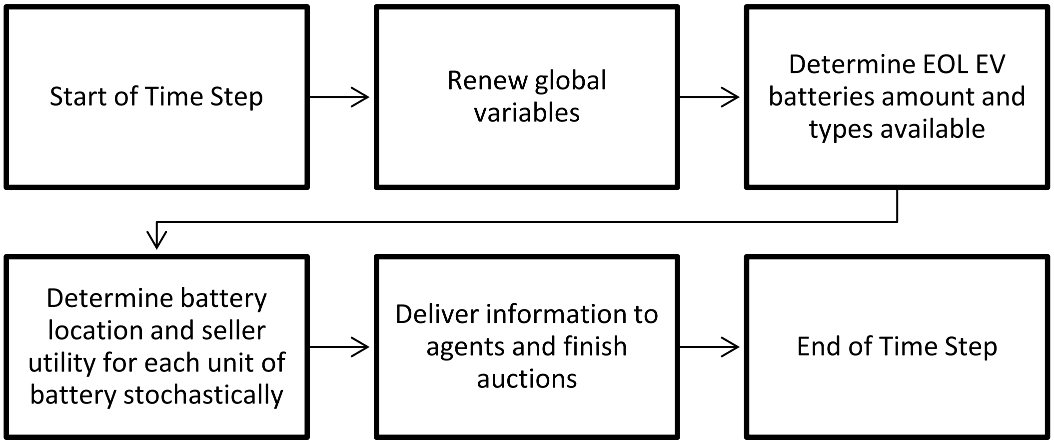

Figure 4.1. Model flow chart

4.3.4 Recycler Agents

The 20 plus 1 recycler agents are modeled to make decisions on each auction in each time step. Their parameters inputs are shown in Table 4.1**Error! Reference source not found.**. By comparing projected EOL EV batteries available with known recycler capacities, it is unlikely that the recycler capacities will be fully utilized by year 2025 [50]. Thus, the model did not impose capacity restrictions on recycler agents.

Meanwhile, the model assumes that all legal agents utilize similar recycling process and have same base cost towards a certain type of batteries. For illegal agent, environmental and tax costs are deducted from the total costs. The model assumes a recovery efficiency of 90%, following the Guangda report setting [50]. Since the data source does not provide reuse cost for LFP, data from another report on battery dismantle cost is utilized [53].

Since for a second price open auction, the dominant strategy is to bid until one's auction value or maximum willingness to pay is reached [56]. For each auction, the recycler agents add up their base cost for that battery type with transportation cost, and calculate their auction value which can be summarized into the following formula:

$$v_i = r_i \times \rho - (c_{base,i} + c_{transport} \times d_{i,battery})$$

here v_i is the value and the maximum bidding price for agent i, r_i is the revenue from recycling or reusing the sold EOL battery, $c_{base,i}$ is the base recycling or reuse cost, and $d_{i,battery}$ is the road distance between the battery and the recycler. As mentioned above, a portion of gross margin ρ is reserved. For each auction, after bidding price for each agent is calculated, the agent with highest bidding price wins the auction and the payment is equal to the second highest bidding price.

Table 4.1. Recycler agents' parameters

Parameters	**Value**	**References**
Transportation Cost	2.39 CNY/km	[28]
Base Recycling Cost, NMC	8300 CNY/t	[50]
Base Recycling Cost, LFP	7800 CNY/t	[50]
Base Reuse Cost, LFP	4964 CNY/t	[50] [53]
Base Energy Density, LFP	2.4kg/kWh	[50]
Base Price Reduction, LFP	30%	[50]
Base Environmental Cost, NMC	470 CNY/t	[50]
Base Environmental Cost, LFP	400 CNY/t	[50]
LFP Reuse Failure Rate	10%	[50]

Based on recycler information, five types of agents exist and are listed in Table 4.2. For recycler agents with only recycling process, LFP battery revenue is evaluated only by recycling process. For reuse only agents, LFP battery revenue is calculated by reuse process. Since the predicted probability for LFP battery failure is 10% [50], reuse only agents will have another 10% reduction in their revenue as they need to resell the battery. For all-purpose agents and illegal agents, the profits for LFP battery recycling and reuse are compared, and the agents only utilize the more profitable process unless they encounter a failed LFP battery.

Table 4.2. Recycler type table

Recycler Type	**EOL battery bid**	**Available process**
Reuse only	LFP	Reuse
Recycle only	LFP, NMC	Recycling
NMC only	NMC	Recycling
All-purpose	LFP, NMC	Recycling, Reuse
Illegal	LFP, NMC	Recycling, Reuse

The revenue of recycler agents, on the other hand, depends on current material prices and new battery prices. The price setting on sellable products is listed in Table 4.3**Error! Reference source not found.**. For critical material prices, as they are highly volatile, historical high price and low price are also listed and scenarios are created based on different price estimation. It should be noted that LFP battery expected price is adjusted by lithium price, since cathode cost count for roughly 20% of total LFP manufacturing cost [48].

Table 4.3. Recycling or reuse product price table

Product	**Current Price**	**Reference**
Lithium	930000 CNY/t (historical high: 935000, historical low: 390000)	[50] [54]
Nickle	146000 CNY/t (historical high: 154000, historical low: 64200)	[50] [54]
Cobalt	404200 CNY/t (historical high: 664200, historical low: 194200)	[50] [54]
Manganese	43800 CNY/t (historical high: 43800, historical low: 9300)	[50] [54]
Other Materials, total, NMC	3540 CNY per ton of battery	[55]
Other Materials, total, LFP	2703 CNY per ton of battery	[55]
LFP battery expected price (With lithium price at 495000)	0.71 CNY/Wh to 0.55 CNY/Wh	[50]

By taking a 90% recovery efficiency and a 40% (roughly 30% for LFP) cathode mass percentage in EV batteries, the recycled material weights deducted from the report are listed in Table 4.4 [50] [55]. Therefore, corresponding recycling revenue and profit can be calculated. When participating in an auction, a recycler will always bid for its maximum willingness to pay, as it is a dominant strategy of the auction [56].

Table 4.4. Recycled product mass table, per ton of batteries

Battery Type	Li (kg)	Ni (kg)	Co (kg)	Mn (kg)	Reference
LFP	24.2	0	0	0	[48] [50]
NMC 333	25.9	73.0	73.3	68.3	[50]
NMC 532	25.9	109.4	43.9	61.4	[50]
NMC 622	25.9	130.8	43.8	40.1	[50]
NMC 811	25.7	173.8	21.8	20.3	[50]

4.3.5 Seller Agent

The seller agent mainly provides EOL EV batteries for auction. During each time step, available batteries is read from input data [50]. Then for each tonnage of batteries, a collection location is stochastically determined based on known distribution [51], and an auction is initiated. The seller agent repeatedly open auctions until all EOL EV batteries are cleared out for current time step.

The total amount of batteries available and their type is shown in Table 4.5. Within the same year, the number of batteries assigned to a single month is evenly distributed. As Tang et. al pointed out, some EOL battery sellers are more aware of factors other than selling price [26]. As a result, for each auction, a seller's preference tied to the survey result is stochastically assigned [26]. The probability distribution of seller preferences and their actual influence on the model is shown in Table 4.6.

Table 4.5. EOL EV batteries available by type (t)

Type	2021	2022	2023	2024	2025
NMC 333	15750	32000	24250	3750	2250
NMC 532	14500	37500	106250	133250	119500
NMC 622	0	6000	19250	30500	36500
NMC 811	0	0.00	2500	7500	35000
LFP	52000	48200	55200	54100	68600

Table 4.6. Seller preferences

Preference	Probability Weight	Sells to
Recycling convenience	207	Legal, illegal
Recycling price	239	Legal, illegal
Environmentally friendly	146	Legal only
Formal channel	78	Legal only

4.3.6 Scenarios

To address uncertainties and policy influence over the market, several scenarios are created and listed below:

1. Metal price change: the base case model utilized current price of recycled products to predict revenues. However, price may drastically change during the 5-year simulation period. Since current metal prices are already at peak level comparing to historical data [50] [54], scenario with higher predicted price is not considered.
2. Government recycling subsidies: According to news report, local government in China had issued a 10 CNY/kWh subsidy to EV batteries recycling enterprises [58]. This scenario explores the possibility of a nation-wide subsidy to enhance the competitiveness of legal recyclers.
3. Banning of LFP reuse: Chinese government had imposed a new regulation to ban large energy storage plants from utilizing reused EV batteries [57]. This may further impact demand of repurposed EV batteries. To simulate this situation, a scenario is created that for each tonnage of EOL LFP battery, there is a 50% chance that it cannot be reused due to lack of demand and must be recycled, representing a shrink in LFP reuse demand.

4.3.7 Model Verification and Validation

A model needs to be verified and validated before putting into use. To verify that the model itself is valid and runs as intended, an internal validity test and an extreme condition test are conducted to prove that the base model properly functions. The internal validity test is conducted by running the model repeatedly, to identify whether the model is robust. The extreme condition test on cost, profit for illegal and legal recyclers and metal prices shows no abnormal behaviors for the model.

To validate the model, maximum possible recycling price is compared with current recycling price on a legal platform [59]. Also, a test run using historical price provided by the report [50] is conducted to compare maximum recycling price with estimated battery cost.

The internal validity test result is shown in   It can be seen that the model properly converges with no apparent outlier situation.

Table 4.7 It can be seen that the model properly converges with no apparent outlier situation.

Table 4.7. Internal validity test, 50 runs

Variable	Average (in 1000 CNY)	Standard Deviation
Average LFP called price, month 60, legal	4.462	0.0136
Average LFP called price, month 60, illegal	4.958	0.00936
Average NMC called price, month 60, legal	28.049	0.336
Average NMC called price, month 60, illegal	28.818	0.00773

The comparison of modelled result with historical data or assumption is listed in Table 4.8.

Table 4.8. Comparison with historical data

Data	Modeled result, average of 10 runs	Historical data	Reference
EOL NMC battery collection price, 2021	28526 CNY	22230-28080 (*1.17 for tax)	[59]
EOL LFP battery collection price, 2021	7825 CNY	6552-7254 (*1.17 for tax)	[59]

4.4 Results and Discussion

The baseline model result is shown in Figure 4.2. Under current price peak for EV battery raw material, both LFP reuse and NMC recycling processes are profitable. However, due to the cheaper cost for illegal recyclers, only 31% of all EOL batteries are legally recycled. Meanwhile, the change of monthly average collection price is shown in Figure 4.3. As LFP reuse has better return than direct recycling, all LFP batteries are bought to reuse. Since new LFP batteries become cheaper during the simulation, reused LFP battery price falls correspondingly. On the other hand, due to the static price of raw material metals, EOL NMC buying price remains steady. Therefore, the change of NMC chemistry will not impact recycling revenue too much under current price levels. During the last year of simulation period, as the market share of NMC811 increased, average buying price of NMC batteries dropped by roughly 600 CNY/t due to lower recycling value of the chemistry. Illegal recycler holds an average price advantage of 652 CNY/t comparing to legal recyclers on NMC collection, and an advantage of 492 CNY/t on LFP collection price.

Under such biding market setting, illegal competitors with cost advantage can dominate the market unless the sellers have preference other than maximum profit.

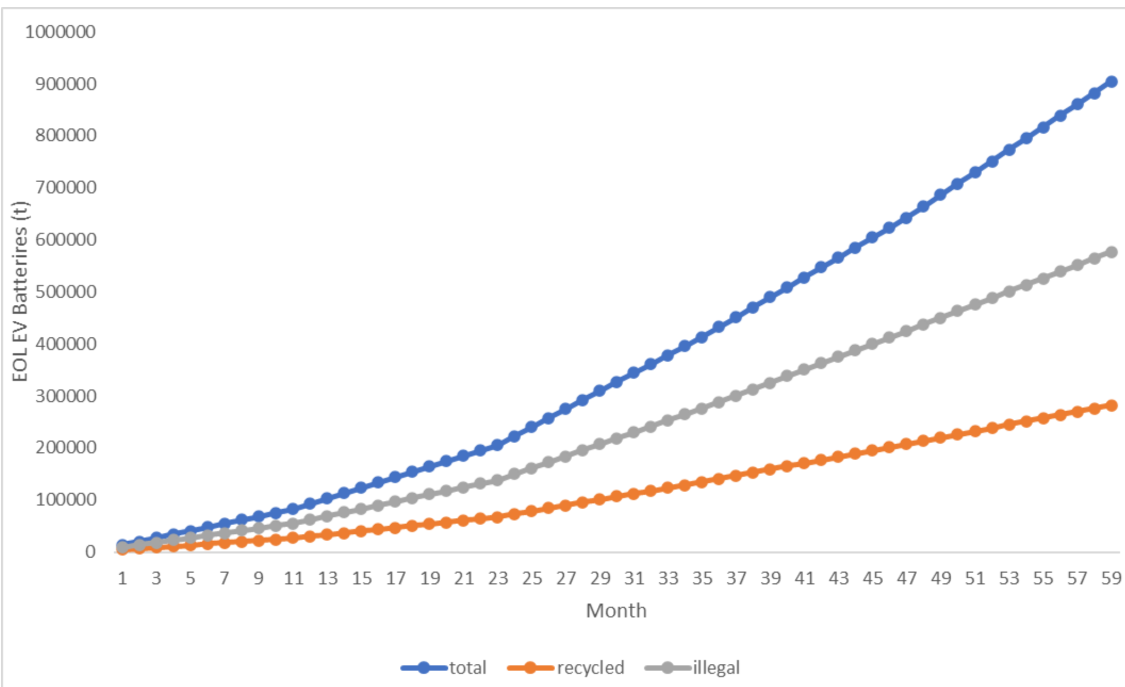

Figure 4.2. Recycling rate, baseline case

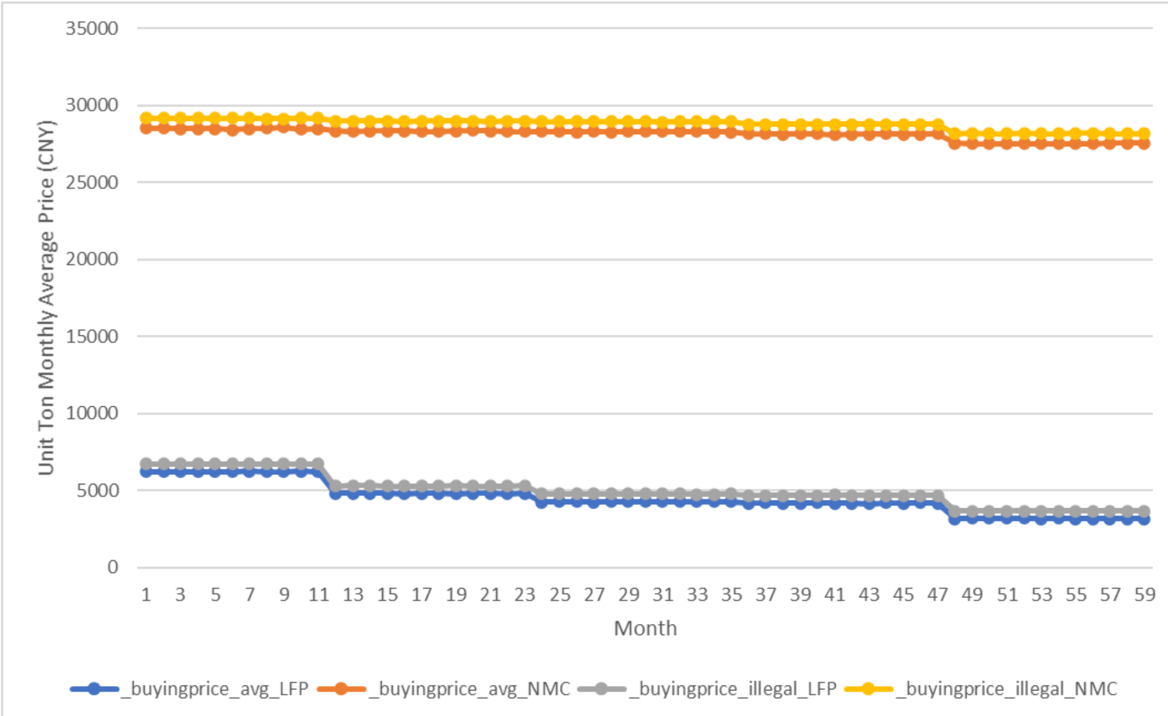

Figure 4.3. Biding price, baseline case

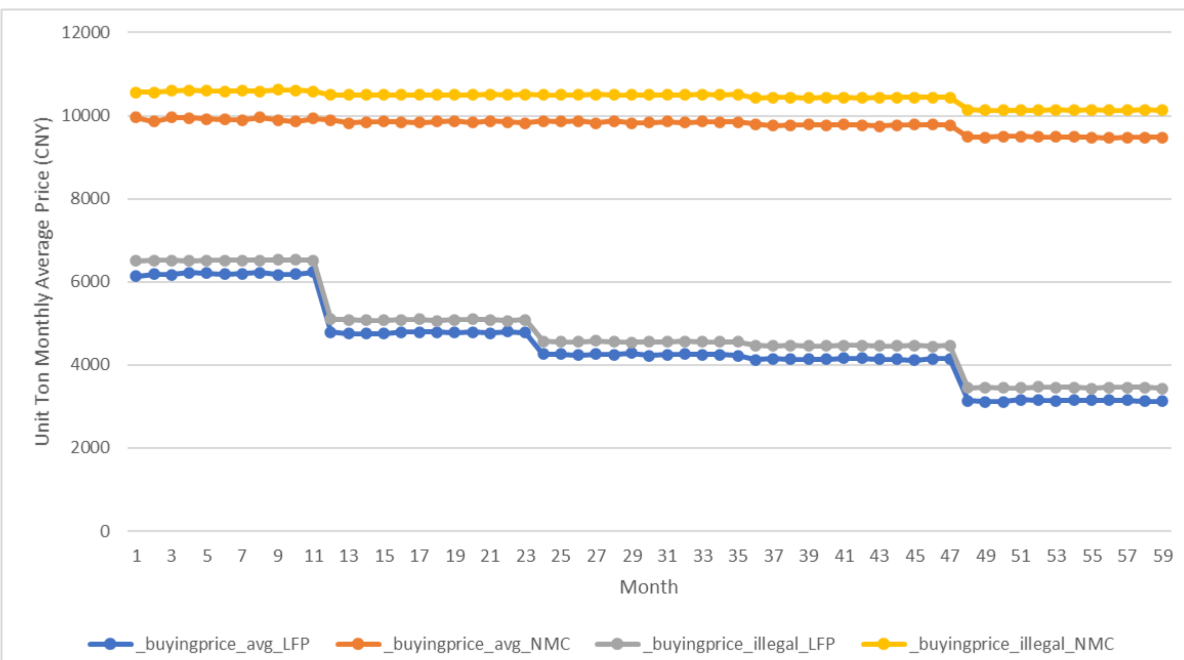

Figure 4.4. Biding price, low-price scenario

Under a historical low-price scenario, the illegal recycler still holds a price advantage over legal recyclers, thus making no difference in recycling rate. On the other hand, the average NMC battery bid price significantly falls for both types of recyclers, as shown in Figure 4.4. This results from the heavy dependency for NMC recycling price on raw material metal price. If the sellers are willing to hold the battery and wait for a high bid price to sell, the recyclers will have to either raise their bids by losing profit or waiting for a better raw material price. Since LFP reuse value is more connected to new LFP battery price and only indirectly influenced by lithium price, it is less impacted by the raw material price change than NMC recycling process.

For government subsidy scenario, considering a 2.4 kg/kWh cathode energy density for LFP battery and 30% LFP cathode mass percentage in a whole battery, the 10 CNY/kWh subsidy issued by Shenzhen local government is equivalent to a 1,250 CNY/t subsidy [50] [58]. To better illustrate the effect of subsidies, a series of runs are conducted with different subsidy values. The result is shown in Figure 4.5. It is implied that for a subsidy of 1,670 CNY/t or more, the cost advantage between illegal and legal recyclers on local NMC battery recycling is denied. However, to cover the additional inter-province transportation cost, additional subsidy needs to be applied.

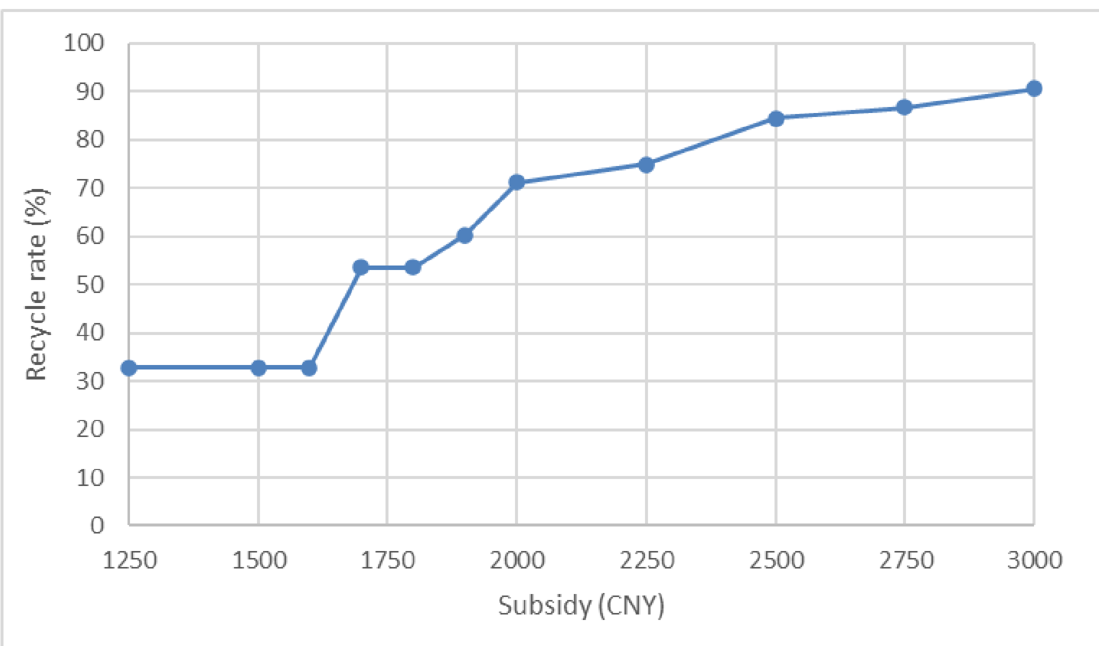

Figure 4.5. Subsidy effect

Finally, by impose an LFP reuse maximum share, the LFP bid price for both type of agents is shown in Figure 4.6. The total amount of batteries recycled did not change due to the high lithium price, but LFP bid price is reduced by one third comparing to the baseline case. With a low-price projection however, LFP recycling will no longer be profitable under current gross margin reserve.

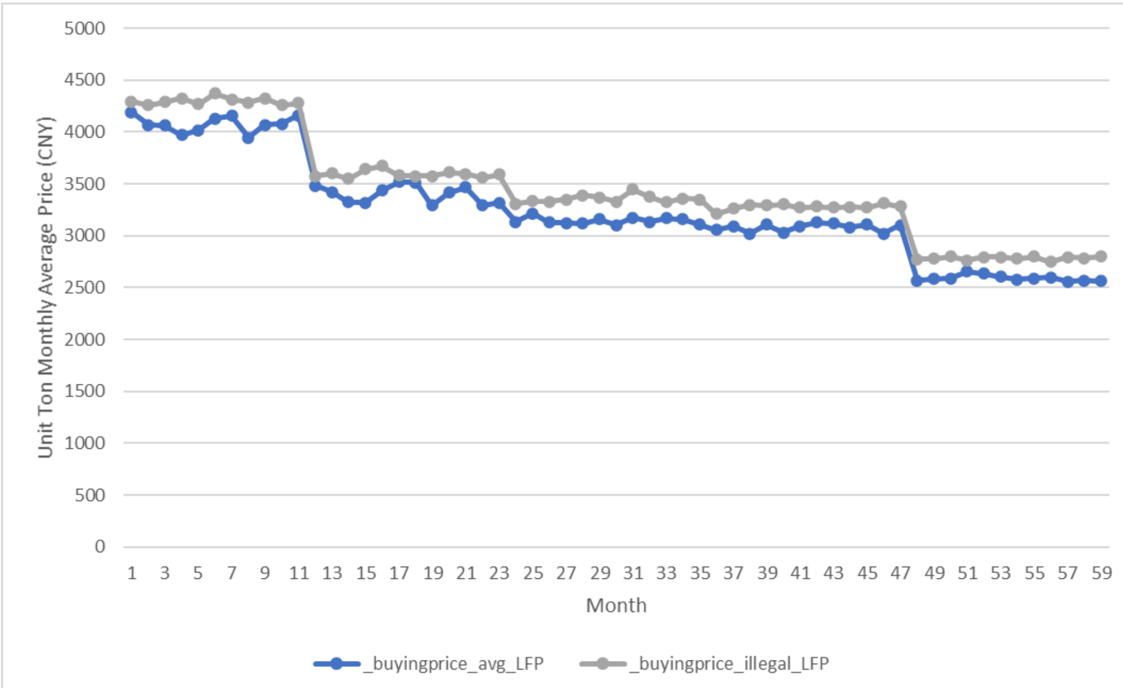

Figure 4.6. LFP reuse restriction, 50% maximum share

4.5 Conclusion and Future Work

In this study, EOL battery recycling market is modelled as an agent-based auction system, which captures the fact that illegal recyclers are dominating the market due to cost advantage. For government facing the situation, aside from directly eliminate illegal recyclers, subsidy would be a useful measure to improve the competitiveness of legal recyclers. On the contrary, any regulations that reduce the profit of illegal recyclers are likely to also harm the legal ones.

Meanwhile, it may be important to create a complete reverse supply chain, as discussed by Alamerew et al. [60]. Except for cost-benefit driven methods solely depending on recyclers, manufacturers can utilize several mechanics, such as battery renting contracts, to ensure the legal recycling of batteries [61].

This study is still crude and can undergo several improvements. Firstly, cost data from Chinese report are largely distinct with those reported by studies from other regions [7]. It may be worthwhile to identify the reason of the gap. Secondly, this work did not separate third party recyclers from battery manufacturers taking part in EOL battery recycling. Since manufacturers can achieve a closed-loop recycling via supply chain optimization, manufacturing scheme, and policies [28] [62], it is interesting to integrate such considerations into the model. Finally, it is valuable to include more layers of elements into the model. For instance, instead of one single sell agent, the model can incorporate a group of agents imitating EV customers in the real world. By modeling customer behavior, the model would become more realistic and provide more insights on the recycling market.

4.6 References

[1] Faiz, A., Weaver, C. S., & Walsh, M. P. (1996). Air pollution from motor vehicles: standards and technologies for controlling emissions. World Bank Publications.

[2] Weinert, J., Ma, C., & Cherry, C. (2007). The transition to electric bikes in China: history and key reasons for rapid growth. Transportation, 34(3), 301-318.

[3] GeekCar (2019). an unofficial Chinese EV history. https://www.sohu.com/a/339884944_120865 (In Chinese)

[4] Gu, R., Wu, J. (2012). "Eleventh Plan" 863 energy saving and new energy vehicle project passed final evaluation. http://www.gov.cn/jrzg/2012-09/14/content_2224960.htm (In Chinese)

[5] Brandsher, K. (2021). As Cars Go Electric, China Builds a Big Lead in Factories https://www.nytimes.com/2021/05/04/business/china-electric-cars.html

[6] Department of Energy (2021). Model Year 2021 Alternative Fuel and Advanced Technology Vehicles https://afdc.energy.gov/vehicles/search/download.pdf?year=2021

[7] Environmental, K. (2019). Research Study on Reuse and Recycling of Batteries Employed in Electric Vehicles: The Technical, Environmental, Economic, Energy and Cost Implications of Reusing and Recycling EV Batteries. Kelleher Environmental, Toronto.

[8] Tan, Q., Yin, B., Zhao, Y. (2019). In-depth report on electric vehicle batteries recycling industries http://www.invest-data.com/eWebEditor/uploadfile/2020032220135974696011.pdf (In Chinese)

[9] Zhou Z, Lai Y, Peng Q, Li J. Comparative Life Cycle Assessment of Merging Recycling Methods for Spent Lithium Ion Batteries. Energies. 2021; 14(19):6263. https://doi.org/10.3390/en14196263

[10] Ministry of Industry and Information Technology, China (2019) the Requirements of the Industry Standards for the Comprehensive Utilization of Waste Power Storage Batteries of New Energy Vehicles https://www.miit.gov.cn/n1146285/n1146352/n3054355/n3057542/n3057555/c7595145/part/7595160.pdf (In Chinese)

[11] Ministry of Industry and Information Technology, China (2021) Companies conform to "the Requirements of the Industry Standards for the Comprehensive Utilization of Waste Power Storage Batteries of New Energy Vehicles", second batch https://finance.sina.com.cn/money/future/indu/2021-01-22/doc-ikftssan9490810.shtml (In Chinese)

[12] Gu, Z. New energy vehicle batteries recycling maze investigation http://news.xhby.net/index/202104/t20210412_7044298.shtml (In Chinese)

[13] Tanong, K., Coudert, L., Mercier, G., & Blais, J. F. (2016). Recovery of metals from a mixture of various spent batteries by a hydrometallurgical process. Journal of environmental management, 181, 95-107..

[14] Yao, Y., Zhu, M., Zhao, Z., Tong, B., Fan, Y., & Hua, Z. (2018). Hydrometallurgical processes for recycling spent lithium-ion batteries: a critical review. ACS Sustainable Chemistry & Engineering, 6(11), 13611-13627.

[15] Ferreira, D. A., Prados, L. M. Z., Majuste, D., & Mansur, M. B. (2009). Hydrometallurgical separation of aluminium, cobalt, copper and lithium from spent Li-ion batteries. Journal of Power Sources, 187(1), 238-246.

[16] Kim, S., Bang, J., Yoo, J., Shin, Y., Bae, J., Jeong, J., ... & Kwon, K. (2021). A comprehensive review on the pretreatment process in lithium-ion battery recycling. Journal of Cleaner Production, 126329.

[17] Jia, W., Wang, Q., Yang, J., Fan, C., Wang, L., & Li, J. (2017). Pretreatment of lithium surface by using iodic acid (HIO3) to improve its anode performance in lithium batteries. ACS applied materials & interfaces, 9(8), 7068-7074.

[18] Makuza, B., Tian, Q., Guo, X., Chattopadhyay, K., & Yu, D. (2021). Pyrometallurgical options for recycling spent lithium-ion batteries: A comprehensive review. Journal of Power Sources, 491, 229622.

[19] Zhao, Y., Yuan, X., Jiang, L., Wen, J., Wang, H., Guan, R., ... & Zeng, G. (2020). Regeneration and reutilization of cathode materials from spent lithium-ion batteries. Chemical Engineering Journal, 383, 123089.

[20] Song, X., Hu, T., Liang, C., Long, H. L., Zhou, L., Song, W., ... & Liu, J. W. (2017). Direct regeneration of cathode materials from spent lithium iron phosphate batteries using a solid phase sintering method. RSC advances, 7(8), 4783-4790.

[21] Schuster, S. F. (2016). Reuse of automotive lithium-ion batteries: An assessment from the cell aging perspective (Doctoral dissertation, Technische Universität München).

[22] Neubauer, J. S., Wood, E., & Pesaran, A. (2015). A second life for electric vehicle batteries: answering questions on battery degradation and value. SAE International Journal of Materials and Manufacturing, 8(2), 544-553.

[23] Pagliaro, M., & Meneguzzo, F. (2019). Lithium battery reusing and recycling: A circular economy insight. Heliyon, 5(6), e01866.

[24] Richa, K., Babbitt, C. W., & Gaustad, G. (2017). Eco‐efficiency analysis of a lithium‐ion battery waste hierarchy inspired by circular economy. Journal of Industrial Ecology, 21(3), 715-730.

[25] Ma, X., Ma, Y., Zhou, J., & Xiong, S. (2018, June). The recycling of spent power battery: Economic benefits and policy suggestions. In IOP Conference Series: Earth and Environmental Science (Vol. 159, No. 1, p. 012017). IOP Publishing.

[26] Qiao, Q., Zhao, F., Liu, Z., & Hao, H. (2019). Electric vehicle recycling in China: Economic and environmental benefits. Resources, Conservation and Recycling, 140, 45-53.

[27] Neubauer, J., Smith, K., Wood, E., & Pesaran, A. (2015). Identifying and overcoming critical barriers to widespread second use of PEV batteries (No. NREL/TP-5400-63332). National Renewable Energy Lab.(NREL), Golden, CO (United States).

[28] Dai, Q., Spangenberger, J., Ahmed, S., Gaines, L., Kelly, J. C., & Wang, M. (2019). EverBatt: A closed-loop battery recycling cost and environmental impacts model (No. ANL-19/16). Argonne National Lab.(ANL), Argonne, IL (United States).

[29] Kamath, D., Arsenault, R., Kim, H. C., & Anctil, A. (2020). Economic and environmental feasibility of second-life lithium-ion batteries as fast-charging energy storage. Environmental science & technology, 54(11), 6878-6887.

[30] Unterreiner, L., Jülch, V., & Reith, S. (2016). Recycling of battery technologies–ecological impact analysis using Life Cycle Assessment (LCA). Energy Procedia, 99, 229-234.

[31] Silvestri, L., Forcina, A., Arcese, G., & Bella, G. (2020). Recycling technologies of nickel–metal hydride batteries: an LCA based analysis. Journal of Cleaner Production, 273, 123083.

[32] Unterreiner, L., Jülch, V., & Reith, S. (2016). Recycling of battery technologies–ecological impact analysis using Life Cycle Assessment (LCA). Energy Procedia, 99, 229-234.

[33] Ziemann, S., Müller, D. B., Schebek, L., & Weil, M. (2018). Modeling the potential impact of lithium recycling from EV batteries on lithium demand: a dynamic MFA approach. Resources, conservation and recycling, 133, 76-85.

[34] Blumberga, A., Timma, L., Romagnoli, F., & Blumberga, D. (2015). Dynamic modeling of a collection scheme of waste portable batteries for ecological and economic sustainability. Journal of Cleaner Production, 88, 224-233.

[35] Li, X., Mu, D., Du, J., Cao, J., & Zhao, F. (2020). Game-based system dynamics simulation of deposit-refund scheme for electric vehicle battery recycling in China. Resources, Conservation and Recycling, 157, 104788.

[36] Liu, S., & Gong, D. (2014). Modeling and simulation on recycling of electric vehicle batteries–using agent approach. International Journal of Simulation Modeling, 13(1), 79-92.

[37] Tang, Y., Zhang, Q., Li, Y., Wang, G., & Li, Y. (2018). Recycling mechanisms and policy suggestions for spent electric vehicles' power battery-A case of Beijing. Journal of Cleaner Production, 186, 388-406.

[38] Liu, H., Lei, M., Deng, H., Leong, G. K., & Huang, T. (2016). A dual channel, quality-based price competition model for the WEEE recycling market with government subsidy. Omega, 59, 290-302.

[39] Murata, H., Yokono, N., Fukushige, S., & Kobayashi, H. (2018). A lifecycle simulation method for global reuse. International Journal of Automation Technology, 12(6), 814-821.

[40] Yang Q. (2019). The "black society" of battery recycling. Retrieved from https://tech.ifeng.com/c/7pwbePn8TDC

[41] Zhao Y. et al. (2015). Recycling of traction battery used in electric vehicle—Management specification—Part 1 : Packing and transporting. Retrieved from http://std.samr.gov.cn/gb/search/gbDetailed?id=5DDA8BA21D9918DEE05397BE0A0A95A7

[42] Ringler, P., Keles, D., & Fichtner, W. (2016). Agent-based modeling and simulation of smart electricity grids and markets–a literature review. Renewable and Sustainable Energy Reviews, 57, 205-215.

[43] Sheoratan, S., Dijkema, G., Nikolic, I., Kleijn, R., Ghorbani, A., Meskers, C., & Art, I. S. (2011). Agent Based Modeling the e-waste recycling sector in Bangalore (Doctoral dissertation, M. Sc. Thesis, Delft University of Technology, Leiden University).

[44] Baindur, D., & Viegas, J. M. (2011). An agent based model concept for assessing modal share in inter-regional freight transport markets. Journal of Transport Geography, 19(6), 1093-1105.

[45] Kawai, K. (2011). Auction Design and the Incentives to Invest: Evidence from Procurement Auctions. NYU Stern.

[46] Kamo, T. (2011). Overview of the waste plastic recycling system in Japan and future tasks. In 6th international symposium on feedstock recycling of polymeric materials, Toledo (pp. 15-18).

[47] Riddle, M., Macal, C. M., Conzelmann, G., Combs, T. E., Bauer, D., & Fields, F. 2015. Global critical materials markets: An agent-based modeling approach. Resources Policy, 45, 307-321.

[48] Green & Low-Carbon Development Foundation (2018). Research on the Power Battery Recycling Mechanism and Policy for Shenzhen. Retrieved from https://www.efchina.org/Attachments/Report/report-ctp-20180710/%E6%B7%B1%E5%9C%B3%E5%B8%82%E5%8A%A8%E5%8A%9B%E7%94%B5%E6%B1%A0%E5%9B%9E%E6%94%B6%E5%88%A9%E7%94%A8%E6%9C%BA%E5%88%B6%E4%B8%8E%E6%94%BF%E7%AD%96%E7%A0%94%E7%A9%B6.pdf (In Chinese)

[49] Jian, L. I. U. (2017). Second use potential of retired EV batteries in power system and associated cost analysis# br. Energy Storage Science and Technology, 6(2), 243.

[50] Yin, Z., Ma, R., Hao, Y., Huang, S., Chen, W. (2021). Industry Research: EV batteries recycling. Retrieved from https://data.eastmoney.com/report/zw_industry.jshtml?infocode=AP202103251476026177 (In Chinese)

[51] Ren, Z., Lian, Y., Guo, S. (2020). China Clean Energy Vehicles Development Report 2020. Retrieved from http://pdf.dfcfw.com/pdf/H3_AP202009231416468578_1.pdf (In Chinese)

[52] Lazar, A. A., & Semret, N. (1998). Design, analysis and simulation of the progressive second price auction for network bandwidth sharing. Columbia University (April 1998).

[53] Jia, X., Feng, Q., Tao, Z., & Wang, B. (2018). Study on the echelon used scenario and technical recycling economy of power battery. Auto Engineer, 6, 14-19.

[54] Current price retrieved from: https://metal. com/

[55] Edelman, B., Ostrovsky, M., & Schwarz, M. (2007). Internet advertising and the generalized second-price auction: Selling billions of dollars worth of keywords. American economic review, 97(1), 242-259.

[56] Gaines, L., & Nelson, P. (2009, March). Lithium-ion batteries: possible materials issues. In 13th international battery materials recycling seminar and exhibit, Broward County Convention Center, Fort Lauderdale, Florida (p. 16).

[57] Shen, J. (2021). China to ban large energy storage plants from using retired EV batteries Retrieved from https://technode.com/2021/06/24/china-to-ban-large-energy-storage-plants-from-using-retired-ev-batteries/

[58] sznews, (2019). New energy vehicles subsidy standard 2018 published. Retrieved from http://www.sznews.com/news/content/2019-01/14/content_21345624.htm (In Chinese)

[59] Lihuitong (2021). Wasted Lithium battery price. Retrieved from, http://www.wukuangxunhuan.net/

[60] Alamerew, Y. A., & Brissaud, D. (2020). Modeling reverse supply chain through system dynamics for realizing the transition towards the circular economy: A case study on electric vehicle batteries. Journal of Cleaner Production, 254, 120025.

[61] Li, Z., & Ouyang, M. (2011). A win–win marginal rent analysis for operator and consumer under battery leasing mode in China electric vehicle market. Energy Policy, 39(6), 3222-3237.

[62] Gu, X., Ieromonachou, P., Zhou, L., & Tseng, M. L. (2018). Developing pricing strategy to optimise total profits in an electric vehicle battery closed loop supply chain. Journal of cleaner production, 203, 376-385.

5. CONCLUSION

The above works demonstrate three different applications of agent-based modeling, each exploring a different layer of a clean energy related market. The objective of the study is to better understand and give projections to different layers of clean energy technology markets, utilizing agent-based model in conjunction with other tools to provide bottom-up views of a market in question, which is seldom done by other methods. This is especially useful to identify the nature of emerging markets with fierce competitions or technology innovations. Since these markets are usually directly or indirectly involved with supply and demand of raw materials that are critical to clean energy development, this study focus its effort on catching the core characteristic of these markets, make projections, and identify possible bottlenecks created by demand from clean energy products and supply of critical material itself.

The initial work focuses its effort on LED lighting market in residential lighting sector. This market directly tied clean energy products to consumers. Understanding the growth of the market can help to make projections on LED lighting development and provide insights on demand increase over related critical materials, especially Gallium and Germanium [1]. Since most domestic consumers are not fully rational, the adoption of LED lighting involves utilities aside from cost-benefit analysis. This work utilizing agent-based modeling to operate a network of irrational customers, with several different schemes to change their opinions between incandescent CFL and LED. By construct several real-world related scenarios, the work identified possible measurements to promote LED adoption while reducing GHG emission and total energy consumption. In the process, possible bound effect created by overuse of LED is also identified, and projections of the market are properly given.

The second study directly explores a vital process of critical material supply. Indium is a by-product metal that cannot be solely mined due to economic concerns. Meanwhile, the emerge of CIGS photovoltaic technology may incur a significant increase in demand to the limited market. The task is to address the competitive and profit-driven nature of the refineries defines a non-cooperative market with high uncertainties. To better imitate these characteristics, the study employed agent-based modeling along with other powerful tools, such as mathematical regression and equilibrium theory to imitate the complicated market. The study successfully set up an agent-based model for indium refining market. The model is built on historical data and covers most real-world characteristics of the market. From the model, indium supply and demand projections can be given under various conditions.

The most recent work addresses a newly arose problem, which is the recycling of EOL electric vehicle batteries. Specifically, the situation in China is vastly different comparing to other countries due to the existence of dominating illegal recyclers. The research aims at understanding the market advantage of illegal recyclers and promoting the recycling rate via possible policies. To accomplish this, an agent-based model inspired by online auction is created to explain the situation. Cost-benefit analysis is done to identify the gap between illegal and legal recyclers. Projections on the recovery of important raw materials, such as lithium, cobalt and manganese are taken into considerations. The work successfully identifies the collection cost gap between recyclers and makes projections about the effects of certain policies and uncertainties.

In all, these works aim at understanding different layers of clean energy markets, try to establish novel bottom-up views towards them. In the process, either the supply and demand of critical material is directly discussed, or relevant markets are discussed to expose potential supply and demand changes. The study employs agent-based modeling to better demonstrate the competing and innovative nature of clean energy related markets and look around with possible scenarios to explore possible futures of the market.

6. FUTURE WORK

Although much has been done by numerous researches including this work, there are still many topics left to be explored. This work shows the possibility and adaptability of agent-based modeling, but it could also be used to connect multiple layers of the market and provide a compete view of dynamic critical material flows in the market.

Taking the indium model as an example, an additional layer of agents could be added to the model, representing indium-containing mines. Although indium is normally not suitable for direct mining, it may become economic feasible to do so when supply shortage occurs and indium price rises. Besides, old mine tails may contain rich indium concentrations. It is possible to expand existing models based on fresh data and identify economical or technical requirements of expanding indium supply. Meanwhile, recycling of indium only happens in-process. Research have been done on EOL indium recycling, including economical assessment. It may be possible to also expand the model on recycling perspective and identify possible secondary supply of indium.

Another thought is about EV market. This work narrows its effort on EOL recycling. However, it is still possible to incorporate multiple layers of agents into the model, from manufacturers to EV consumers. One biggest challenge would be data collecting, since clean energy markets are relatively new and evolves quickly. It may be possible to cooperate with insiders of the market and extend existing models based on close-informed data.

6.1 Reference

[1] Pavel, C. C., Marmier, A., Tzimas, E., Schleicher, T., Schüler, D., Buchert, M., & Blagoeva, D. (2016). Critical raw materials in lighting applications: substitution opportunities and implication on their demand. physica status solidi (a), 213(11), 2937-2946.

PUBLICATIONS

Choi, C. H., Cao, J., & Zhao, F. (2016). System dynamics modeling of indium material flows under wide deployment of clean energy technologies. Resources, Conservation and Recycling, 114, 59-71.

Cao, J., Choi, C. H., & Zhao, F. (2017). Agent-based modeling of the adoption of high-efficiency lighting in the residential sector. Sustainable Energy Technologies and Assessments, 19, 70-78.

Choi, C. H., Eun, J., Cao, J., Lee, S., & Zhao, F. (2018). Global strategic level supply planning of materials critical to clean energy technologies–A case study on indium. Energy, 147, 950-964.

Li, X., Mu, D., Du, J., Cao, J., & Zhao, F. (2020). Game-based system dynamics simulation of deposit-refund scheme for electric vehicle battery recycling in China. Resources, Conservation and Recycling, 157, 104788.

Cao, J., Choi, C. H., & Zhao, F. (2021). Agent-Based Modeling for By-Product Metal Supply—A Case Study on Indium. Sustainability, 13(14), 7881.